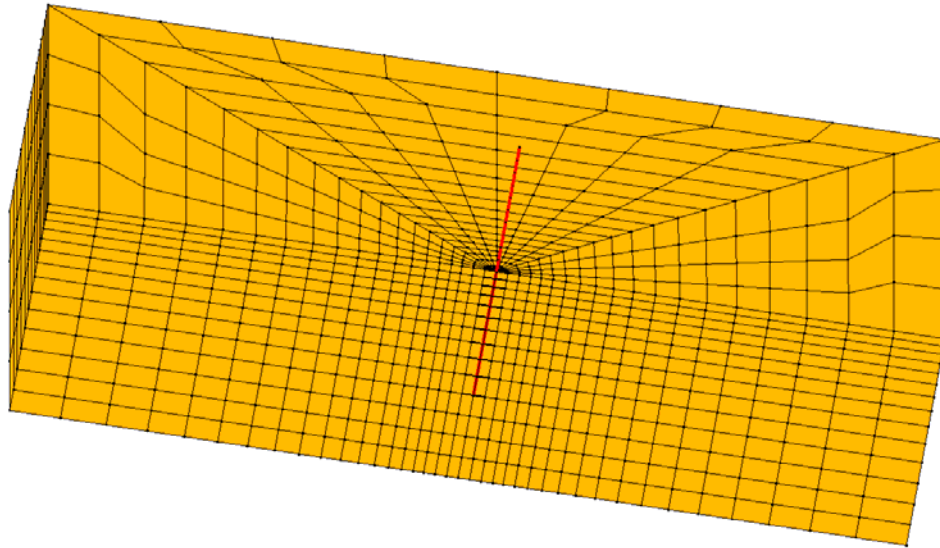


OpenSeesPL: 3D Lateral Pile-Ground Interaction

User Manual (Beta 1.0)



<http://cyclic.ucsd.edu/openseespl/>

Jinchi Lu, Ahmed Elgamal, and Zhaohui Yang

University of California, San Diego
Department of Structural Engineering

December 2011

For conversion between SI and English Units, please check:

<http://www.unit-conversion.info/>

(1 kPa = 0.1450378911491 psi)

(1 psi = 6.89475 kPa)

Table of Contents

TABLE OF FIGURES	IV
1. INTRODUCTION	1
1.1 OVERVIEW	1
1.2 SYSTEM REQUIREMENTS	2
1.3 INSTALLATION	2
1.4 ACKNOWLEDGMENTS	3
2. GETTING STARTED	4
2.1 START-UP	4
2.2 INTERFACE	4
2.2.1 <i>Menu Bar</i>	5
2.2.2 <i>Model Input Window</i>	6
2.2.3 <i>Finite Element Mesh Window</i>	6
3. PILE MODEL	8
3.1 PILE PARAMETERS	8
3.2 PILE PROPERTIES	9
3.2.1 <i>Linear Beam Element</i>	9
3.2.2 <i>Nonlinear Beam Element</i>	9
4. SOIL PARAMETERS	19
4.1 SOIL PARAMETERS	19
4.1.1 <i>Analysis Options</i>	20
4.1.2 <i>Additional Viscous Damping</i>	20
4.2 SOIL PROPERTIES	23
4.2.1 <i>Theory of Soil Models</i>	23
4.2.2 <i>Predefined Materials</i>	26
4.2.3 <i>User-Defined Materials</i>	31
4.2.4 <i>Material Properties for Pile Zone</i>	43
4.2.5 <i>Pile-Soil Interfacing Layer Properties</i>	44
4.2.6 <i>Outermost Zone Properties</i>	44
5. MESH GENERATION	46
5.1 GENERAL MESH DEFINITION	46
5.2 HORIZONTAL MESHING	46
5.3 VERTICAL MESHING	46
5.4 MESH SCALING	47
6. PUSHOVER & EIGENVALUE ANALYSES	50
6.1 PUSHOVER ANALYSIS	50
6.1.1 <i>Analysis Types</i>	50
6.1.2 <i>Load Pattern</i>	52
6.1.3 <i>Running the Analysis</i>	53
6.1.4 <i>Output for Pushover Analysis</i>	54
6.2 EIGENVALUE ANALYSIS	59
7. BASE SHAKING ANALYSIS	61
7.1 BASE SHAKING	61
7.1.1 <i>Step-by-Step Time Integration</i>	61

7.1.2	<i>Input Motion</i>	62
7.1.3	<i>Model Inclination</i>	64
7.2	TIME HISTORY OUTPUT	65
7.2.1	<i>Soil Response Time Histories</i>	65
8.	PILE GROUP	67
8.1	PILE GROUP PARAMETERS	67
8.2	PILE GROUP MESHING	67
8.3	OUTPUT FOR A PILE GROUP MODEL	69
APPENDIX A	HOW TO DEFINE THE SOIL FINITE ELEMENT MESH	73
APPENDIX B	OWN WEIGHT APPLICATION WITH DRY AND SATURATED SOIL CASES	77
APPENDIX C	BENCHMARK LINEAR FINITE ELEMENT ANALYSIS OF Laterally Loaded Single Pile Using OpenSees & Comparison with Analytical Solution	83
APPENDIX D	FINITE ELEMENT ANALYSIS OF ARKANSAS TEST SERIES PILE #2 USING OPENSEES (WITH LPILE COMPARISON)	96
APPENDIX E	FINITE ELEMENT ANALYSIS OF STANDARD CALTRANS 16" CIDH PILE USING OPENSEES FOR GENERAL COMPARISON WITH LPILE (WITH DEFAULT P-Y MULTIPLIER = 1.0)	107
APPENDIX F	FINITE ELEMENT ANALYSIS OF CALTRANS 42" CIDH PILE USING OPENSEES FOR GENERAL COMPARISON WITH LPILE (WITH DEFAULT P-Y MULTIPLIER = 1.0)	115
APPENDIX G	FINITE ELEMENT ANALYSIS OF STANDARD CALTRANS 16" CIDH PILE SUBJECTED TO AXIAL LOAD	128
APPENDIX H	MOMENT-CURVATURE ANALYSIS OF CIRCULAR NONLINEAR RC BEAM (FIBER SECTION)	133
REFERENCES		145
OPENSEESPL-RELATED REFERENCES		146

Table of Figures

Figure 2.1: OpenSeesPL main window.	4
Figure 2.2: OpenSeesPL's menu bar and submenu bars: a) menu bar; b) menu File; c) menu Execute; d) menu Display; and e) menu Help.....	5
Figure 2.3: OpenSeesPL copyright message.	6
Figure 2.4: Buttons available in the Finite Element Mesh window.....	7
Figure 3.1: Definition of pile model.	8
Figure 3.2: Definition of linear pile properties.	9
Figure 3.3: Definition of nonlinear pile properties (Aggregator Section).	10
Figure 3.4: Definition of nonlinear pile properties (Fiber Section).	12
Figure 3.5: Moment-curvature response for the pile (with default steel and concrete parameters)	14
Figure 3.6: Material Parameters of the Concrete01 material (Mazzoni et al. 2006)	15
Figure 3.7: Typical hysteretic stress-strain relation of the Concrete01 material (Mazzoni et al. 2006)	15
Figure 3.8: Material Parameters of the Steel01 material (Mazzoni et al. 2006)	16
Figure 3.9: Typical hysteretic behavior of model with Isotropic hardening of the Steel01 material (Mazzoni et al. 2006)	16
Figure 3.10: Schematic of fiber section definition for a circular cross section (Mazzoni et al. 2006)	17
Figure 3.11: Schematic of patch definition for a circular cross section (Mazzoni et al. 2006)	17
Figure 3.12: Schematic of layer definition for a circular cross section (Mazzoni et al. 2006).....	18
Figure 4.1: Soil strata definition.	19
Figure 4.2: Analysis options.	21
Figure 4.3: Rayleigh damping coefficients.....	22
Figure 4.4: OpenSees parameters.	23
Figure 4.5: Multi-yield surfaces in principal stress space and deviatoric plane (Prevost 1985; Parra 1996; Yang 2000)	24
Figure 4.6: Shear-effective confinement and shear stress-strain response (Yang and Elgamal 2002; Yang et al. 2003).	25
Figure 4.7: Von Mises multi-surface kinematic plasticity model (Yang 2000; Yang et al. 2003).	26
Figure 4.8: Soil materials in OpenSeesPL.	27
Figure 4.9: Soil backbone curve and yield surfaces.	30
Figure 4.10: Backbone curves for Medium Sand.	31
Figure 4.11: U-Sand1A.....	32
Figure 4.12: Initial yield domain at low levels of effective confinement (Yang et al. 2003).	36
Figure 4.13: Schematic of constitutive model response showing (a) octahedral stress τ - effective confinement p' response, (b) octahedral stress τ - octahedral strain γ response, and (c) configuration of yield domain (Yang et al. 2003).	36
Figure 4.14: U-Sand1B.	37
Figure 4.15: U-Clay1.	40
Figure 4.16: U-Clay2.	41
Figure 4.17: U-Sand2A.....	42

Figure 4.18: U-Sand2B.	43
Figure 4.19: Pile zone material.	44
Figure 4.20: Pile-soil interfacing layer material.	45
Figure 4.21: Outermost zone material.	45
Figure 5.1: Definition of meshing parameters.	48
Figure 6.1: Pushover analysis.	51
Figure 6.2: Pushover load pattern.	52
Figure 6.3: User-defined pushover load pattern (U-Push).	53
Figure 6.4: Analysis running progress window.	54
Figure 6.5: Zoom in.	54
Figure 6.6: Zoom out.	55
Figure 6.7: Response time histories and profiles for pile.	56
Figure 6.8: Response relationships for pile.	57
Figure 6.9: Deformed mesh and contour fill.	58
Figure 6.10: 2D plane ($Y = 0$) view of the longitudinal displacement contour in the deformed mesh window.	59
Figure 6.11: Output for an Eigenvalue analysis.	60
Figure 7.1: Newmark Time Integration.	61
Figure 7.2: Definition of 3D base excitation and boundary conditions.	63
Figure 7.3: User-defined input motion (U-Shake).	64
Figure 7.4: Response time histories window.	66
Figure 8.1: Pile group definition.	67
Figure 8.2: Pile group horizontal meshing.	68
Figure 8.3: Sample mesh of a 3 by 3 pile group model (half mesh configuration).	69
Figure 8.4: Pile response profiles for a pile group model.	70
Figure 8.5: Pile response time histories for a pile group model.	70
Figure 8.6: Pile response relationships for a pile group model.	71
Figure 8.7: Pile response relationships at the pile cap for a pile group model.	71
Figure 8.8: Deformed mesh of a pile group model.	72
Figure A.1: Finite element mesh created with default values.	73
Figure A.2: Mesh refinement example 1: a) Change “Num of Slices” to 32; b) the resulting mesh.	74
Figure A.3: Mesh refinement example 2: a) Change “Number of Mesh Layers” in the vertical direction; b) the resulting mesh.	75
Figure A.4: Mesh refinement example 3: a) Change meshing controlling parameters in the horizontal direction; b) the resulting mesh.	76
Figure C.1: Finite element mesh employed in this study.	85
Figure C.2: Comparison of pile deflection profiles ($v_s=.25$, $l/a=50$).	86
Figure C.3: Comparison of pile bending moment profiles ($v_s=.25$, $l/a=50$).	87
Figure C.4: Sample pile deflection ($h/a=.1$, $l/a=50$) under an applied pure pile-head horizontal load (Abedzadeh and Pak, 2004).	89
Figure C.5: Sample pile bending moment ($h/a=.1$, $l/a=50$) under an applied pure pile-head horizontal load (Abedzadeh and Pak, 2004).	90
Figure C.6: Comparison of the load-deflection curves for the linear and nonlinear runs.	91
Figure C.7: Comparison of the pile deflection profiles for the linear and nonlinear runs.	92

Figure C.8: Comparison of the pile bending moment profiles for the linear and nonlinear runs.	93
Figure C.9: Stress ratio contour fill of the nonlinear run at different load levels (red color shows yielded soil elements).....	95
Figure D.1: Finite element mesh employed in this study.	98
Figure D.2: Comparison of the load-deflection curves for the linear and nonlinear runs.	99
Figure D.3: Comparison of the pile deflection profiles for the linear and nonlinear runs.....	100
Figure D.4: Comparison of the pile bending moment profiles for the linear and nonlinear runs.	101
Figure D.5: Stress ratio contour fill of the nonlinear run at different load levels (red color shows yielded soil elements).....	103
Figure D.6: Comparison of the pile deflection profiles for the linear and nonlinear runs.....	104
Figure D.7: Comparison of the pile bending moment profiles for the linear and nonlinear runs.	105
Figure E.1: Finite element mesh employed in this study.....	109
Figure E.2: Comparison of pile deflection profiles for load case 1.....	110
Figure E.3: Comparison of pile rotation profiles for load case 1.....	111
Figure E.4: Comparison of bending moment profiles for load case 1.....	111
Figure E.5: Comparison of shear force profiles for load case 1.	112
Figure E.6: Comparison of pile deflection profiles for load case 2.....	112
Figure E.7: Comparison of pile rotation profiles for load case 2.....	113
Figure E.8: Comparison of bending moment profiles for load case 2.....	113
Figure E.9: Comparison of shear force profiles for load case 2.	114
Figure E.10: Stress ratio contour fill for load case 1 (red color shows yielded soil elements)...	114
Figure E.11: Stress ratio contour fill for load case 2 (red color shows yielded soil elements)...	114
Figure F.1: Finite element mesh employed in this study.....	117
Figure F.2: Comparison of pile deflection profiles for the fixed-head condition.....	118
Figure F.3: Comparison of pile rotation profiles for the fixed-head condition.	118
Figure F.4: Comparison of bending moment profiles for the fixed-head condition.	119
Figure F.5: Comparison of shear force profiles for the fixed-head condition.	119
Figure F.6: Comparison of pile deflection profiles for the free-head condition.....	120
Figure F.7: Comparison of pile rotation profiles for the free-head condition.	120
Figure F.8: Comparison of bending moment profiles for the free-head condition.....	121
Figure F.9: Comparison of shear force profiles for the free-head condition.	121
Figure F.10: Stress ratio contour fill of the nonlinear run for the fixed-head condition (red color shows yielded soil elements).....	122
Figure F.11: Stress ratio contour fill of the nonlinear run for the free-head condition (red color shows yielded soil elements).....	123
Figure F.12: Comparison of pile deflection profiles for the fixed-head condition.....	124
Figure F.13: Comparison of pile rotation profiles for the fixed-head condition.	124
Figure F.14: Comparison of bending moment profiles for the fixed-head condition.....	125
Figure F.15: Comparison of shear force profiles for the fixed-head condition.	125
Figure F.16: Comparison of pile deflection profiles for the free-head condition.....	126
Figure F.17: Comparison of pile rotation profiles for the free-head condition.	126
Figure F.18: Comparison of bending moment profiles for the free-head condition.....	127

Figure F.19: Comparison of shear force profiles for the free-head condition.	127
Figure G.1: Finite element mesh employed in this study.	130
Figure G.2: Pile profile response at the axial load of 243 kips.	131
Figure G.3: Close-up of final deformed mesh (factor of 120).	131
Figure G.4: Stress ratio contour fill for the nonlinear analysis (red color shows yielded soil elements).	132
Figure H.1: Schematic of the fiber section definition for the circular pile cross section.	135
Figure H.2: Material properties for the Fiber section.	135
Figure H.3: Finite element mesh employed in this study.	136
Figure H.4: Comparison of the moment-curvature curves calculated by using OpenSeesPL and OpenSees Example.	136
Figure H.5: Displacement response profiles histories of the pile.	138
Figure H.6: Lateral (longitudinal) shear versus displacement at the pile head.	138
Figure H.7: Moment-curvature relation at the maximum moment location (ground surface) in OpenSeesPL.	139

1. Introduction

OpenSeesPL is a graphical user interface (GUI) for three dimensional (3D) ground and ground-structure response. The OpenSees Finite Element (FE) Computational Analysis framework (<http://opensees.berkeley.edu>) is employed to conduct all analyses. The OpenSeesPL graphical interface (pre- and post-processor) is focused on facilitating a wide class of 3D studies (with additional capabilities yet under development). In the current version, OpenSeesPL may be employed to study a number of geometries and configurations of interest including:

- Linear and nonlinear (incremental plasticity based) 3D ground seismic response with capabilities for 3D excitation, and multi-layered soil strata. Multi-yield surface cohesionless (Drucker-Prager cone model), and (Mises or J2) soil models are available. The coupled solid-fluid analysis option allows for conducting liquefaction studies.
- Inclusion of a pile or shaft in the above 3D ground mesh (circular or square pile in a soil island). The pile can extend above ground and can support a bridge deck, or a point mass at the pile top. The bridge deck can be specified to only translate laterally, or to undergo both lateral translation and rotation. In addition to the seismic excitation option, the pile system may be subjected to monotonic or cyclic lateral push-over loading (in prescribed displacement or prescribed force modes). Soil within the zone occupied by the pile (as specified by pile diameter for instance) can be specified independently, allowing for a variety of useful modeling scenarios.
- Various Ground Modification scenarios may be studied by appropriate specification of the material within the pile zone. For instance, liquefaction countermeasures in the form of gravel drains, stone columns, and solidification/cementation may all be analyzed. Of particular importance and significance in these scenarios is the ability to include the effect of mild infinite-slope inclination (i.e., allowing estimates of accumulated ground deformation, effect of liquefaction countermeasures, pile-pinning effects, and liquefaction-induced lateral loading).
- Slopes and pile systems embedded in sloping ground are also currently being simulated.

1.1 Overview

OpenSeesPL is a FE user-interface for 3D lateral pile-ground interaction response. This interface allows conducting pushover pile analyses as well as seismic (earthquake) simulations. The FE analysis engine for this interface is the Pacific Earthquake Engineering Research (PEER) Center OpenSees Framework, developed under the leadership of Professor Gregory Fenves of UC Berkeley. For more information, please visit <http://opensees.berkeley.edu/>.

OpenSeesPL allows simulations for any size of pile and pile diameter. The pile cross section can be circular or square. Linear and nonlinear material properties options are available for pile definition.

OpenSeesPL allows for definition of multiple soil strata. Nonlinearity of soil materials is simulated by incremental plasticity models to allow for modeling permanent deformation and for generation of hysteretic damping. In addition, OpenSeesPL allows including user-defined soil materials.

OpenSeesPL allows for convenient pre-processing and graphical visualization of the analysis results including the deformed mesh, ground response time histories and pile responses. OpenSeesPL makes it possible for geotechnical and structural engineers/researchers to quickly build a model, run FE analysis and evaluate the performance of the pile-ground system.

OpenSeesPL was developed by Dr. Jinchi Lu (jinlu@ucsd.edu), Dr. Ahmed Elgamal (elgamal@ucsd.edu), and Dr. Zhaohui Yang (yangaaa@gmail.com). The OpenSees geotechnical simulation capabilities were developed by Dr. Zhaohui Yang and Dr. Ahmed Elgamal. For more information, please visit <http://cyclic.ucsd.edu/opensees/>. OpenSeesPL operates in SI and English units.

NOTE: Seismically-induced deformations are complex mechanisms. Much expertise and sound engineering judgment are necessary in interpreting the OpenSeesPL computational results.

1.2 System Requirements

OpenSeesPL runs on PC compatible systems using Windows (NT V4.0, 2000, XP, Vista or Windows 7). The system should have a minimum hardware configuration appropriate to the particular operating system.

Internet Explorer 3.0 or above (or compatible Browser) with Java Applet enabled is needed to view the graphic results. For best results, your system's video should be set to 1024 by 768 or higher.

1.3 Installation

After downloading the OpenSeesPL installation file (OpenSeesPL_Setup.exe), double-click on the icon and the installation procedure will start. Once installed, the default case in OpenSeesPL is a good way to go through the steps involved in conducting an OpenSeesPL analysis. The interface will allow the user to prepare and save an input file, to run the analysis, and to display the response.

Note: Tcl/tk 8.5 must be installed in order to run OpenSeesPL. Please restart the computer after the installation of Tcl/tk 8.5 for the change to take effect.

To download Tcl/tk 8.5, please visit <http://cyclic.ucsd.edu/openseespl/>.

1.4 Acknowledgments

OpenSeesPL is based on research underway since the early 1990s, and a partial list of related publications is included in the Appendix section. The OpenSeesPL graphical interface is written in Microsoft Visual C++ 2005 with the Microsoft Foundation Class (MFC) libraries. The Java Applet package used to display graphical results in OpenSeesPL is obtained from the website <http://ptolemy.eecs.berkeley.edu/>. GIF images are generated with GNUPLOT for MS-Windows 32 bit Version 3.7, available at <http://www.gnuplot.org/>.

2. Getting Started

2.1 Start-Up

On Windows start OpenSeesPL from the Start button, or from an icon on your desktop. To Start OpenSeesPL from the Start button:

1. Click Start, and then select Programs.
2. Select the OpenSeesPL folder
3. Click on OpenSeesPL

The OpenSeesPL main window is shown in Figure 2.1.

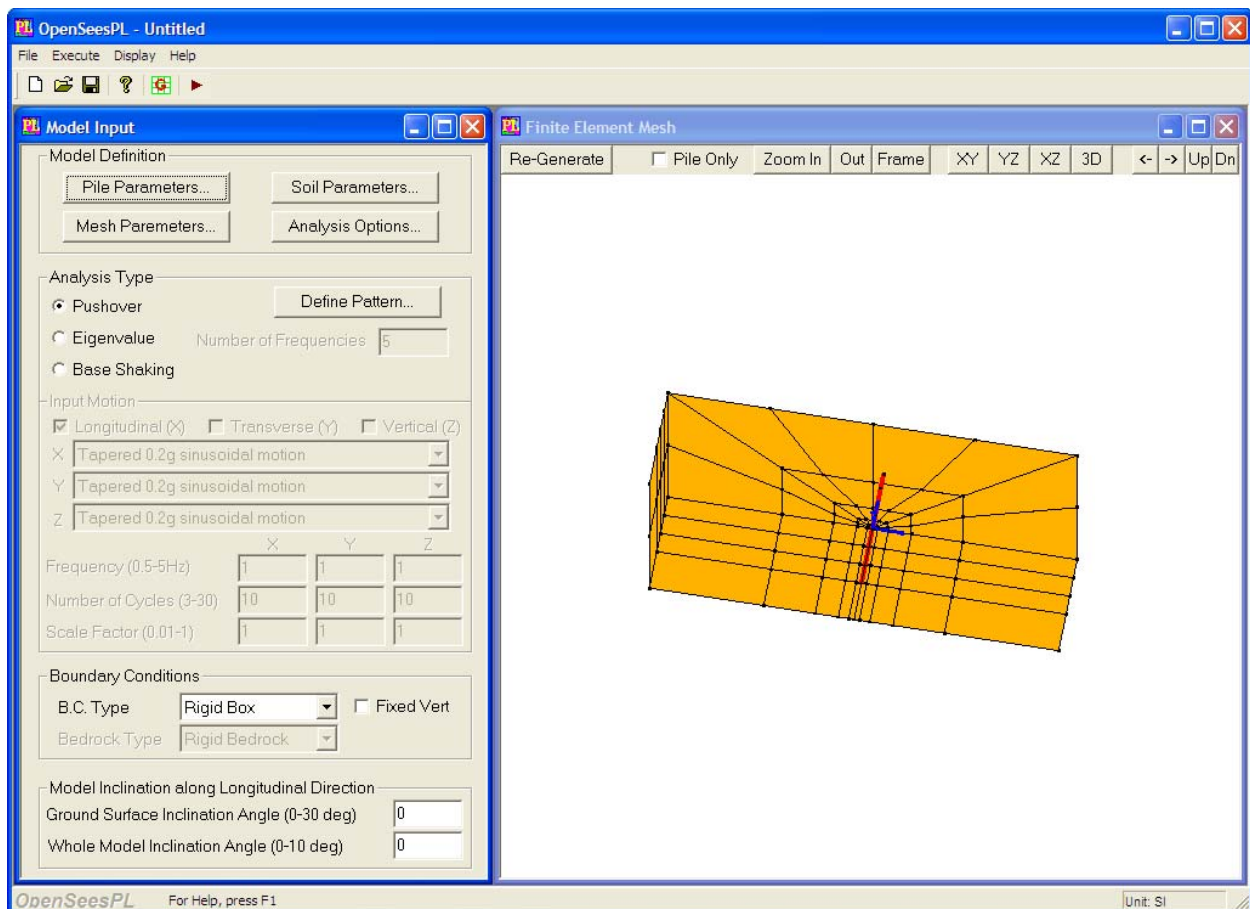


Figure 2.1: OpenSeesPL main window.

2.2 Interface

There are 3 main regions in the OpenSeesPL window – menu bar, the model input window, and the finite element mesh window.

2.2.1 Menu Bar

The menu bar, shown in Figure 2.2, offers rapid access to most of OpenSeesPL's main features.

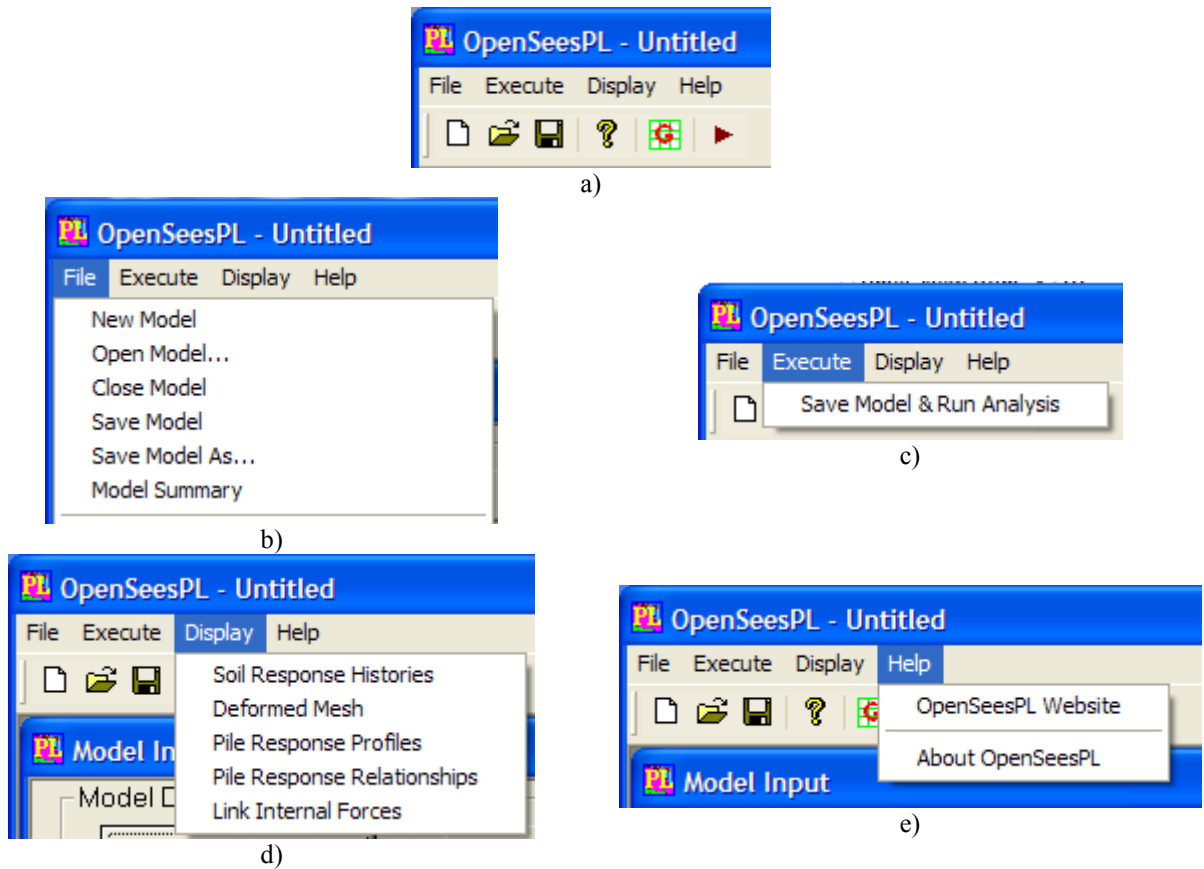


Figure 2.2: OpenSeesPL's menu bar and submenu bars: a) menu bar; b) menu File; c) menu Execute; d) menu Display; and e) menu Help.

OpenSeesPL's main features are organized into the following menus:

- **File:** Controls reading, writing and printing of model definition parameters, and exiting OpenSeesPL.
- **Execute:** Controls running analyses.
- **Display:** Controls displaying of the analysis results.
- **Help:** Visits OpenSeesPL website and display the copyright info (Figure 2.3).



Figure 2.3: OpenSeesPL copyright message.

2.2.2 Model Input Window

The model input window controls definitions of the model and analysis options, which are organized into four regions (Figure 2.1):

- **Model Definition:** Controls definitions of pile and soil strata including material properties. Meshing parameters are also defined.
- **Analysis Types:** Controls analysis options: pushover analysis, Eigenvalue analysis or base shaking simulation.
- **Boundary Conditions:** Controls boundary conditions.
- **Model Inclination:** Controls the inclination angles for the ground surface and the whole model.

2.2.3 Finite Element Mesh Window

The finite element mesh window (Figure 2.1) displays the mesh generated. Once the mesh window is focused, the mesh can be rotated by dragging the mouse, moved in 4 directions by pressing keys of LEFT ARROW, RIGHT ARROW, UP ARROW or DOWN ARROW

respectively. The view can be zoomed in (by pressing key 'F9'), out (by pressing key 'F10') or frame (by pressing key 'F11').

To display a 2D view, press key 'F2' (for Plane XY, where X is the longitudinal direction, Y the transverse direction), 'F3' (for Plane YZ, where Z is the vertical direction) or 'F4' (for Plane XZ). An isometric view of the mesh can be achieved by pressing key 'F5'.

Alternatively, users can press the corresponding button shown in Figure 2.4.



Figure 2.4: Buttons available in the Finite Element Mesh window.

3. Pile Model

To define pile geometry, click **Pile Parameters** in the **Model Input** window. The pile geometry is defined by the following parameters (Figure 3.1):

The 'Pile' dialog box is divided into several sections:

- Pile Section:** Includes a dropdown for 'Pile Type' (set to 'Circular'), and input fields for 'Diameter/Side Length (D)' (1 [m]), 'Total Pile Length' (12 [m]), and 'Pile Length above Surface' (6 [m]).
- Pile Head:** Includes radio buttons for 'Fixed' (selected) and 'Free/Pinned', and input fields for 'Pile Head Mass' (0 [ton]) and 'Axial Load' (0 [kN]).
- Pile Group:** A checkbox labeled 'Pile Group' is present. Below it, a 'Group Info' section contains input fields for 'Number of Piles' (3), 'Spacing (xD)' (3), and 'Y-Dir.' (3).
- Linear Beam Properties:** Includes radio buttons for 'Linear Beam Element' (selected), 'Nonlinear Beam Element - Aggregator Section', and 'Nonlinear Beam Element - Fiber Section'. The 'Linear Beam Element' section contains input fields for 'Young's Modulus' (30000000 [kPa]), 'Moment of Inertia' (0.0490873 [m4]), and 'Mass Density' (0 [ton/m3]), along with a 'Re-Calculate' button.
- Buttons:** 'OK' and 'Cancel' buttons are at the bottom.

Figure 3.1: Definition of pile model.

3.1 Pile Parameters

Parameters to define the geometrical configurations of the pile include (refer to Figure 3.1):

Pile Type The pile cross section can be circular or square.

Pile Diameter/Side Length (D) The diameter (if a circular pile is chosen), or the side length (if a square pile is chosen) of the pile cross section. The value entered must be greater than zero.

Total Pile Length The total length of the pile. The value entered must be greater than zero.

Pile Length above Surface The height of the pile above the ground surface. The value entered must be greater than zero.

Fixed or Free Head Free Head or Fixed Head can be chosen.

Pile Head Mass The mass applied at the pile head.

Axial Load The axial load applied at the pile head (positive as compression).

If checkbox **Pile Group** is enabled (note that the pile group option might not be available in the version you have), users can activate pile group by checking **Pile Group**. Please see Chapter 8 for the detailed information.

3.2 Pile Properties

In OpenSeesPL, the element types available for the pile are **elasticBeamColumn**, which represents elastic beam-column element, and **nonlinearBeamColumn**, which represents a nonlinear beam-column element based on the non-iterative (or iterative) force formulation. Detail information can be found in the OpenSees User Manual (Mazzoni et al. 2006).

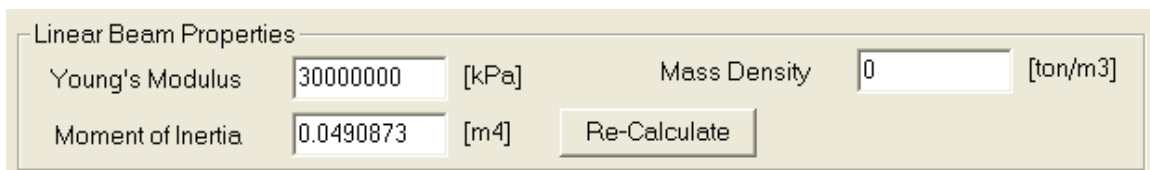
3.2.1 Linear Beam Element

The material properties of the pile for the linear beam element (**elasticBeamColumn**) are defined by the following parameters (Figure 3.2):

Young's Modulus (E) Young's Modulus of the pile.

Mass Density The Mass Density of the pile.

Moment of Inertia (I) The Moment of Inertia of the pile. This can be specified directly or calculated based on the pile diameter.



Linear Beam Properties			
Young's Modulus	<input type="text" value="30000000"/>	[kPa]	Mass Density <input type="text" value="0"/> [ton/m3]
Moment of Inertia	<input type="text" value="0.0490873"/>	[m4]	<input type="button" value="Re-Calculate"/>

Figure 3.2: Definition of linear pile properties.

3.2.2 Nonlinear Beam Element

OpenSees uses the **Section** command to define the nonlinear beam-column element (a section defines the stress resultant force-deformation response at a cross section of a beam-column element). Two types of sections are available in OpenSeesPL for the nonlinear beam element (**nonlinearBeamColumn**): **Aggregator** Section or **Fiber** Section. Detail information can be found in the OpenSees User Manual (Mazzoni et al. 2006).

3.2.2.1 Aggregator Section

The **Aggregator** Section is defined by the following parameters in OpenSeesPL (Figure 3.3):

Flexural Rigidity \mathbf{My} & \mathbf{Mz} The Flexural Rigidity of the pile which is equal to the product of Young's Modulus (E) and the Moment of Inertia (I). \mathbf{My} corresponds the moment-curvature about section local y-axis and \mathbf{Mz} corresponds the moment-curvature about section local z-axis.

Yield Moment The Yield Moment of the pile.

Kinematic Hardening Parameter The Kinematic Hardening Modulus.

Isotropic Hardening Parameter The Isotropic Hardening Modulus.

Shear Rigidity \mathbf{Vy} & \mathbf{Vz} The Shear Rigidity of the pile which is equal to the product of the Shear Modulus (G) and the area of the pile cross section (A). \mathbf{Vy} corresponds the shear force-deformation along section local y-axis and \mathbf{Vz} corresponds the shear force-deformation along section local z-axis.

Torsional Rigidity \mathbf{T} The Torsional Rigidity of the pile which is equal to the product of the Shear Modulus (G) and J .

Axial Rigidity \mathbf{P} The Axial Rigidity of the pile which is equal to the product of Young's Modulus (E) and the area of the pile cross section (A).

Parameter	Value	Unit
My & Mz: Flexural Rigidity EI	158600	[kN-m ²]
Yield Moment	1200	[kN-m]
Kinematic Hardening Parameter	0	[kN-m]
Isotropic Hardening Parameter	0	[kN-m ²]
Vy & Vz: Shear Rigidity GA	3378000	[kN]
T: Torsional Rigidity GJ	42200	[kN-m ²]
P: Axial Rigidity EA	8785000	[kN]

Figure 3.3: Definition of nonlinear pile properties (Aggregator Section).

3.2.2.2 Fiber Section

The dialog of defining Fiber Section is shown in Figure 3.4 (the Fiber Section is only available to circular pile in this version of OpenSeesPL). Two materials are available: **Concrete01** and **Steel01** in this version of OpenSeesPL. **Concrete01** (Figure 3.6) is defined by the following parameters (for **Core** and **Cover**, see Figure 3.10):

Concrete Compressive Strength The concrete compressive strength at 28 days (\$fpc in Figure 3.6).

Concrete Strain at Maximum Strength The concrete strain at maximum strength (\$epsc0 in Figure 3.6).

Concrete Crushing Strength The concrete crushing strength (\$fpcu in Figure 3.6).

Concrete Strain at Crushing Strength The concrete strain at crushing strength (\$epsU in Figure 3.6).

Note that the compressive concrete parameters should be input as negative values. Typical hysteretic stress-strain relation of the Concrete01 material is shown in Figure 3.7).

Steel01 is defined by the following parameters (Figure 3.8 and Figure 3.9):

Yield Strength The yield strength of steel.

Initial Elastic Tangent The initial elastic tangent of steel.

Strain-hardening Ratio The strain-hardening ratio (ratio between post-yield tangent and initial elastic tangent)

Patch (Figure 3.10) is defined by the following parameters (for both **Core** and **Cover**):

Number of Subdivisions (fibers) in the Circumferential Direction The number of subdivisions (fibers) in the circumferential direction of the pile circular cross section (\$numSubdivCirc in Figure 3.11).

Number of Subdivisions (fibers) in the Radial Direction The number of subdivisions (fibers) in the radial direction of the pile circular cross section (\$numSubdivRad in Figure 3.11).

Internal Radius The internal radius of the patch (\$intRad in Figure 3.11).

External Radius The external radius of the patch (\$extRad in Figure 3.11).

The values of \$yCenter and \$zCenter (y & z-coordinates of the center of the circle) as shown in Figure 3.11 are zeros. And the \$startAng (starting angle) and \$endAng (ending angle) are set to 0 and 360 degrees respectively in OpenSeesPL since only a full mesh is available for fiber section nonlinear beam element).

Layer is defined by the following parameters (Figure 3.12):

Number of Reinforcing Bars along Layer The number of reinforcing bars along layer (\$numBars in Figure 3.12).

Area of Individual Reinforcing Bar The area of individual reinforcing bar.

Radius of Reinforcing Layer The radius of reinforcing layer (\$radius in Figure 3.12) .

The values of \$yCenter and \$zCenter (y & z-coordinates of the center of the circle) as shown in Figure 3.12 are zeros. And the \$startAng (starting angle) and \$endAng (ending angle) are set to 0 and 360 degrees respectively in OpenSeesPL since only a full mesh is available for fiber section nonlinear beam element).

Material		Core	Cover	
Concrete01:	Concrete Compressive Strength	-29000	-22332	[kPa]
	Concrete Strain at Maximum Strength	-0.004	-0.002	
	Concrete Crushing Strength	-22332	0	[kPa]
	Concrete Strain at Crushing Strength	-0.014	-0.006	
Steel01:	Yield Strength	460000		[kPa]
	Initial Elastic Tangent	200000000		[kPa]
	Strain-hardening Ratio	0.01		

Circular Shape		Core	Cover	
Patch:	Number of Subdivisions (fibers) in the Circumferential Direction	16	16	
	Number of Subdivisions (fibers) in the Radial Direction	4	4	
	Internal Radius	0	0.457	[m]
	External Radius	0.457	0.61	[m]
Layer:	Number of Reinforcing Bars along Layer	16		
	Area of Individual Reinforcing Bar	0.00014		[m ²]
	Radius of Reinforcing Layer	0.457		[m]

OK Cancel View Moment-Curvature Response

Figure 3.4: Definition of nonlinear pile properties (Fiber Section).

The moment-curvature response for the pile is shown in Figure 3.5 (for default steel and concrete parameters).

Material: Concrete

	Core	Cover	
Compressive Strength	-29000	-22332	[kPa]
Strain at Max. Strength	-0.004	-0.002	
Crushing Strength	-22332	0	[kPa]
Strain at Crushing Strength	-0.014	-0.006	

Material: Steel

Yield Strength	460000	[kPa]
Initial Elastic Tangent	2000000000	[kPa]
Strain-hardening Ratio	0.01	

Patch

	Core	Cover	
Number of Fibers in Circumferential Direction	16	16	
Number of Fibers in Radial Direction	4	4	
Internal Radius	0	0.457	[m]
External Radius	0.457	0.61	[m]

Layer

Number of Reinforcing Bars along Layer	16	
Area of Individual Reinforcing Bar	0.00014	[m ²]
Radius of Reinforcing Layer	0.457	[m]

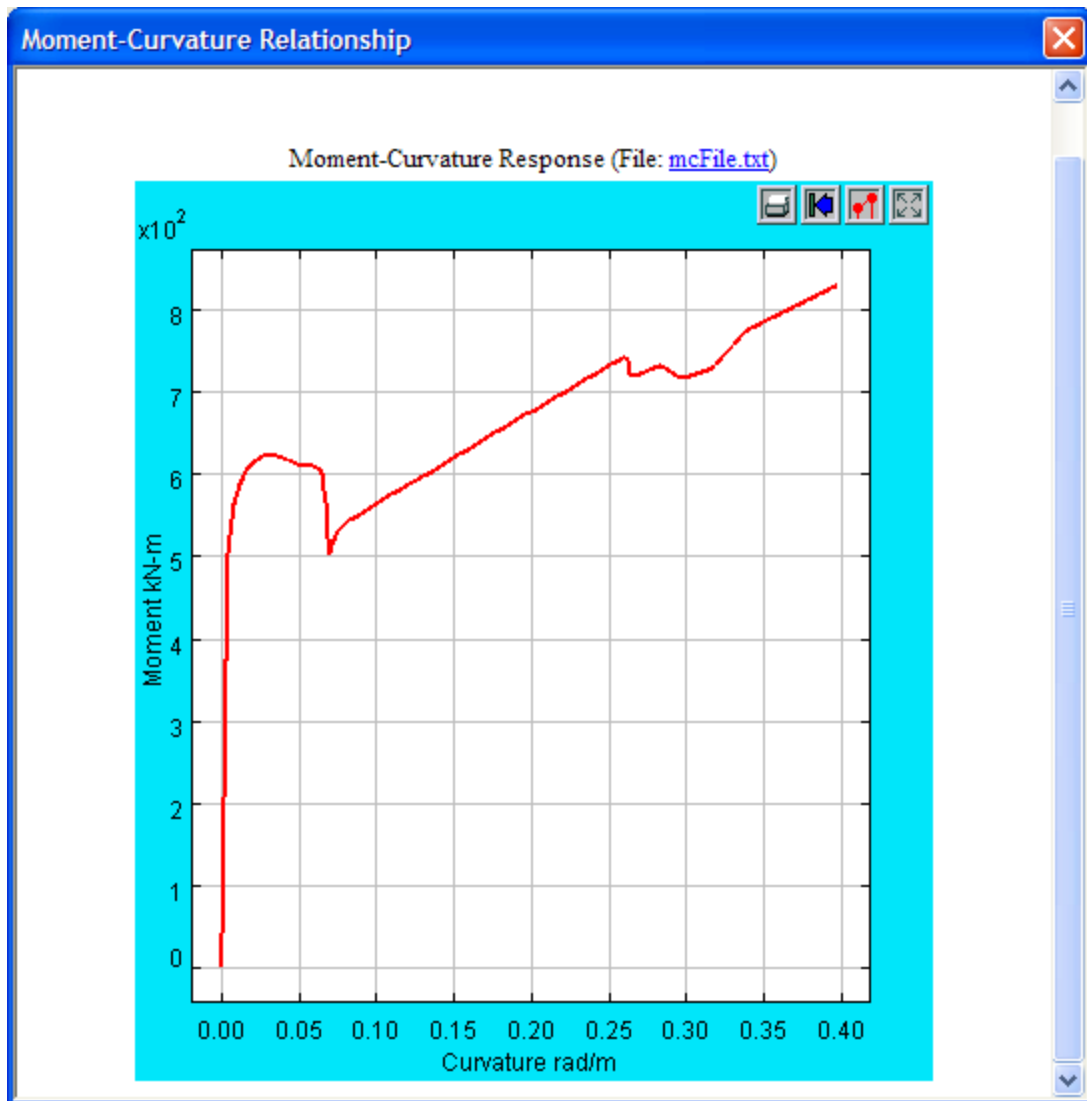
Axial Load	100	[kN]
Maximum Curvature	0.3937	[rad/m]
Number of Analysis Increments to Max. Curvature	100	

Re-calculate Response

OK

a)

13



b)

Figure 3.5: Moment-curvature response for the pile (with default steel and concrete parameters)

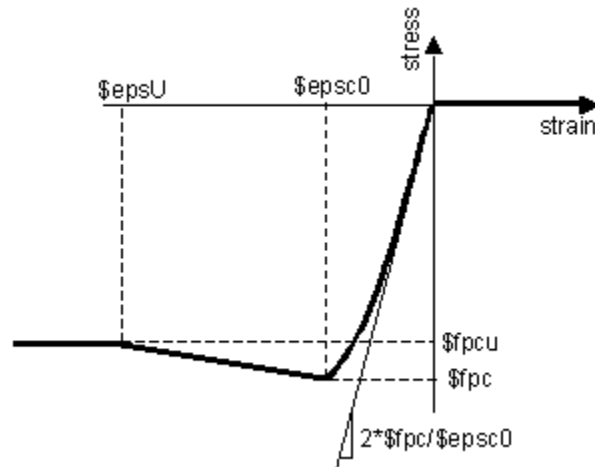


Figure 3.6: Material Parameters of the Concrete01 material (Mazzoni et al. 2006) .

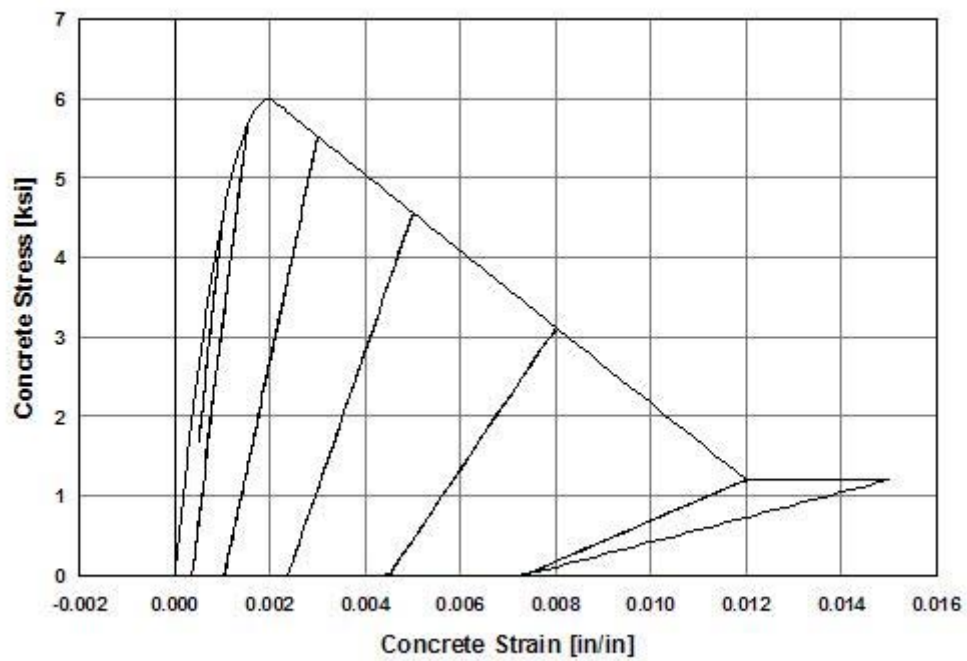


Figure 3.7: Typical hysteretic stress-strain relation of the Concrete01 material (Mazzoni et al. 2006) .

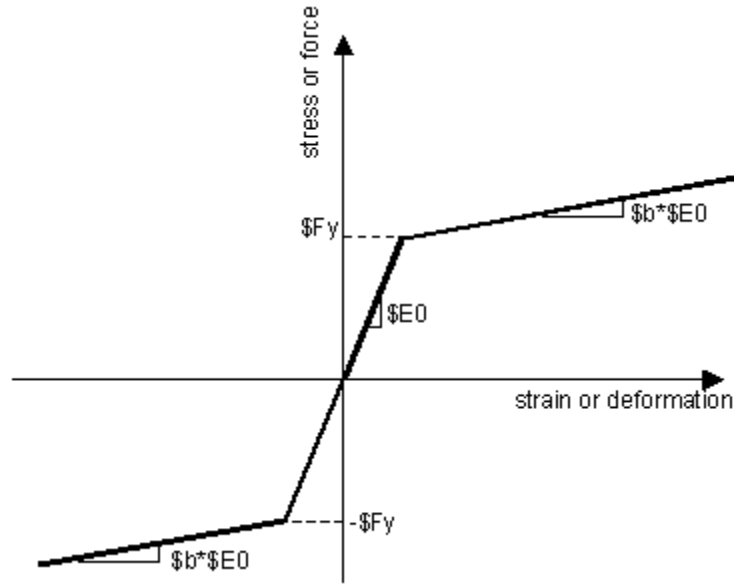


Figure 3.8: Material Parameters of the Steel01 material (Mazzoni et al. 2006) .

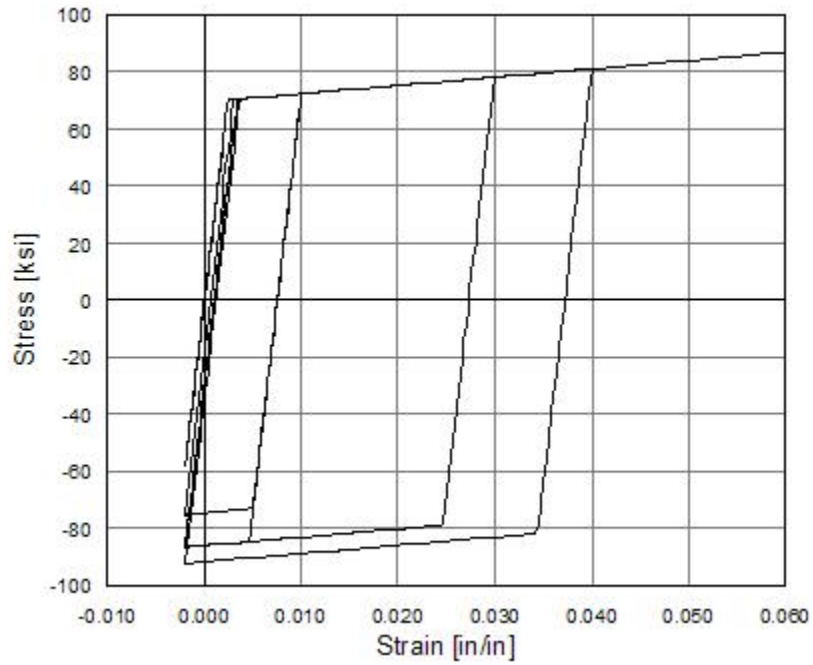


Figure 3.9: Typical hysteretic behavior of model with Isotropic hardening of the Steel01 material (Mazzoni et al. 2006) .

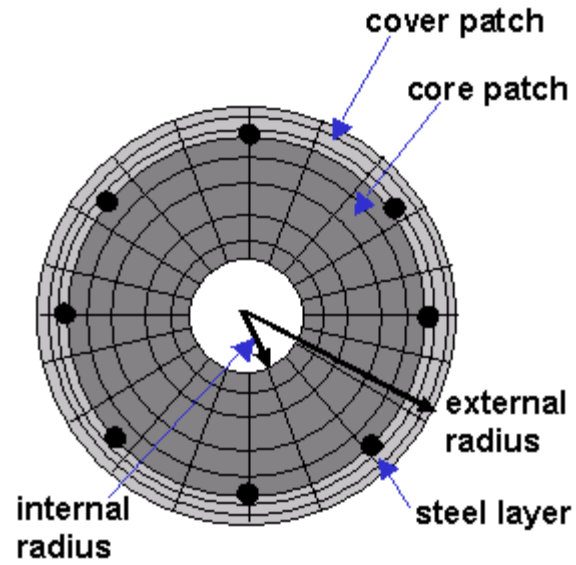


Figure 3.10: Schematic of fiber section definition for a circular cross section (Mazzoni et al. 2006) .

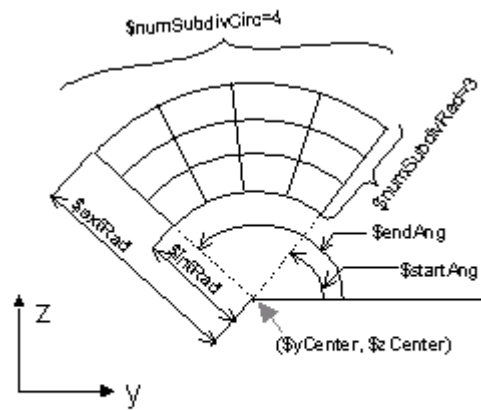


Figure 3.11: Schematic of patch definition for a circular cross section (Mazzoni et al. 2006)

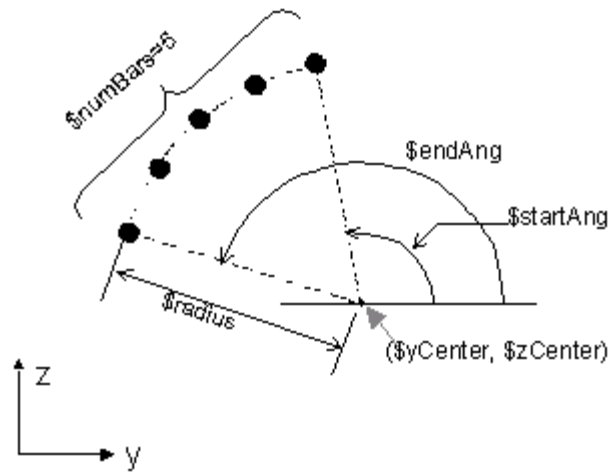


Figure 3.12: Schematic of layer definition for a circular cross section (Mazzoni et al. 2006)

4. Soil Parameters

To define soil strata, click **Soil Parameters** in the **Model Input** window (Figure 4.1).

Soil Layer # (From topdown)	Thickness [m]	Soil Type	Residual Shear Strength [kPa]	P	L	C
1:	10	22: U-Clay2 (PressureIndependentMultiYield)...	0.2	<input checked="" type="radio"/>	<input type="radio"/>	<input type="radio"/>
2:	0		0.2	<input type="radio"/>	<input type="radio"/>	<input type="radio"/>
3:	0		0.2	<input type="radio"/>	<input type="radio"/>	<input type="radio"/>
4:	0		0.2	<input type="radio"/>	<input type="radio"/>	<input type="radio"/>
5:	0		0.2	<input type="radio"/>	<input type="radio"/>	<input type="radio"/>
6:	0		0.2	<input type="radio"/>	<input type="radio"/>	<input type="radio"/>
7:	0		0.2	<input type="radio"/>	<input type="radio"/>	<input type="radio"/>
8:	0		0.2	<input type="radio"/>	<input type="radio"/>	<input type="radio"/>
9:	0		0.2	<input type="radio"/>	<input type="radio"/>	<input type="radio"/>
10:	0		0.2	<input type="radio"/>	<input type="radio"/>	<input type="radio"/>

☐ Saturated Soil Analysis Water Table Depth (Below Ground Surface) [m]

☐ Activate Pile Zone ☐ Top Layer Same as Soil

☐ Activate Interfacing Layer Thickness (xD) ☐ Top Layer Same as Soil

☐ Activate Outermost Zone Thickness [m] ☐ Top Layer Same as Soil

☐ Activate Tension Cutoff for Cohesive Soil

Note: P, L and C represents Parabolic, Linear increasing and Constant variation of soil modulus with depth, respectively.

Figure 4.1: Soil strata definition.

4.1 Soil Parameters

A total of 10 soil strata can be defined in OpenSeesPL (Figure 4.1). The profile of the soil strata can be defined by using the follow parameters:

Thickness The thickness for a soil layer. Definitions following a zero height will be ignored. In other words, the total number of soil layers in use will be equal to the number of the last soil layer that contain no zero values, e.g., if you need 5 strata, enter nonzero heights for Stratum #1 through Stratum #5.

To perform a liquefaction analysis, check the checkbox **Saturated Soil Analysis** (Figure 4.1) and specify the water table depth:

Water Table Depth The Water Table Depth refers to the depth below ground surface.(e .g., 0.0 corresponds to a fully saturated soil profile, 1.0 is 1m below ground surface). Dry sites should specify water table depth to be equal to the entire model depth.

4.1.1 Analysis Options

First, some important master control options are defined by clicking **Analysis Options** as shown in Figure 2.1. This will display the interface shown in Figure 4.2. Here you can:

1. Select to keep the soil properties as defined by their linear properties, or opt to conduct nonlinear soil computations (note that the default is Linear),
2. Select among a number of available Brick elements in OpenSees,
3. Apply own weight of the soil using a global lateral stress coefficient, and a single value of Young's modulus that is user defined (this will reduce initial shear stresses in the mesh due to own weight application, but generally will have minimal impact on the subsequent earthquake computations anyway),
4. Apply own weight of the soil using a global permeability (horizontal & vertical), e.g., one can specify a large permeability value for the application of own weight in a saturated soil analysis,
5. by clicking **Rayleigh Damping** (Figure 4.3) you can change the viscous damping characteristics of the model, and
6. by clicking **OpenSees Parameters** (Figure 4.4) you can OpenSees analysis parameters (advanced feature, please exercise with care).

4.1.2 Additional Viscous Damping

In OpenSeesPL, additional viscous Rayleigh-type damping is available of the form:

$$\mathbf{C} = A_m \mathbf{M} + A_k \mathbf{K}$$

where \mathbf{M} is the mass matrix, \mathbf{C} is the viscous damping matrix, \mathbf{K} is the initial stiffness matrix. A_m and A_k are two user-specified constants.

The damping ratio curve $\xi(f)$ is calculated based on the following equation:

$$\xi = \frac{A_m}{4\pi f} + A_k \pi f$$

where f is frequency.

Figure 4.2: Analysis options.

(1) Specification of A_m and A_k By Defining Damping Ratios

The user can define damping coefficients (Figure 4.3) by specifying two frequencies, f_1 and f_2 (must be between 0.1 and 50 Hz), and two damping ratios, ξ_1 and ξ_2 (suggested values are between 0.2% and 20%).

The Rayleigh damping parameters A_m and A_k are obtained by solving the follow equations simultaneously:

$$\xi_1 = \frac{A_m}{4\pi f_1} + A_k \pi f_1$$

$$\xi_2 = \frac{A_m}{4\pi f_2} + A_k \pi f_2$$

(2) Direct Specification of A_m and A_k :

The user can also directly define Rayleigh damping coefficients A_m and A_k (Figure 4.3).

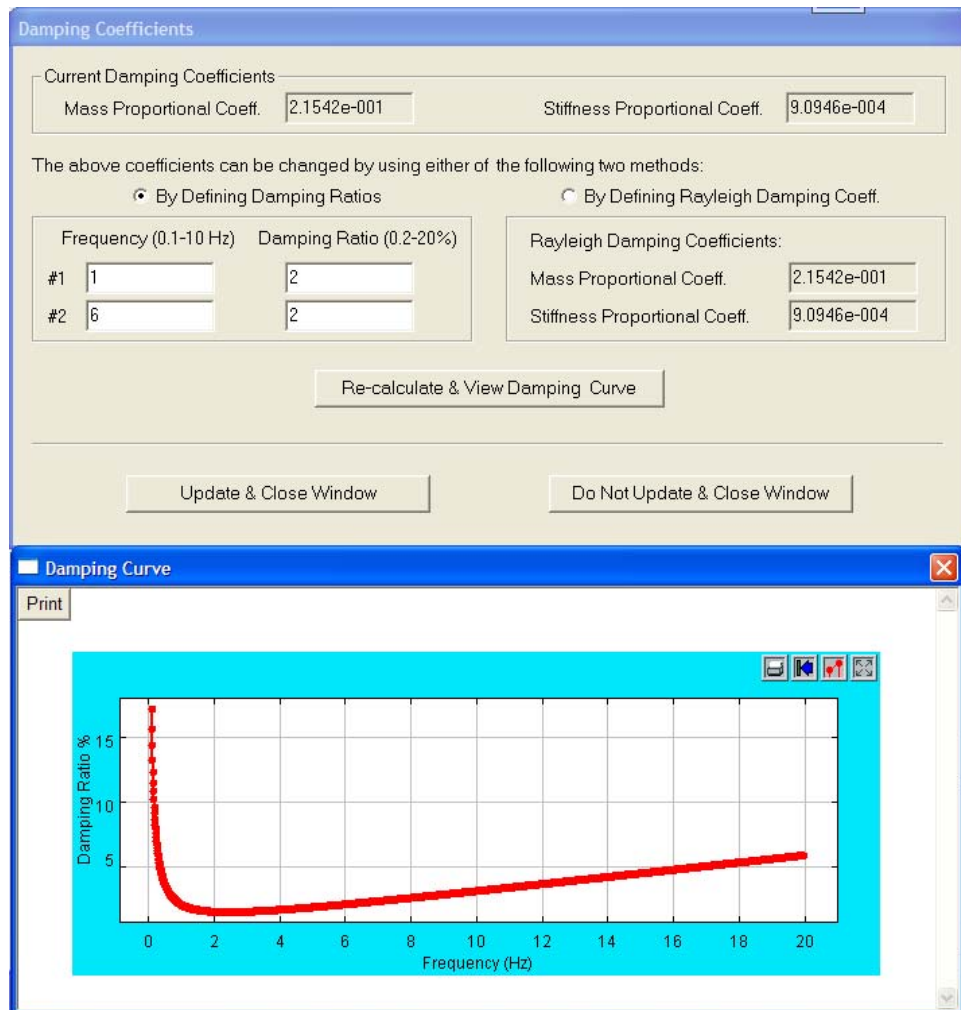


Figure 4.3: Rayleigh damping coefficients.

OpenSees Parameters

Parameters for Dry Soil Analysis

1st Run

Tolerance \$tol (for OpenSees command: test NormDisplncr) Max. number of iterations \$maxNumIter

Number of steps (for OpenSees command: analyze) Time step \$dt

Run for Horizontal Gravity Application (Activated if Model Inclination Degree is not zero)

Number of steps for linearly increasing loading part Time step \$dt

Number of steps for constant loading part afterwards

2nd Run

Number of steps (for OpenSees command: analyze) Time step \$dt

3rd Run

Tolerance \$tol (for OpenSees command: test NormDisplncr) Max. number of iterations \$maxNumIter

Number of steps for linearly increasing loading part Time step \$dt

Number of steps for constant loading part afterwards

Last Run

Tolerance \$tol (for OpenSees command: test NormDisplncr) Max. number of iterations \$maxNumIter

Newmark Integrator \$gamma Time step \$dt

Figure 4.4: OpenSees parameters.

4.2 Soil Properties

4.2.1 Theory of Soil Models

In OpenSees, the soil model (Figure 4.5) for cohesionless soils is developed within the framework of multi-yield-surface plasticity (e.g., Prevost 1985). In this model, emphasis is placed on controlling the magnitude of cycle-by-cycle permanent shear strain accumulation (Figure 4.6) in clean medium to dense sands (Parra 1996; Yang 2000; Yang et al. 2003). Furthermore, appropriate loading-unloading flow rules were devised to reproduce the observed strong dilation tendency, and resulting increase in cyclic shear stiffness and strength (the “Cyclic Mobility” mechanism). The material types for the cohesionless soils in OpenSees are called **PressureDependMultiYield** and **PressureDependMultiYield02**.

Clay material is modeled as a nonlinear hysteretic material (Parra 1996; Yang 2000; Yang et al. 2003) with a Von Mises multi-surface (Iwan 1967; Mroz 1967) kinematic plasticity model (Figure 4.7). In this regard, focus is on reproduction of the soil hysteretic elasto-plastic shear response (including permanent deformation). In this material, plasticity is exhibited only in the deviatoric stress-strain response. The volumetric stress-strain response is linear-elastic and is independent of the deviatoric response. This constitutive model simulates monotonic or cyclic response of materials whose shear behavior is insensitive to the confinement change. Plasticity is formulated based on the multi-surface (nested surfaces) concept, with an associative flow rule (according to the well-known Provost approach). In the clay model, the nonlinear shear stress-strain back-bone curve is represented by the hyperbolic relation (Kondner 1963), defined by the two material constants, low-strain shear modulus and ultimate shear strength. The material type for the cohesive soils in OpenSees is called **PressureIndependentMultiYield**.

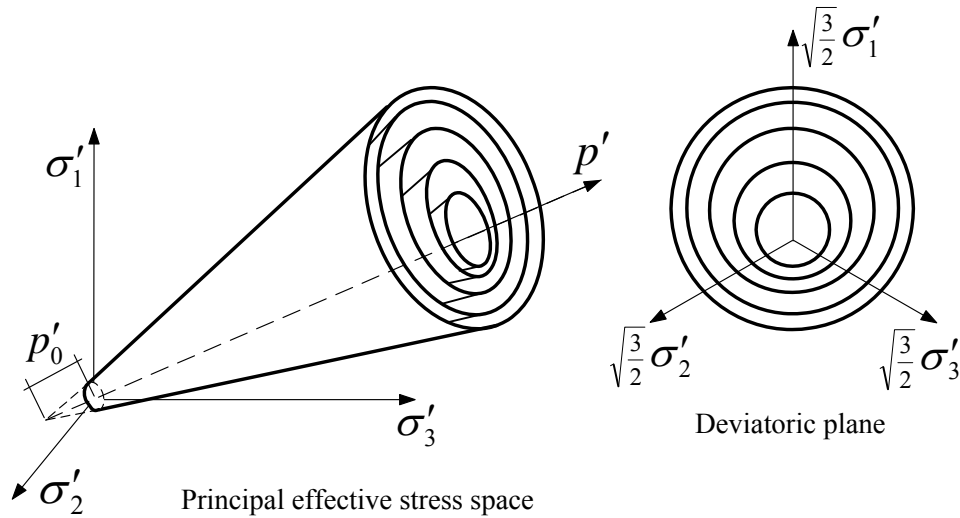


Figure 4.5: Multi-yield surfaces in principal stress space and deviatoric plane (Prevost 1985; Parra 1996; Yang 2000)

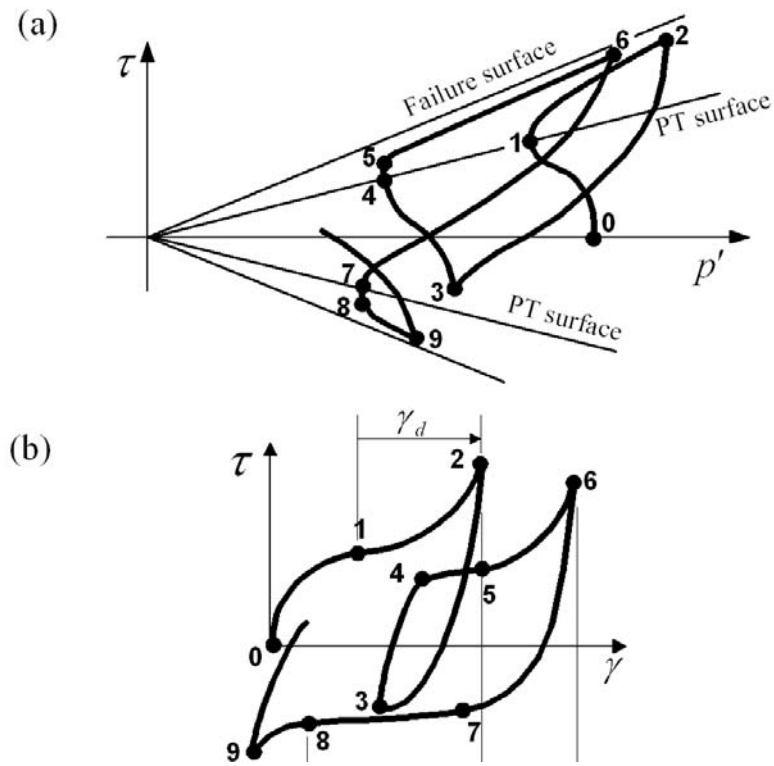
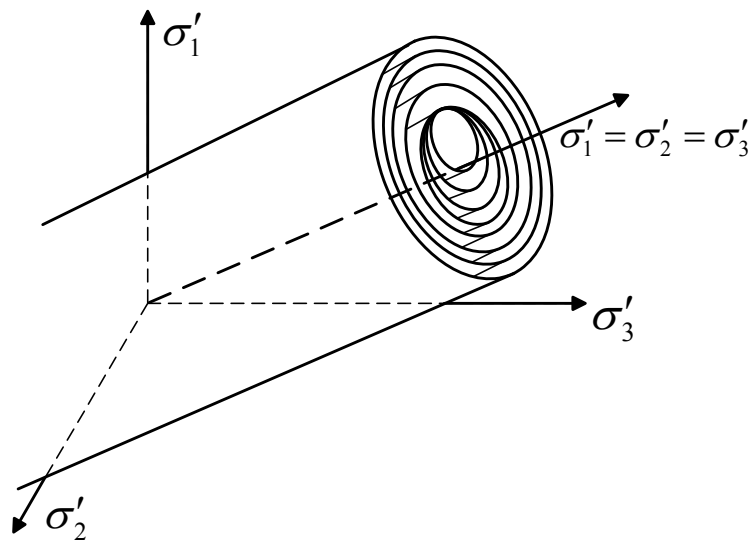
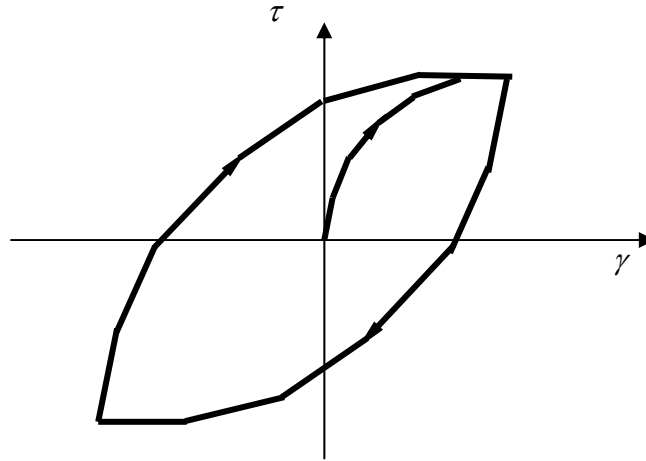


Figure 4.6: Shear-effective confinement and shear stress-strain response (Yang and Elgamal 2002; Yang et al. 2003).



(a) Von Mises multi-surface.



(b) Hysteretic shear response.

Figure 4.7: Von Mises multi-surface kinematic plasticity model (Yang 2000; Yang et al. 2003).

4.2.2 Predefined Materials

As shown in Figure 4.1, the soil materials can be selected from an available menu of cohesionless and cohesive soil materials (Figure 4.8). There are 18 predefined materials using the **PressureDependMultiYield** soil model. Basic model parameter values for these materials are listed in Table 4.1.

If ‘Cohesionless very loose’ is chosen, the user is allowed to define the residual shear strength (0.2 kPa is specified by default). The cohesionless very loose soil is same as the cohesionless loose soil except the user is allowed to specify the residual shear strength for the very loose one.

In addition, user-defined cohesionless and cohesive soil materials (**U-Sand1A**, **U-Sand1B**, **U-Clay1**, **U-Clay2**, **U-Sand2A**, and **U-Sand2B**) are also available to choose. U-Sand1A and U-Sand1B use **PressureDependMultiYield** model while U-Sand2A and U-Sand2B use **PressureDependMultiYield02** model.

As shown in Figure 4.1, parabolic variation of soil modulus with depth is used if **P** is selected. Linear variation of soil modulus with depth is used if **L** is selected. And the constant soil modulus with depth is used if **C** is selected;

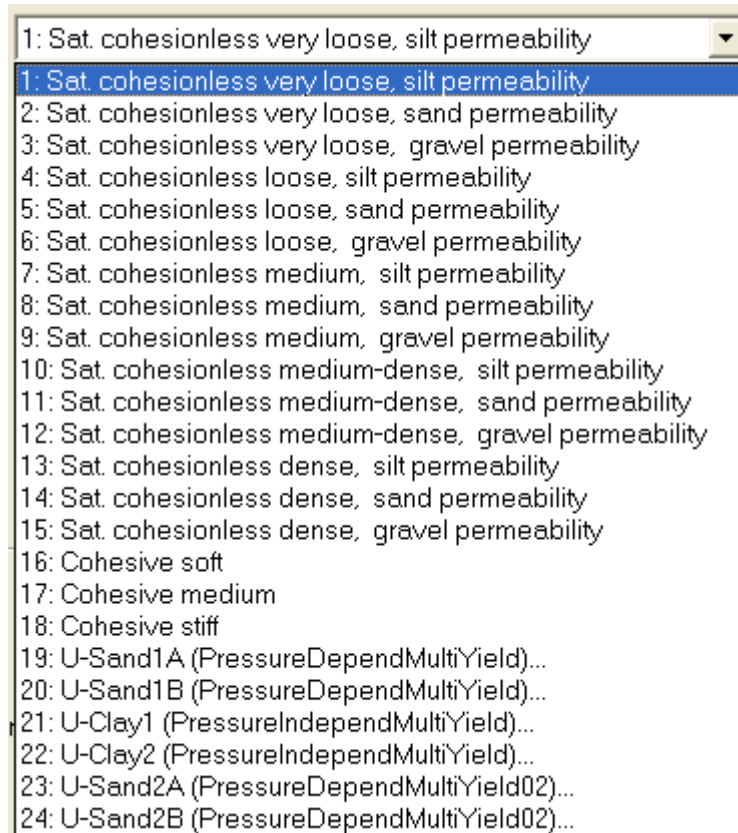


Figure 4.8: Soil materials in OpenSeesPL.

Table 4.1: Predefined soil materials in OpenSeesPL

Cohesionless Soil	Reference shear modulus G_r (kPa, at $p'_r=80\text{kPa}$)¹	Reference bulk modulus B_r (kPa, at $p'_r=80\text{kPa}$)	Friction angle ϕ (degrees)²	Permeability coeff.³ (m/s)	Mass density⁴ (ton/m³)
Very loose, silt permeability	5.5E+04	1.5E+05	29	1.0E-07	1.7
Very loose, sand permeability	5.5E+04	1.5E+05	29	6.6E-05	1.7
Very loose, gravel permeability	5.5E+04	1.5E+05	29	1.0E-02	1.7
Loose, silt permeability	5.5E+04	1.5E+05	29	1.0E-07	1.7
Loose, sand permeability	5.5E+04	1.5E+05	29	6.6E-05	1.7
Loose, gravel permeability	5.5E+04	1.5E+05	29	1.0E-02	1.7
Medium, silt permeability	7.5E+04	2.0E+05	33	1.0E-07	1.9
Medium, sand permeability	7.5E+04	2.0E+05	33	6.6E-05	1.9
Medium, gravel permeability	7.5E+04	2.0E+05	33	1.0E-02	1.9
Medium-dense, silt permeability	1.0E+05	3.0E+05	37	1.0E-07	2.0
Medium-dense, sand permeability	1.0E+05	3.0E+05	37	6.6E-05	2.0
Medium-dense, gravel permeability	1.0E+05	3.0E+05	37	1.0E-02	2.0
Dense, silt permeability	1.3E+05	3.9E+05	40	1.0E-07	2.1
Dense, sand permeability	1.3E+05	3.9E+05	40	6.6E-05	2.1
Dense, gravel permeability	1.3E+05	3.9E+05	40	1.0E-02	2.1
Cohesive Soil	Shear modulus G (kPa)	Bulk modulus B (kPa)	Cohesion c (kPa)⁵	Permeability coeff.³ (m/s)	Mass density⁴ (ton/m³)
Soft	1.3E+04	6.5E+04	18.0	1.0E-09	1.3
Medium	6.0E+04	3.0E+05	37.0	1.0E-09	1.5
Stiff	1.5E+05	7.5E+05	75.0	1.0E-09	1.8

1. Where p'_r is the reference mean effective confining pressure at which soil appropriate soil properties are defined.

2. Friction angles for cohesionless soils are based on Table 7.4 (p.425) of Das, B.M. (1983).

3. Permeability values are based on Fig. 7.6 (p.210) of Holtz and Kovacs (1981).

4. Mass density is based on Table 1.4 (p.10) of Das (1995).

5. Cohesion for cohesive soils are based on Table 7.5 (p.442) of Das (1983).

Backbone Curve

At a constant confinement p' , the shear stress τ (octahedral) - shear strain γ (octahedral) nonlinearity is defined by a hyperbolic curve (backbone curve, see Figure 4.9):

$$\tau = \frac{G_r \gamma}{1 + \frac{\gamma}{\gamma_r}} \quad (4.1)$$

where G_r is the low-strain shear modulus (see 4.2.3.1), and γ_r satisfies the following equation at p'_r :

$$\tau_f = \frac{2\sqrt{2} \sin \phi}{3 - \sin \phi} p'_r = \frac{G_r \gamma_{\max}}{1 + \gamma_{\max} / \gamma_r} \quad (\text{for sands}) \quad (4.2a)$$

and,

$$\tau_f = \frac{2\sqrt{2} \sin \phi}{3 - \sin \phi} p'_r + \frac{2\sqrt{2}}{3} c = \frac{G_r \gamma_{\max}}{1 + \gamma_{\max} / \gamma_r} \quad (\text{for clays}) \quad (4.2b)$$

where τ_f is the peak (octahedral) shear strength, ϕ is the friction angle, c is the cohesion, and γ_{\max} is the maximum shear strain (10% is employed in OpenSeesPL).

The octahedral shear stress τ is defined as:

$$\tau = \frac{1}{3} \left[(\sigma_{xx} - \sigma_{yy})^2 + (\sigma_{yy} - \sigma_{zz})^2 + (\sigma_{xx} - \sigma_{zz})^2 + 6\sigma_{xy}^2 + 6\sigma_{yz}^2 + 6\sigma_{xz}^2 \right]^{1/2}$$

and the octahedral shear strain γ is defined as:

$$\gamma = \frac{2}{3} \left[(\varepsilon_{xx} - \varepsilon_{yy})^2 + (\varepsilon_{yy} - \varepsilon_{zz})^2 + (\varepsilon_{xx} - \varepsilon_{zz})^2 + 6\varepsilon_{xy}^2 + 6\varepsilon_{yz}^2 + 6\varepsilon_{xz}^2 \right]^{1/2}$$

The number of yield surfaces used for the predefined sands and clays is 20.

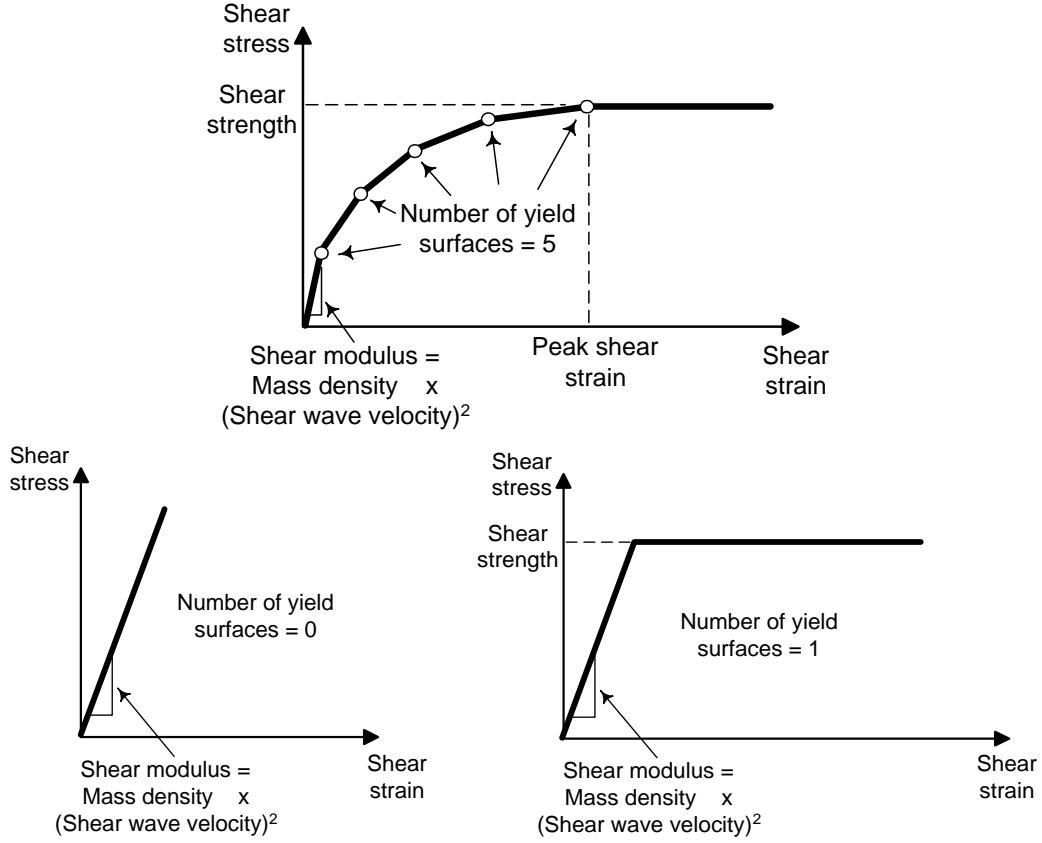


Figure 4.9: Soil backbone curve and yield surfaces.

From Eq. (4.2), we can obtain:

$$\gamma_r = \frac{\tau_f \gamma_{\max}}{G_r \gamma_{\max} - \tau_f} \quad (4.3a)$$

Or

$$\gamma_{\max} = \frac{\tau_f \gamma_r}{G_r \gamma_r - \tau_f} \quad (4.3b)$$

Substituting Eq. (4.3a) into Eq. (4.1), we can obtain:

$$\tau = \frac{G_r \gamma}{1 + \left(\frac{G_r}{\tau_f} - \frac{1}{\gamma_{\max}} \right) \gamma} \quad (4.4)$$

Take Medium Sand (Table 4.1) as an example, $G_r = 75,000$ kPa, $p'_r = 80$ kPa, $\phi = 33^\circ$.

Substituting the above values into Eq. (4.2a), we can obtain:

$$\tau_f = \frac{2\sqrt{2} \sin(33^\circ)}{3 - \sin(33^\circ)}(80) = 50.2 \text{ kPa} \quad (4.5)$$

Substituting the above into Eq. (4.4), we can obtain:

$$\tau = \frac{(75000) \gamma}{1 + (1494 - \frac{1}{\gamma_{\max}}) \gamma} \quad (4.6)$$

Figure 4.10 shows the backbone curves at $\gamma_{\max} = 2\%$, 5% and 10% , based on Eq. (4.6).

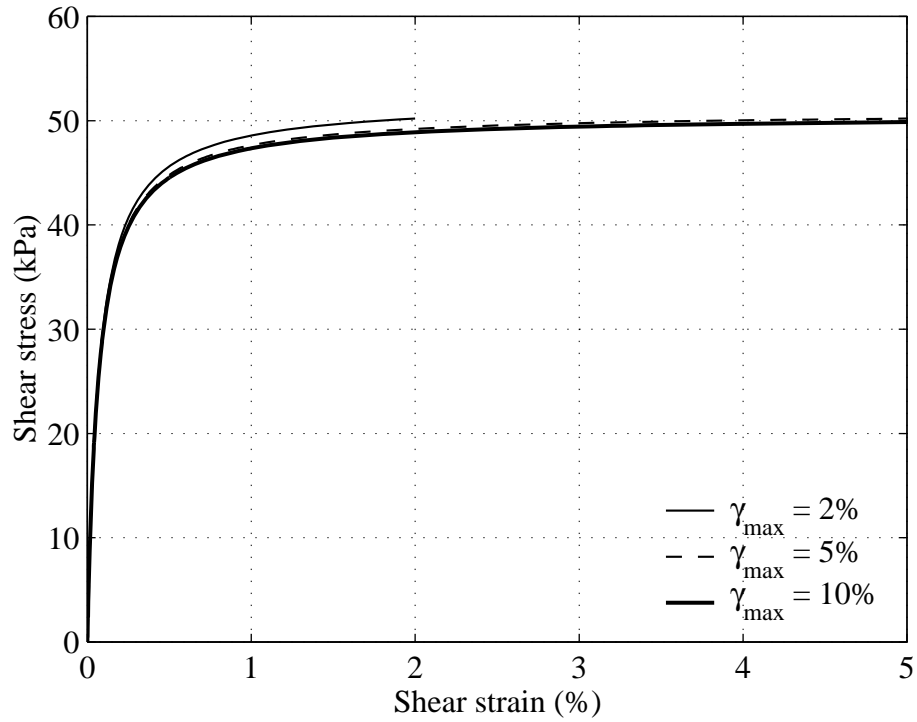


Figure 4.10: Backbone curves for Medium Sand.

4.2.3 User-Defined Materials

User-defined materials include user-defined sand (U-Sand1 and U-Sand2) with confinement-dependent material properties, and user-defined clay (U-Clay1 and U-Clay2) with properties independent of confinement variation. To define the parameters of a user-defined material, click the list of soil materials and select **U-Sand1A**, **U-Sand1B**, **U-Clay1**, **U-Clay2**, **U-Sand2A**, or **U-Sand2B** accordingly (Figure 4.8).

4.2.3.1 User Defined Sand1A (U-Sand1A)

Sandy soil (**PressureDependMultiYield**) with confinement-dependent shear response can be defined by specifying the following parameters (see Figure 4.6 and Figure 4.11):

U-Sand1A (PressureDependMultiYield) for Soil Layer #1

Reset All Based on -> Please select...

Soil Elastic Properties

Saturated Mass Density: 2 [ton/m³]
Reference Pressure: 80 [kPa]
Pressure Dependence Coefficient: 0.5
Gmax: 100000 [kPa]
Bmax: 300000 [kPa]

Soil Nonlinear Properties

Peak Shear Strain (%): 10
Friction Angle: 35 [degree]

Fluid Properties

Fluid Mass Density: 1 [ton/m³]
Combined Bulk Modulus: 2200000 [kPa]
Horizontal Permeability: 0.0001 [m/s]
Vertical Permeability: 0.0001 [m/s]

Modulus Reduction Curve

Number of Points Defining Curve: 0

	Shear strain (%)	G/Gmax
1.	0.0001	0.999
2.	0.0003	0.995
3.	0.001	0.99
4.	0.003	0.96
5.	0.01	0.85
6.	0.03	0.64
7.	0.1	0.37
8.	0.3	0.18
9.	1	0.08
10.	3	0.03
11.	10	0.01
12.	0	0
13.	0	0

Dilatancy/Liquefaction Parameters

Phase Transformation Angle: 30 [degree]
Contraction param: 0
Dilation param1: 0
Dilation param2: 0
Liquefaction param1: 0 [kPa]
Liquefaction param2: 0
Liquefaction param3: 0

OK
Cancel
View Backbone Curve

Figure 4.11: U-Sand1A.

Saturated Mass Density The saturated mass density of the cohesionless soil.

Reference Pressure The reference mean effective confining pressure (p'_r) at which soil appropriate soil properties below are defined.

G_{max} The reference low-strain shear modulus G_r , specified at a reference mean effective confining pressure p'_r .

B_{max} The reference bulk modulus B_r , specified at a reference mean effective confining pressure p'_r .

Pressure Dependence Coefficient (d) A positive constant defining variations of G and B as a function of instantaneous effective confinement p' :

$$G = G_r \left(\frac{p'}{p'_r} \right)^d \quad B = B_r \left(\frac{p'}{p'_r} \right)^d \quad (4.7)$$

Peak Shear Strain An octahedral shear strain at which the maximum shear strength is reached, specified at a reference mean effective confining pressure p'_r . The suggested values are between 0.001% and 20%.

Friction Angle The friction angle (ϕ) at peak shear strength in degrees. The suggested values are between 5 and 65 degrees.

Fluid Mass Density The mass density of the fluid, which is usually 1.0 ton/m³..

Combined Bulk Modulus The combined undrained bulk modulus B_c relating changes in pore pressure and volumetric strain, may be approximated by:

$$B_c \approx B_f / n \quad (4.8)$$

where B_f is the bulk modulus of fluid phase (2.2×10^6 kPa for water typically), and n the initial porosity.

Horizontal Permeability The permability along the horizontal direction.

Vertical Permeability The permability along the vertical direction.

User Defined Nonlinear Shear Stress-Strain Backbone Curve:

The nonlinear shear stress-strain backbone curve can be defined by specifying a G/G_{max} curve (Figure 4.11). To specify the G/G_{max} curve, first enter “number of points defining G/G_{max} curve” and then enter pairs of shear strain and G/G_{max} values. The maximum number of points that can be entered is 13 (the backbone curve becomes horizontal after point 13). In addition:

- If the number of points is zero, then the built-in hyperbolic curve will be used instead.
- If the number of points is 1, the material is elastic-perfectly-plastic.

The user-defined backbone curve is activated if the number of points is greater than zero. In this case, the user specified friction angle ϕ is ignored. Instead, ϕ is defined as follows:

$$\sin \phi = \frac{3\sqrt{3} \sigma_m / p'_r}{6 + \sqrt{3} \sigma_m / p'_r} \quad (3.9)$$

where σ_m is the product of the last modulus and strain pair in the modulus reduction curve. Therefore, it is important to adjust the backbone curve so as to render an appropriate ϕ . If the resulting ϕ is smaller than the phase transformation angle ϕ_{PT} , ϕ_{PT} is set equal to ϕ .

Also remember that improper modulus reduction curves can result in strain softening response (negative tangent shear modulus), which is not allowed in the current model formulation. Finally, note that the backbone curve varies with confinement, although the variations are small within commonly interested confinement ranges. Backbone curves at different confinements can be obtained using the OpenSees element recorder facility (Mazzoni et al. 2006).

The dilatancy/liquefaction parameters include:

Phase Transformation (PT) Angle The transformation angle (degrees) of the cohesionless soil.

Contraction Parameter c_1 A non-negative constant defining the rate of shear-induced volume decrease (contraction) or pore pressure buildup. A larger value corresponds to faster contraction rate (Table 4.2).

The contraction rule is defined by:

$$P'' = \frac{1 - (\eta / \eta_{PT})^2}{1 + (\eta / \eta_{PT})^2} c_1 \quad (4.10)$$

where η is the stress ratio and η_{PT} is the stress ratio along the PT surface (Yang et al. 2003).

Dilation Parameters d_1 & d_2 Non-negative constants defining the rate of shear-induced volume increase (dilation). Larger values correspond to stronger dilation rate (Table 4.2).

The dilation rule is defined by:

$$P'' = \frac{1 - (\eta / \eta_{PT})^2}{1 + (\eta / \eta_{PT})^2} d_1 \exp(d_2 \gamma_d) \quad (4.11)$$

where γ_d is the octahedral shear strain accumulated during a dilation phase (Yang et al. 2003).

Liquefaction Parameters l_1 , l_2 and l_3 Parameters (Table 4.2) controlling the mechanism of liquefaction-induced perfectly plastic shear strain accumulation, i.e., cyclic mobility. **Set $l_1 = 0$ to deactivate this mechanism altogether.**

(Post-liquefaction) yield domain radius:

$$\gamma_y = l_2 \cos^3\left(\frac{\pi p'}{2 l_1}\right) \quad (3.12)$$

l_1 defines the effective confining pressure (e.g., 10 kPa) below which the mechanism is in effect (l_1 is actually p'_y in Figure 4.12). Smaller values should be assigned to denser sands. l_2 defines the maximum amount of perfectly plastic shear strain developed at zero effective confinement during each loading phase (l_2 is actually $\gamma_{s\max}$ in Figure 4.12). Smaller values should be assigned to denser sands.

Maximum extent of biased-loading yield domain (γ_y is actually γ_s in Figure 4.12)

$$\gamma_{ry} = l_3 \gamma_y \quad (4.13)$$

l_3 defines the maximum amount of biased perfectly plastic shear strain γ_b accumulated at each loading phase under biased shear loading conditions, as $\gamma_b = l_2 \times l_3$ (γ_{ry} is actually γ_r , and l_3 is R in Figure 4.13). Typically, l_3 takes a value between 0.0 and 3.0. Smaller values should be assigned to denser sands.

Table 4.2: Suggested values for contraction and dilation parameters

	Loose Sand (15%-35%)	Medium Sand (35%-65%)	Medium-dense Sand (65%-85%)	Dense Sand (85%-100%)
$c1$	0.21	0.07	0.05	0.03
$d1$	0.	0.4	0.6	0.8
$d2$	0	2	3	5
l_1 (kPa)	10	10	5	0
l_2	0.02	0.01	0.003	0
l_3	1	1	1	0

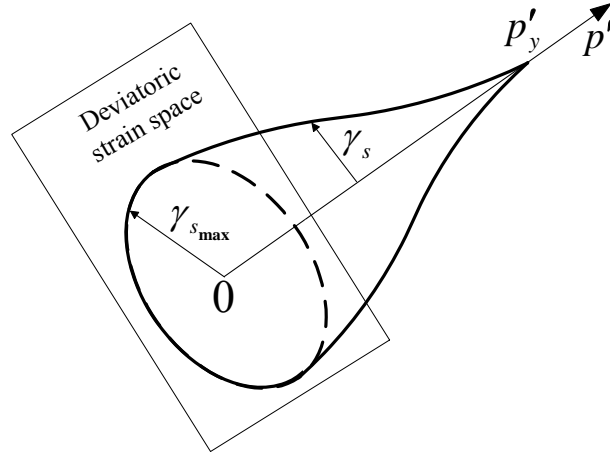


Figure 4.12: Initial yield domain at low levels of effective confinement (Yang et al. 2003).

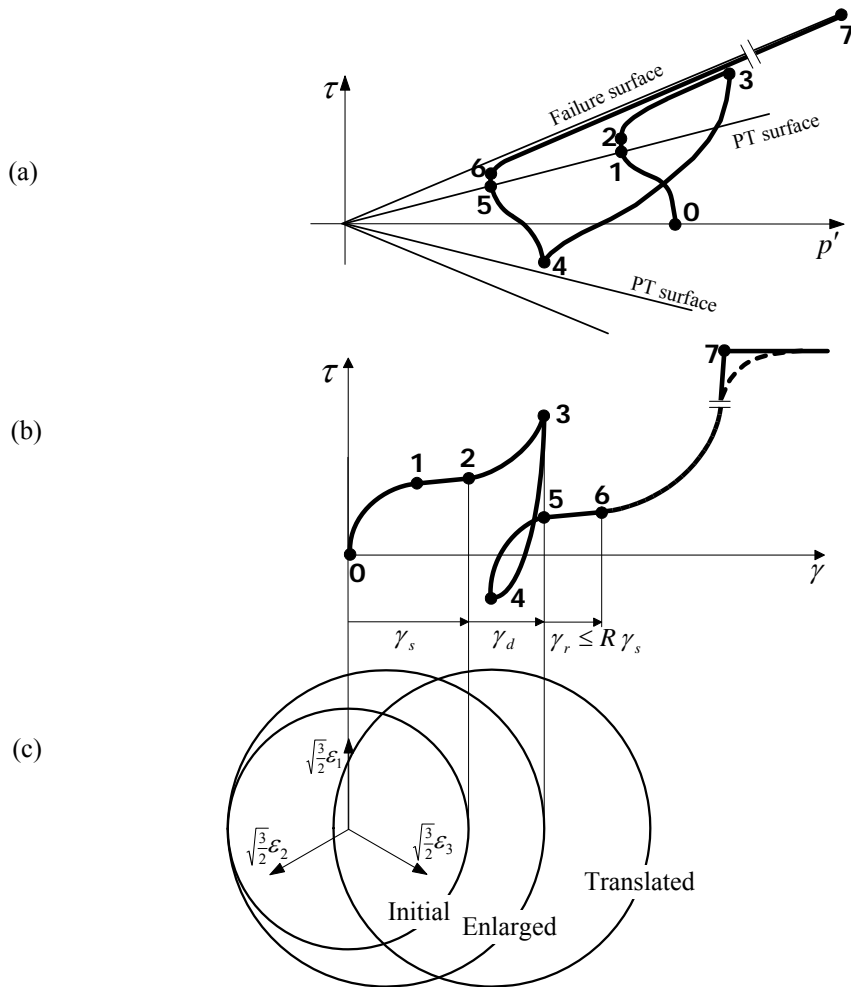


Figure 4.13: Schematic of constitutive model response showing (a) octahedral stress τ - effective confinement p' response, (b) octahedral stress τ - octahedral strain γ response, and (c) configuration of yield domain (Yang et al. 2003).

4.2.3.2 User Defined Sand1B (U-Sand1B)

The second type of user-defined sandy soil (**PressureDependMultiYield**, U-Sand1B) can be defined by specifying the following parameters (Figure 4.14):

U-Sand1B (PressureDependMultiYield) for Soil Layer #1

Mass Density	2.1	[ton/m ³]
Reference Mean Confinement	80	[kPa]
Reference Shear Wave Velocity	300	[m/s]
Confinement Dependence Coeff. (0.1-1.0)	0.5	
Poisson's Ratio	0.4	
Cohesion	0	[kPa]
Friction Angle (5-65 degrees)	40	
Peak Shear Strain (0.001-20%)	3	
Number of Yield Surfaces (0-30)	20	

Advanced Options

- ☐ Use K0 for Elastic Own Weight
- Initial Lateral/Vertical Confinement Ratio (0.1-0.9): 0.5
- ☐ Young's Modulus for Elastic Own Weight: 600000 [kPa]

Buttons: OK, Cancel, View Backbone Curve

Figure 4.14: U-Sand1B.

Note: All parameters shown in Figure 4.14 are defined at the reference mean confinement p_r .

Mass Density The mass density of the cohesionless soil (ρ). The suggested range of values are between 1 and 3 ton/m³.

Reference Shear Wave Velocity The reference shear wave velocity (V_{sr}). The suggested range is between 10 and 6000 m/s. The reference shear modulus $G = \rho V_{sr}^2$.

Reference Mean Confinement The reference mean confinement. This is the confinement level at which shear wave velocity and peak shear strain are defined. The suggested range is between 10 kPa or larger.

Confinement Dependence Coeff. The confinement dependence coefficient. The suggested range is between 0.1 and 10.

Initial Lateral/Vertical Confinement Ratio The initial lateral/vertical stress ratio (also known as coefficient of lateral earth pressure at rest K_0). K_0 is related to Poisson's ratio by the following relation $K_0 = \nu / (1 - \nu)$. The suggested range for K_0 is between 0.1 and 0.9.

Cohesion The suggested range is between 0 and 5000000 kPa. See Section 4.2.3.1 for more information.

Friction Angle The suggested range is between 5 and 65 degrees. See Section 4.2.3.1 for more information.

Peak Shear Strain The suggested range is between 0.001% and 20%. See Section 4.2.3.1 for more information.

Number of Yield Surfaces NYS The suggested range is between 0 and 30. In particular, NYS = 0 dictates an elastic shear response (Cohesion, Friction Angle and Peak Shear Strain are ignored, see Figure 4.9), NYS = 1 indicates an elastic-perfectly plastic shear response (Peak Shear Strain is ignored, see Figure 4.9).

Advanced Options:

Use K0 for Elastic Own Weight If checked, users can specify the initial lateral/vertical confinement ratio K_0 which will be used for the application of own weight at the elastic stage (first run).

Young's Modulus for Elastic Own Weight The elastic modulus used for the application of own weight at the elastic stage.

4.2.3.3 User Defined Clay1 (U-Clay1)

Non-liquefiable clay with shear response properties independent of confinement variation can be defined as shown in Figure 4.7 and Figure 4.15.

Cohesion The apparent cohesion at zero effective confinement.

The nonlinear shear stress-strain backbone curve can be defined by specifying a G/G_{max} curve (Figure 4.15). The user-defined backbone curve is activated if the number of points is greater than zero. In this case, if the user specifies $\phi=0$, cohesion c will be ignored. Instead, c is defined by $c = \sqrt{3} \cdot \sigma_m / 2$, where σ_m is the product of the last modulus and strain pair in the modulus reduction curve. Therefore, it is important to adjust the backbone curve so as to render an appropriate c .

If the user specifies $\phi > 0$, this ϕ will be ignored. Instead, ϕ is defined as follows:

$$\sin \phi = \frac{3(\sqrt{3} \sigma_m - 2c) / p_r'}{6 + (\sqrt{3} \sigma_m - 2c) / p_r'} \quad (3.14)$$

If the resulting $\phi < 0$, we set $\phi = 0$ and $c = \sqrt{3} \sigma_m / 2$.

Also remember that improper modulus reduction curves can result in strain softening response (negative tangent shear modulus), which is not allowed in the current model formulation. Finally, note that the backbone curve varies with confinement, although the variation is small within commonly interested confinement ranges. Backbone curves at different confinements can be obtained using the OpenSees element recorder facility (Mazzoni et al. 2006).

For information about other parameters, see Section 4.2.3.1.

4.2.3.4 User Defined Clay2 (U-Clay2)

The second type of user-defined clay (U-Clay2) can be defined as shown in Figure 4.16. See Section 4.2.3.2 for information about parameters defining U-Clay2.

4.2.3.5 User Defined Sand2A (U-Sand2A)

The third type of user-defined sandy soil (**PressureDependMultiYield02**, U-Sand2A) can be defined as shown in Figure 4.17. **PressureDependMultiYield02** material is modified from **PressureDependMultiYield** material, with: 1) additional parameters (Contraction parameter 3 and Dilation parameter 3 as shown in Figure 4.17) to account for $K\sigma$ effect, 2) a parameter to account for the influence of previous dilation history on subsequent contraction phase, and 3) modified logic related to permanent shear strain accumulation

4.2.3.6 User Defined Sand2B (U-Sand2B)

The third type of user-defined sandy soil (**PressureDependMultiYield02**, U-Sand2B) can be defined as shown in Figure 4.18.

U-Clay1 (PressureIndependentMultiYield) for Soil Layer #-1

Soil Elastic Properties

Saturated Mass Density: 1.8 [ton/m³]

Reference Pressure: 100 [kPa]

Pressure Dependence Coefficient: 0

Gmax: 160000 [kPa]

Bmax: 500000 [kPa]

Soil Nonlinear Properties

Peak Shear Strain (%): 10

Friction Angle: 0 [degree]

Cohesion: 75 [kPa]

Fluid Properties

Fluid Mass Density: 1 [ton/m³]

Combined Bulk Modulus: 2200000 [kPa]

Horizontal Permeability: 1e-009 [m/s]

Vertical Permeability: 1e-009 [m/s]

Modulus Reduction Curve

Number of Points Defining Curve: 0

	Shear Strain (%)	G/Gmax
1.	0.0001	0.999
2.	0.0003	0.995
3.	0.001	0.99
4.	0.003	0.96
5.	0.01	0.85
6.	0.03	0.64
7.	0.1	0.37
8.	0.3	0.18
9.	1	0.08
10.	3	0.03
11.	10	0.01
12.	0	0
13.	0	0

OK

Cancel

View Backbone Curve

Figure 4.15: U-Clay1.

U-Clay2 (PressureIndependentMultiYield) for Soil Layer #1 ✕

Mass Density	<input type="text" value="1.8"/>	[ton/m3]
Shear Wave Velocity	<input type="text" value="300"/>	[m/s]
Poisson's Ratio	<input type="text" value="0.4"/>	
Cohesion (C) multiplied by $((\sqrt{3})/2)$	<input type="text" value="75"/>	[kPa]
Peak shear strain Gamma multiplied by $\sqrt{2}/3$ (from 0.001-20%)	<input type="text" value="3"/>	
Number of Yield Surfaces (0-30)	<input type="text" value="20"/>	

Advanced Options

☐ Use K0 for Elastic Own Weight

Initial Lateral/Vertical Confinement Ratio (0.1-0.9)

☐ Young's Modulus for Elastic Own Weight [kPa]

Figure 4.16: U-Clay2.

U-Sand2A (PressureDependMultiYield02) for Soil Layer #1

Reset All Based on -> Please select...

Soil Elastic Properties

Saturated Mass Density: 1.9 [ton/m3]

Reference Pressure: 101 [kPa]

Pressure Dependence Coefficient: 0.5

Gmax: 100000 [kPa]

Bmax: 233000 [kPa]

Modulus Reduction Curve

Number of Points Defining Curve: 0

	Shear strain (%)	G/Gmax
1.	0.0001	0.999
2.	0.0003	0.995
3.	0.001	0.99
4.	0.003	0.96
5.	0.01	0.85
6.	0.03	0.64
7.	0.1	0.37
8.	0.3	0.18
9.	1	0.08
10.	3	0.03
11.	10	0.01
12.	0	0
13.	0	0

Dilatancy/Liquefaction Parameters

Phase Transformation Angle: 25.5 [degree]

Contraction param 1: 0.045

Contraction param 3: 0.06

Dilation param 1: 0.15

Dilation param 3: 0

Soil Nonlinear Properties

Peak Shear Strain (%): 10

Friction Angle: 33.5 [degree]

Fluid Properties

Fluid Mass Density: 1 [ton/m3]

Combined Bulk Modulus: 2200000 [kPa]

Horizontal Permeability: 0.0001 [m/s]

Vertical Permeability: 0.0001 [m/s]

OK

Cancel

Figure 4.17: U-Sand2A.

U-Sand2B (PressureDependMultiYield02) for Soil Layer #1

Mass Density	1.9	[ton/m3]
Reference Mean Confinement	101	[kPa]
Reference Shear Wave Velocity	300	[m/s]
Confinement Dependence Coeff. (0.1-1.0)	0.5	
Poisson's Ratio	0.4	
Cohesion	0	[kPa]
Friction Angle (5-65 degrees)	33.5	
Peak Shear Strain (0.001-20%)	3	
Number of Yield Surfaces (0-30)	20	

Advanced Options

- ☐ Use K0 for Elastic Own Weight
 - Initial Lateral/Vertical Confinement Ratio (0.1-0.9): 0.5
- ☐ Young's Modulus for Elastic Own Weight: 60000 [kPa]

OK Cancel

Figure 4.18: U-Sand2B.

4.2.4 Material Properties for Pile Zone

The pile zone refers to the pile domain under the ground surface. The material for the pile zone (Figure 4.19) can be selected from an available menu of cohesionless and cohesive soil materials including the elastic isotropic material. In addition, user-defined cohesionless and cohesive soil materials (**U-Sand1A**, **U-Sand1B**, **U-Clay1**, **U-Clay2**, **U-Sand2A**, and **U-Sand2B**) are also available to choose.

If an elastic isotropic material is selected, the user is requested to specify, Young's Modulus, Poisson's Ratio, Mass Density Permeability of the material used for the pile zone.

Pile Zone

Material for Pile Zone
 22: U-Clay2 (PressureIndependentMultiYield)...

Residual Shear Strength (for Very Loose Material Only): 0.2 [kPa]

Soil Modulus Variation with Depth: ☒ P ☐ L ☐ C

Youngs Modulus 100000 [kPa] Poisson's Ratio 0.3

Mass Density 1.5 [ton/m3] Permeability 1e-005 [m/s]

Notes
 P, L, and C represents parabolic, linear and constant variation of soil modulus with depth, respectively.

OK Cancel

Figure 4.19: Pile zone material.

4.2.5 Pile-Soil Interfacing Layer Properties

The material for the pile-soil interfacing layer (Figure 4.20) can be selected from an available menu of cohesionless and cohesive soil materials including the elastic isotropic material. In addition, user-defined cohesionless and cohesive soil materials (**U-Sand1A**, **U-Sand1B**, **U-Clay1**, **U-Clay2**, **U-Sand2A**, and **U-Sand2B**) are also available to choose.

If an elastic isotropic material is selected, the user is requested to specify, Young's Modulus, Poisson's Ratio, Mass Density Permeability of the material used for the pile-soil interfacing layer.

4.2.6 Outermost Zone Properties

The material for the outermost zone (Figure 4.21) can be selected from an available menu of cohesionless and cohesive soil materials including the elastic isotropic material. In addition, user-defined cohesionless and cohesive soil materials (**U-Sand1A**, **U-Sand1B**, **U-Clay1**, **U-Clay2**, **U-Sand2A**, and **U-Sand2B**) are also available to choose.

If an elastic isotropic material is selected, the user is requested to specify, Young's Modulus, Poisson's Ratio, Mass Density Permeability of the material used for the pile-soil interfacing layer.

Column-Soil Interfacing Layer

Material for Pile-Soil Interfacing Layer
 8: Sat. Cohesionless medium, sand permeability

Residual Shear Strength (for Very Loose Material Only): 0.2 [kPa]

Soil Modulus Variation with Depth: ☒ P ☐ L ☐ C

Youngs Modulus 100000 [kPa] Poisson's Ratio 0.3

Mass Density 1.5 [ton/m3] Permeability 1e-005 [m/s]

Notes
 P, L, and C represents parabolic, linear and constant variation of soil modulus with depth, respectively.

OK Cancel

Figure 4.20: Pile-soil interfacing layer material.

Outermost Zone Material

Material for Outermost Zone
 8: Sat. Cohesionless medium, sand permeability

Residual Shear Strength (for Very Loose Material Only): 0.2 [kPa]

Soil Modulus Variation with Depth: ☒ P ☐ L ☐ C

Youngs Modulus 100000 [kPa] Poisson's Ratio 0.3

Mass Density 1.5 [ton/m3] Permeability 1e-005 [m/s]

Notes
 P, L, and C represents parabolic, linear and constant variation of soil modulus with depth, respectively.

OK Cancel

Figure 4.21: Outermost zone material.

5. Mesh Generation

To define the finite element mesh, click **Mesh Parameters** button in the **Model Input** window (Figure 5.1).

5.1 General Mesh Definition

Mesh Scale The mesh scale can be quarter mesh, half mesh or full mesh (to reduce computational effort depending on the situation at hand).

Number of Slices The number of mesh slices in the circumferential direction.

Number of Beam Elements above Ground Surface The number of beam elements used for the pile section above the ground surface.

5.2 Horizontal Meshing

The meshing in the horizontal direction for the single pile definition is controlled by the following parameters (Tab **Horizontal Meshing**, Figure 5.1b):

This section controls mesh refinement along the horizontal direction. **Length** of each soil horizontal layer is defined in the left column. Number of mesh elements in each defined is specified in the column “**Number of Mesh Layers**”. Note that the first mesh layer is starting from the center of the mesh when the pile is located and the length of the first mesh layer is equal to the pile radius. **Ratio of Element Length over Next** is used to obtain a gradually changing element size within a layer if **Uniform Meshing** is unchecked (obviously this option is only valid if the # of mesh layers is 2 or larger).

5.3 Vertical Meshing

The meshing in the vertical direction is controlled by the following parameters (Tab **Vertical Meshing**, Figure 5.1c):

This section defines the soil profile (layering) along the vertical direction starting from the ground surface downwards (looking at the side view from the top downwards. **Height** (thickness) of each soil layer is defined in the left column. Number of mesh elements in each defined is specified in the column “**Number of Mesh Layers**” (at least equal to 1 to define a soil profile consisting of a single type of soil). Height (thickness) of this layer must be equal to the entire soil stratum height. Note that the number of mesh layers in the upper zone (where the pile foundation is embedded) will automatically define the number of beam column elements of this pile (below ground surface). As such, it is generally advisable to select an adequate number of

mesh layers in this zone. Note: If there is any error during mesh generation, please follow the error message instructions to adjust the controlling parameters and then try again.

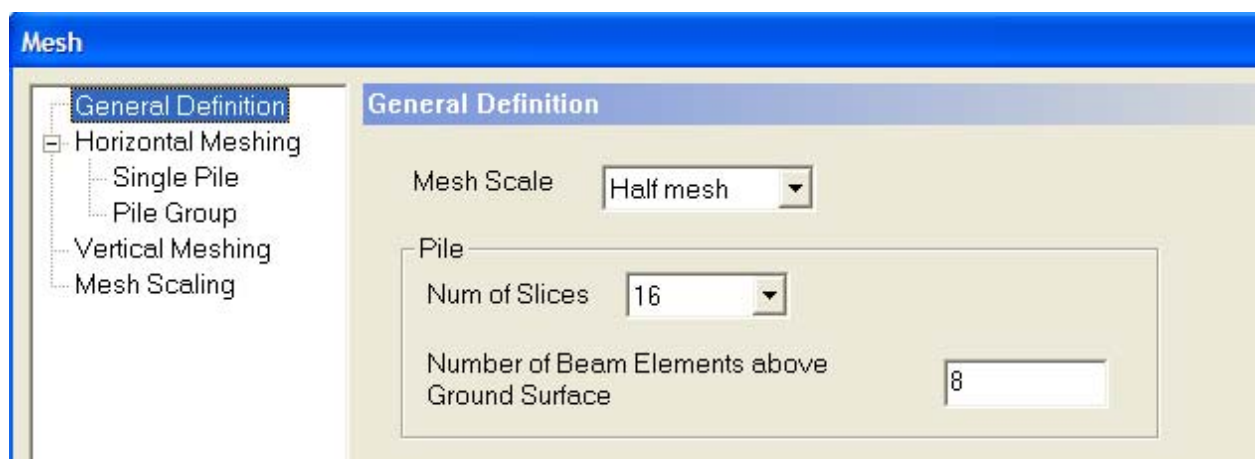
Note: Element size is a parameter that affects frequency content of the ground response. Smaller size elements (particularly along the soil domain height), will permit higher frequencies (if present in the input motion) to propagate to the ground surface with more fidelity.

5.4 Mesh Scaling

The soil domain will be scaled if ‘**Re-scale Soil Domain in Horizontal Directions**’ checkbox is checked (Figure 5.1d):

Model Length The length of the soil domain (along the longitudinal direction) to be scaled.

Model Width The width of the soil domain (along the transverse direction) to be scaled.



a) General Definition

Mesh

General Definition

Horizontal Meshing

Single Pile

Pile Group

Vertical Meshing

Mesh Scaling

Single Pile

Mesh Layer # (From Pile Center)	Length [m]	# of Mesh Layers	Uniform Meshing?	Ratio of Element Length over Next
Pile Radius	0.5	1	<input checked="" type="checkbox"/>	1
1st Layer after Interface	1	2	<input checked="" type="checkbox"/>	1
2nd Layer	18	8	<input type="checkbox"/>	0.8
3rd Layer	0	1	<input checked="" type="checkbox"/>	1
4th Layer	0	1	<input checked="" type="checkbox"/>	1
5th Layer	0	1	<input checked="" type="checkbox"/>	1
6th Layer	0	1	<input checked="" type="checkbox"/>	1
Outermost Zone	1	1	<input checked="" type="checkbox"/>	1

Note: Definitions following a 0-length section will be ignored, e.g., if you do not need the 3rd layer and beyond, enter 0 for the length of the 3rd layer.

b) Horizontal Meshing for Single Pile Models

Figure 5.1: Definition of meshing parameters.

Mesh

- General Definition
- Horizontal Meshing
- Single Pile
- Pile Group
- Vertical Meshing**
- Mesh Scaling

Vertical Meshing

Mesh Layer # (From Topdown)	Height [m]	Number of Mesh Layers	Uniform Meshing?	Ratio of Top Element Height over Bottom
1:	6	8	<input type="checkbox"/>	0.9
2:	4	4	<input checked="" type="checkbox"/>	1
3:	0	1	<input checked="" type="checkbox"/>	1
4:	0	1	<input checked="" type="checkbox"/>	1
5:	0	1	<input checked="" type="checkbox"/>	1
6:	0	1	<input checked="" type="checkbox"/>	1
7:	0	1	<input checked="" type="checkbox"/>	1
8:	0	1	<input checked="" type="checkbox"/>	1
9:	0	1	<input checked="" type="checkbox"/>	1
10:	0	1	<input checked="" type="checkbox"/>	1
11:	0	1	<input checked="" type="checkbox"/>	1

c) Vertical Meshing

Mesh

- General Definition
- Horizontal Meshing
- Single Pile
- Pile Group
- Vertical Meshing
- Mesh Scaling**

Mesh Scaling

☒ Scale Soil Domain in Horizontal Directions (Single Pile Only)

Model Length (Longitudinal Direction) [m]

Model Width (Transverse Direction) [m]

d) Mesh Scaling

Figure 5.1: (continued).

6. Pushover & Eigenvalue Analyses

In a pushover or base-shaking analysis, four runs are conducted in sequence in order to achieve convergence and simulate the actual loading situation.

- 1) 1st run: Gravity of soil domain is applied in this run; all soil materials are prescribed as linear during this run.
- 2) 2nd run: Soil elements are changed to nonlinear if “Nonlinear” is chosen in Analysis Options (see Section 4.1.1 **Error! Reference source not found.**).
- 3) 3rd run: Pile elements are added and gravity of the pile structure is applied in this run.
- 4) 4th run: Pushover or base-shaking analysis is started.

6.1 Pushover Analysis

6.1.1 Analysis Types

To conduct a pushover analysis, click **Pushover** and then click **Define Pattern** in Figure 2.1. Two types of pushover analyses are available (Figure 6.1): Static and Dynamic Pushover.

6.1.1.1 Force-Based Method

The force-based method is used if the **Force-Based Method** radio button is chosen.

Longitudinal (X) Force The force applied in the longitudinal direction.

Transverse (Y) Force The force applied in the transverse direction.

Vertical (Z) Force The force applied in the vertical direction.

Moment of X The applied bending moment about the longitudinal direction (M_x).

Moment of Y The applied bending moment about the longitudinal direction (M_y).

Moment of Z The applied bending moment about the longitudinal direction (M_z).

6.1.1.2 Displacement-Based Method

The displacement-based method is used if the **Displacement-Based Method** radio button is chosen.

Longitudinal Displacement The displacement applied in the longitudinal direction.

Transverse Displacement The displacement applied in the transverse direction.

Vertical Displacement The displacement applied in the vertical direction.

Rotation around X The applied rotation around the longitudinal axis (X).

Rotation around Y The applied rotation around the transverse axis (Y).

Rotation around Z The applied rotation around the vertical axis (Z).

Pushover

Type

- ☒ Static Pushover
- ☐ Dynamic Pushover

Method

- ☒ Force-Based Method
- ☐ Displacement-Based Method

Pattern

- ☒ Monotonic Pushover Loading Duration [sec]
- ☐ Sine Wave Frequency [Hz] Duration [sec]
- ☐ U-Push Amplitude Increasing Slope [Define U-Push...](#)

Loading Afterward

- ☒ Keep
- ☐ Remove

Force Increment (Per Step or Time Step)

Logitudinal (X) Force	<input type="text" value="1"/>	[kN]
Transverse (Y) Force	<input type="text" value="0"/>	[kN]
Vertical (Z) Force	<input type="text" value="0"/>	[kN]
Moment of X	<input type="text" value="0"/>	[kN-m]
Moment of Y	<input type="text" value="0"/>	[kN-m]
Moment of Z	<input type="text" value="0"/>	[kN-m]

Displacement Increment (Per Step or Time Step)

Longitudinal Displacement	<input type="text" value="0.01"/>	[m]
Transverse Displacement	<input type="text" value="0"/>	[m]
Vertical Displacement	<input type="text" value="0"/>	[m]
Rotation around X	<input type="text" value="0"/>	[rad]
Rotation around Y	<input type="text" value="0"/>	[rad]
Rotation around Z	<input type="text" value="0"/>	[rad]

Surface Load Applied at Pile Zone (Ground Surface Level) (Per Step)

Logitudinal (X)	<input type="text" value="0"/>	Transverse (Y)	<input type="text" value="0"/>	Vertical (Z)	<input type="text" value="0"/>	[kPa]
-----------------	--------------------------------	----------------	--------------------------------	--------------	--------------------------------	-------

Total Analysis Time/Steps

Static Pushover:	Number of Steps	<input type="text" value="20"/>		
Dynamic Pushover:	Computation Time	<input type="text" value="20"/> [sec]	Time Step	<input type="text" value="0.1"/> [sec]

Applied Location

- ☒ Pile Head
- ☐ Shear Beam
- ☐ Shear Beam (by Profile Ratios)

Applied Range/Height (Starting from Surface)

 [m]

[Change Profile...](#)

OK Cancel

Figure 6.1: Pushover analysis.

6.1.2 Load Pattern

To conduct a pushover analysis, a load pattern must be defined. The load pattern is shown in Figure 6.2.

Pattern

☐ Monotonic Pushover Loading Duration [sec]

☒ Sine Wave Frequency [Hz]

 Duration [sec]

 Amplitude Increasing Slope

☐ U-Push

Loading Afterward

☒ Keep

☐ Remove

Figure 6.2: Pushover load pattern.

6.1.2.1 Monotonic Pushover

If Static Pushover is chosen, the pushover options include monotonic pushover as well as pushover by a user-defined loading pattern (U-Push). Please see Section 6.1.2.3 for how to define a U-Push. In a monotonic pushover, the pushover load/displacement is linearly increasing with steps. In a dynamic monotonic pushover, users are allowed to define the loading duration.

6.1.2.2 Sine Wave Pushover

If Dynamic Pushover is chosen, a Sine Wave loading pattern is also available (Figure 6.2).

6.1.2.3 Pushover by User-Defined Load Pattern (U-Push)

To define your own load pattern (U-Push), click U-Push in Figure 6.2. The U-Push window is shown in Figure 6.3. Click **Select/Change Pushover File** to change file. The user-defined pushover file should contain single-column data.

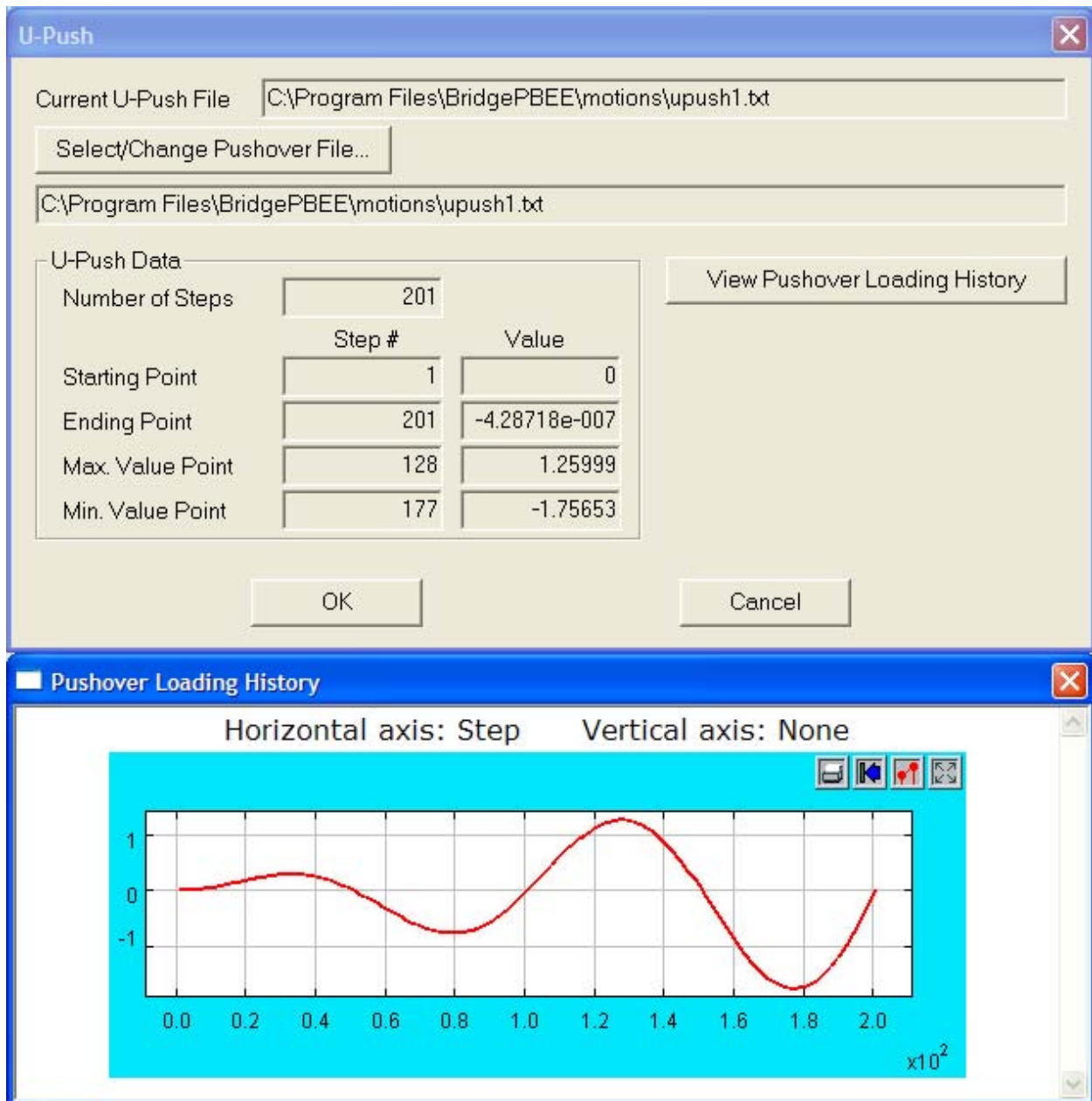


Figure 6.3: User-defined pushover load pattern (U-Push)

6.1.3 Running the Analysis

To run the analysis, click “**Save Model & Run Analysis**” in Menu “**Analyze**”.

Upon the user requests to run the analysis, OpenSeesPL will check all the entries defined by the user to make sure the model is valid. Thereafter, a small window (Figure 6.4) will show the progress of the analysis.

By default, graphical output windows will be opened upon completion of the analysis.

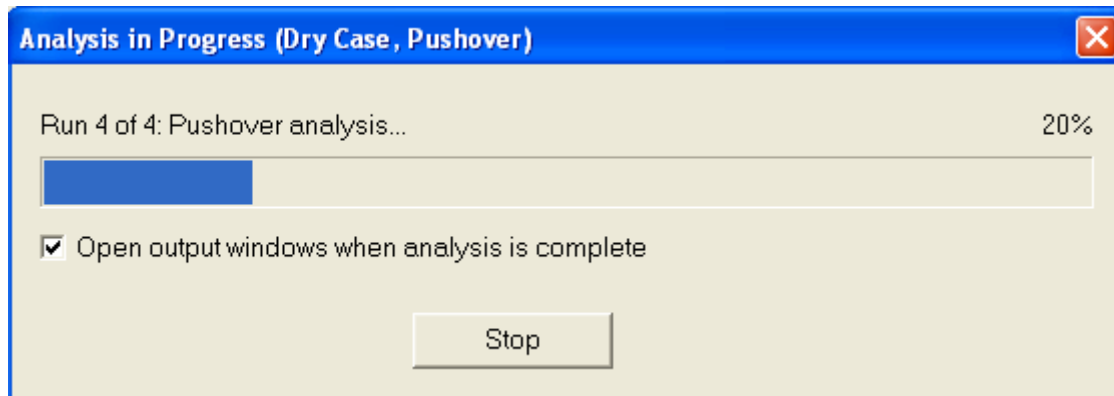


Figure 6.4: Analysis running progress window.

6.1.4 Output for Pushover Analysis

6.1.4.1 Tips on Manipulating Graphs

Response time histories and profiles are displayed by X-Y plot using Java Applet. Therefore, make sure to enable Java Applet in your web browser (Internet Explorer). You may also view the digital data by clicking on the link under the X-Y plot. If occasionally the graph becomes crooked, you can click on the Fill button to refresh it.

To zoom in on any region of the plot, select a box with the mouse pointer (Figure 6.5). Start at the upper left corner of the region you wish to view in more detail and drag downwards and to the right. To bring the graph to the original scale, click on the "fill" button at the upper right corner.

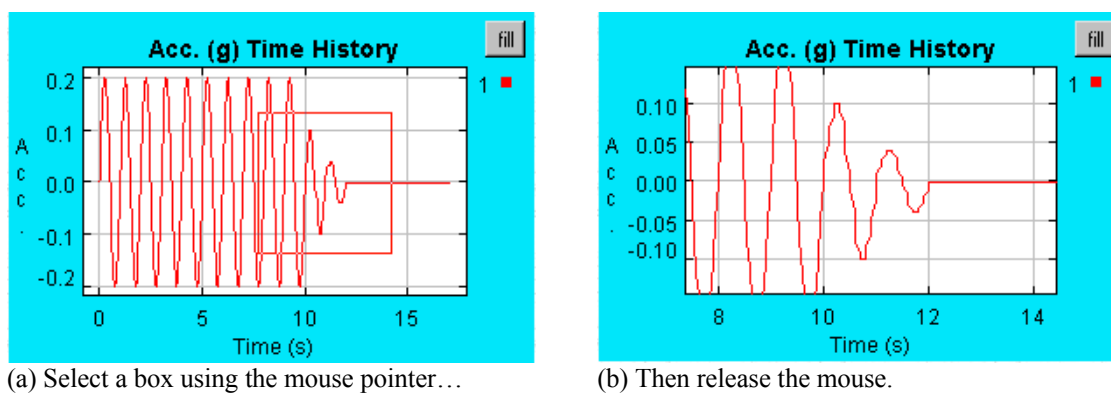
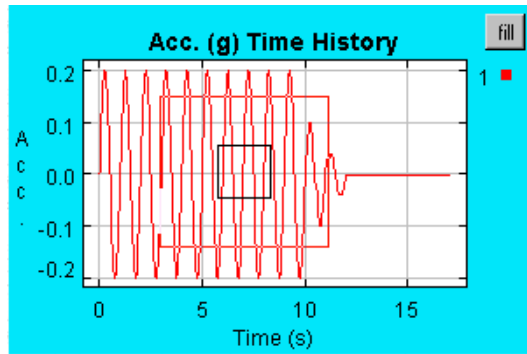
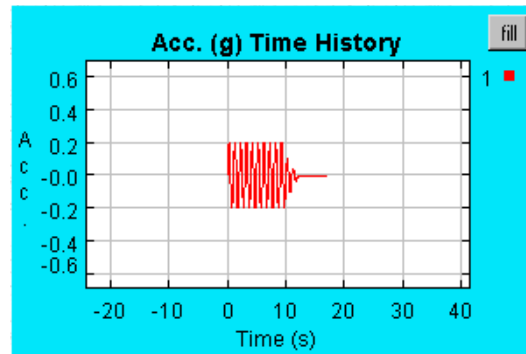


Figure 6.5: Zoom in.



(a) Select a box using the mouse pointer...



(b) Then release the mouse.

Figure 6.6: Zoom out.

To zoom out, drag the mouse pointer upwards (Figure 6.6). When zooming out, a reference box is drawn that will represent the current view, and dragging will cause a box to be displayed that represents the new view. Again, click on the "fill" button at the upper right corner to bring the graph to the original scale.

6.1.4.2 Pile Response Time Histories and Profiles

To view the pile response, click **Pile Response Profiles** in Menu **Display**. The figures show the response time histories and response profiles of the pile. Seven types of response are available (Figure 6.7):

- Displacement
- Acceleration
- Rotation
- Moment
- Shear
- Pressure

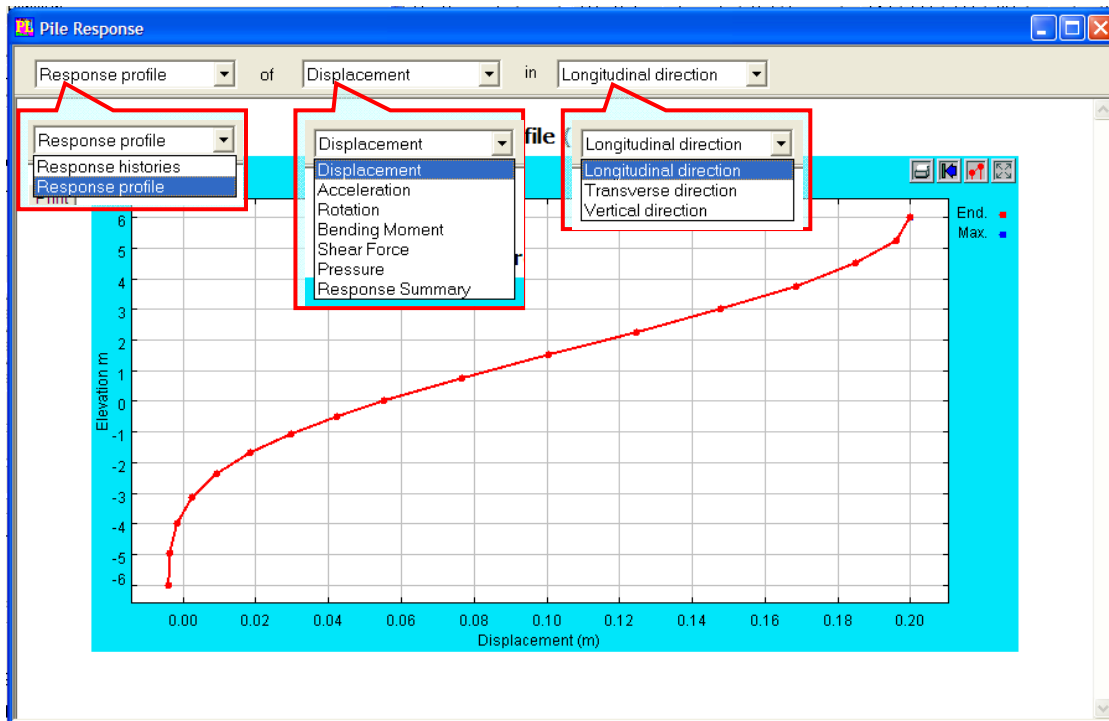


Figure 6.7: Response time histories and profiles for pile.

6.1.4.3 Pile Response Relationships

To view the pile response relationships, click **Pile Response Relationships** in Menu **Display**. The figures show the response relationships of the pile. Two types of response are available (Figure 6.8):

- Load-displacement
- Moment-curvature

To zoom-in or zoom-out, use mouse to select a window. Click "**fill**" to get back to the original figure.

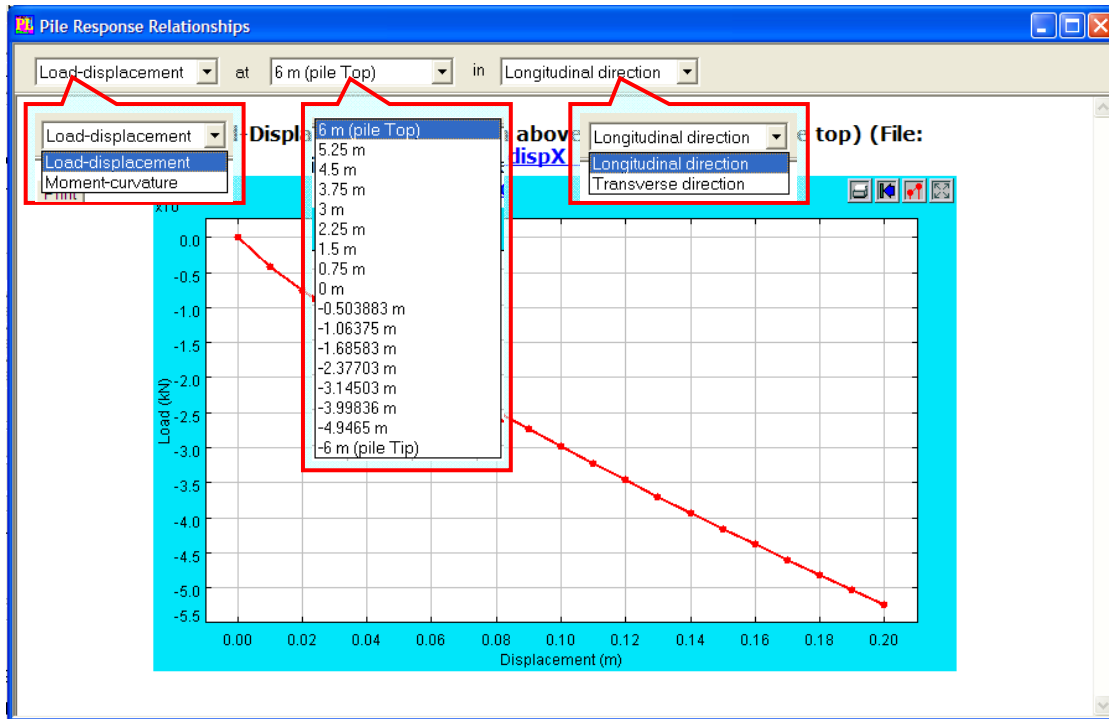


Figure 6.8: Response relationships for pile.

6.1.4.4 Deformed Mesh

By default, the deformed mesh is for the dynamic analysis (if '**Due to Seismic Excitation**' is chosen) or the pushover analysis (if "**Due to Pushover**" is chosen). However, the deformed mesh due to gravity is also available ('**Due to Gravity**' is chosen)

Types of results in the deformed mesh include (Figure 6.9):

- Deformed Mesh
- Displacement Contour Fill
- Longitudinal Displacement Contour Fill (X-disp contour)
- Transverse Displacement Contour Fill (Y-disp contour)
- Vertical Displacement Contour Fill (Z-disp contour)
- Pore Pressure Contour Fill
- Excess Pore Pressure (EPP) Contour Fill
- EPP Ratio Contour Fill
- Vertical Stress Contour Fill
- Shear Stress Contour Fill
- Stress Ratio Contour Fill
- Effective Confinement Contour Fill

The deformed mesh can be viewed in 3D or 2D (can be selected from a list of 2D cut planes, see Figure 6.10).

To view the animation of any given type, click the “**Play Animation**” button. The text of the button will change to “**Stop Animation**” when the animation is being played. To stop the animation, click the “**Stop Animation**” button.

The **Scale Factor** can be changed to improve the viewing effects. The time between playing two frames can be defined by specifying the **Animation Playing Delay** (in millisecond).

Note that the animation will not be played if the current time step is in the last step and “**Endless Playing**” is unchecked.

At any time, the deformed mesh can be rotated by dragging the mouse, moved in 4 directions by pressing keys of LEFT ARROW, RIGHT ARROW, UP ARROW or DOWN ARROW respectively. The view can be zoomed in (by pressing key ‘F9’), out (by pressing key ‘F10’) or frame (by pressing key ‘F11’).

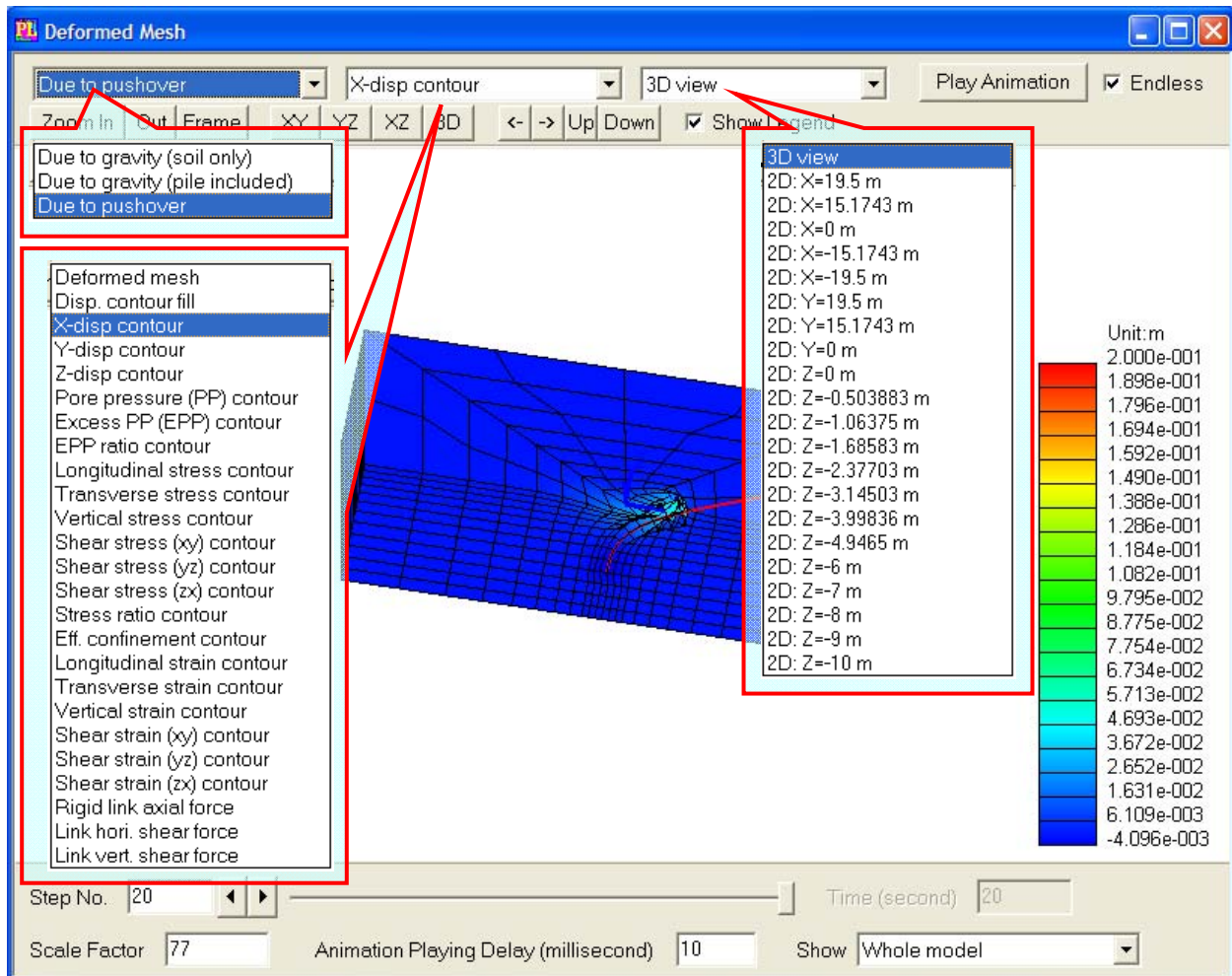


Figure 6.9: Deformed mesh and contour fill

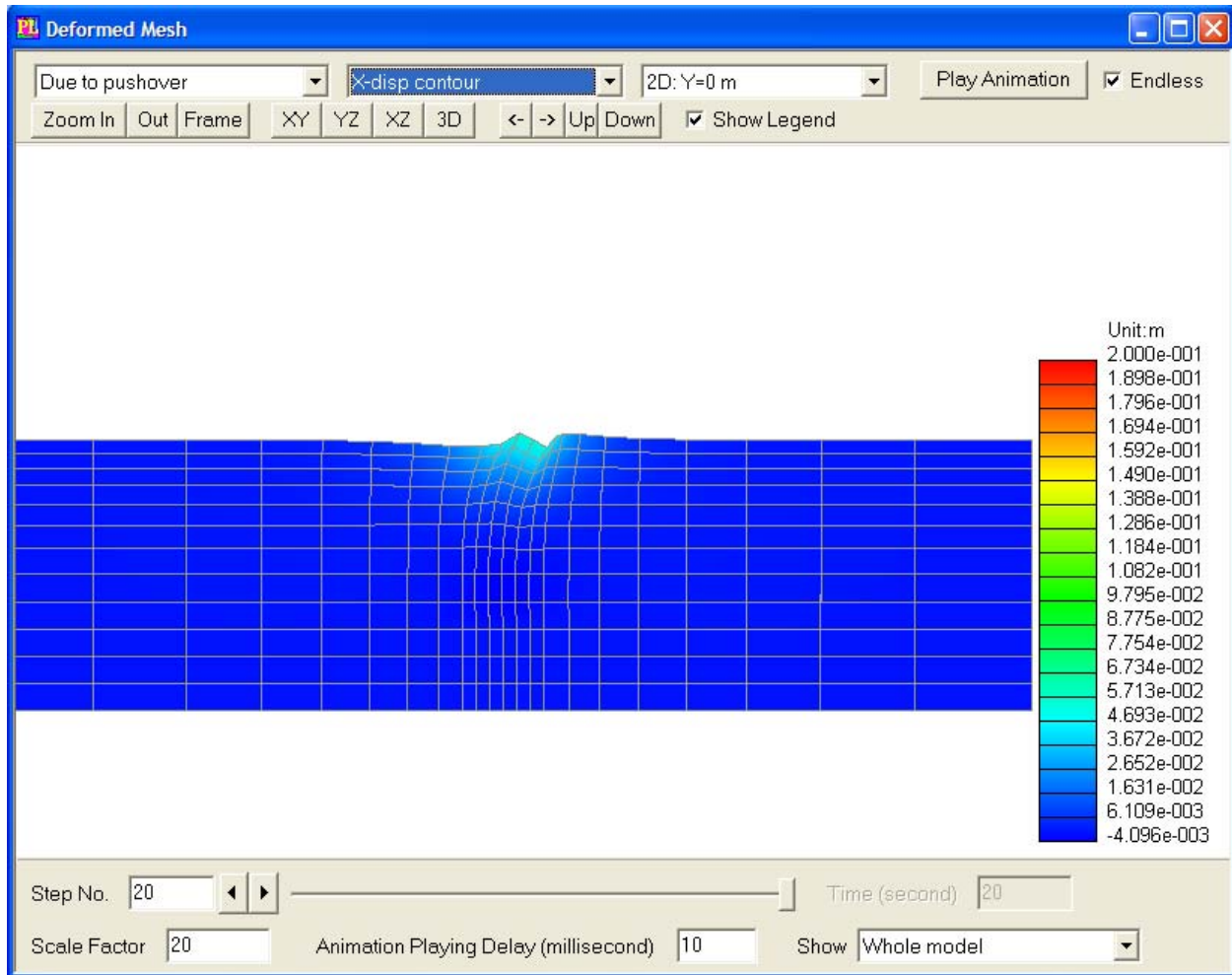


Figure 6.10: 2D plane ($Y = 0$) view of the longitudinal displacement contour in the deformed mesh window.

6.2 Eigenvalue Analysis

To conduct an Eigenvalue analysis, click **Eigenvalue** and then specify **Number of Frequencies** in Figure 2.1. And then click **Save Model & Run Analysis**. Figure 6.11 shows the output window for an Eigenvalue analysis, which can be accessed by clicking menu **Display** and then choosing **Deformed Mesh**.

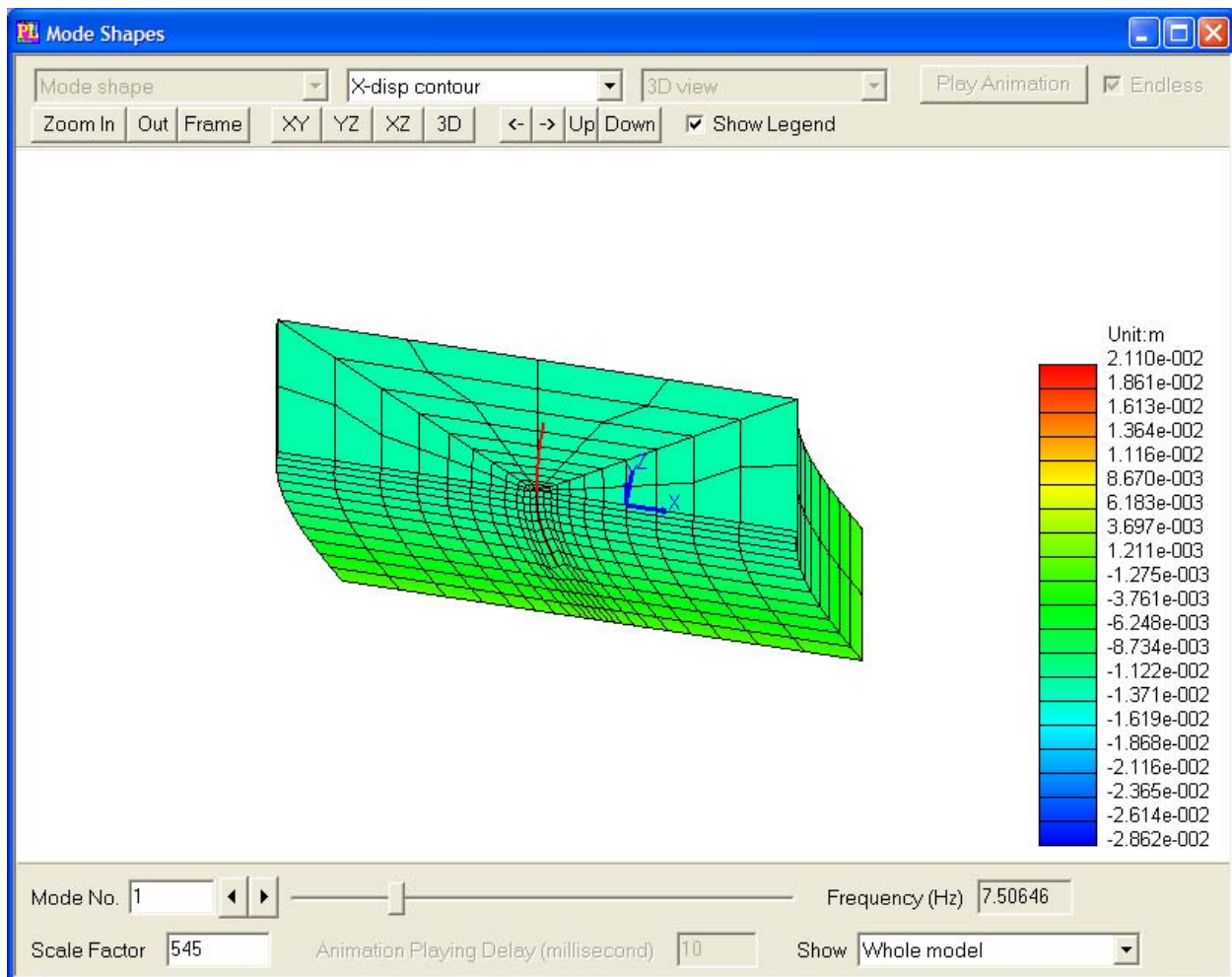


Figure 6.11: Output for an Eigenvalue analysis

7. Base Shaking Analysis

7.1 Base Shaking

7.1.1 Step-by-Step Time Integration

OpenSeesPL employs the Newmark time integration procedure with two user defined coefficients β and γ (Newmark 1959, Chopra 2004). Standard approaches may be adopted by appropriate specification of these constants (Figure 7.1). Default values in OpenSeesPL are $\gamma = 0.55$, and $\beta = ((\gamma + 1/2)^2) / 4$.

Computations at any time step are executed to a convergence tolerance of 10^{-4} (Euclidean Norm of acceleration vector), normalized by the first iteration Error Norm (predictor multi-corrector approach).

Note: An additional fluid-phase (Chan 1988) time integration parameter θ is set to 0.6 in the data file.

$\beta = 1/6 ; \gamma = 1/2$	Linear acceleration (conditionally stable scheme)
$\beta = 1/4 ; \gamma = 1/2$	Average acceleration or trapezoidal rule (unconditionally stable scheme in linear analyses);
$\beta = 1/12 ; \gamma = 1/2$	Fox-Goodwin (fourth order accurate)

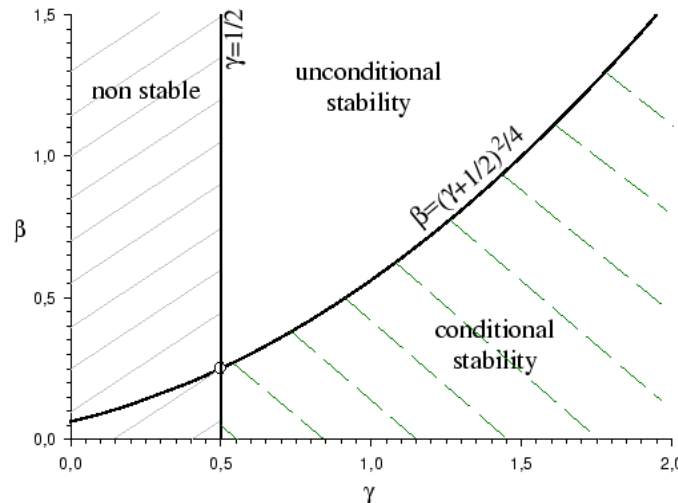


Figure 7.1: Newmark Time Integration

7.1.2 Input Motion

One, two and three directions of excitations are available: longitudinal, transverse and vertical directions (Figure 2.1 and Figure 7.2).

The bedrock is assumed to be rigid, the input motion is total motion; Base seismic excitation can be defined by either of the following two methods:

- i) Via a built-in input motion library. This library includes near-fault soil surface motions as well as long-duration rock outcrop motions recorded during past strong earthquakes worldwide.
- ii) ‘U-Shake’, a user-defined input motion (Figure 7.3). The input motion file to be defined should consist of two columns, Time (seconds) and Acceleration (g), delimited by SPACE(S).

Below is an example of a user-defined input motion file:

```
0.00    0.000
0.02    0.005
...     .....
19.98   0.004
20.00   0.000
```

Note that the user-defined input motion file must be placed in the subfolder “motions/”. (This subfolder also contains all provided built-in input motion files).

The amplitude of the input motion can be scaled by a factor ranging from 0.01 to 1.0. In addition, if ‘0.2g sinusoidal motion’ is chosen, the user must specify excitation frequency and number of cycles (Figure 2.1).

Scale Factor The amplitude of the input motion is multiplied by the Scale Factor. The Scale Factor may be positive or negative.

Frequency The Frequency (in Hz) has to be specified if harmonic “sinusoidal motion” is chosen

Number of Cycles The Number of Cycles has to be specified if “sinusoidal motion” is chosen.

☒ Base Shaking

Input Motion

☒ Longitudinal (X) ☒ Transverse (Y) ☒ Vertical (Z)

X Tapered 0.2g sinusoidal motion

Y Tapered 0.2g sinusoidal motion

Z Tapered 0.2g sinusoidal motion

	X	Y	Z
Frequency (0.5-5Hz)	1	1	1
Number of Cycles (3-30)	10	10	10
Scale Factor (0.01-1)	1	1	1

Boundary Conditions

B.C. Type Rigid Box ☐ Fixed Vert

Bedrock Type Rigid Bedrock

Model Inclination along Longitudinal Direction

Ground Surface Inclination Angle (0-30 deg) 0

Whole Model Inclination Angle (0-10 deg) 0

Figure 7.2: Definition of 3D base excitation and boundary conditions.

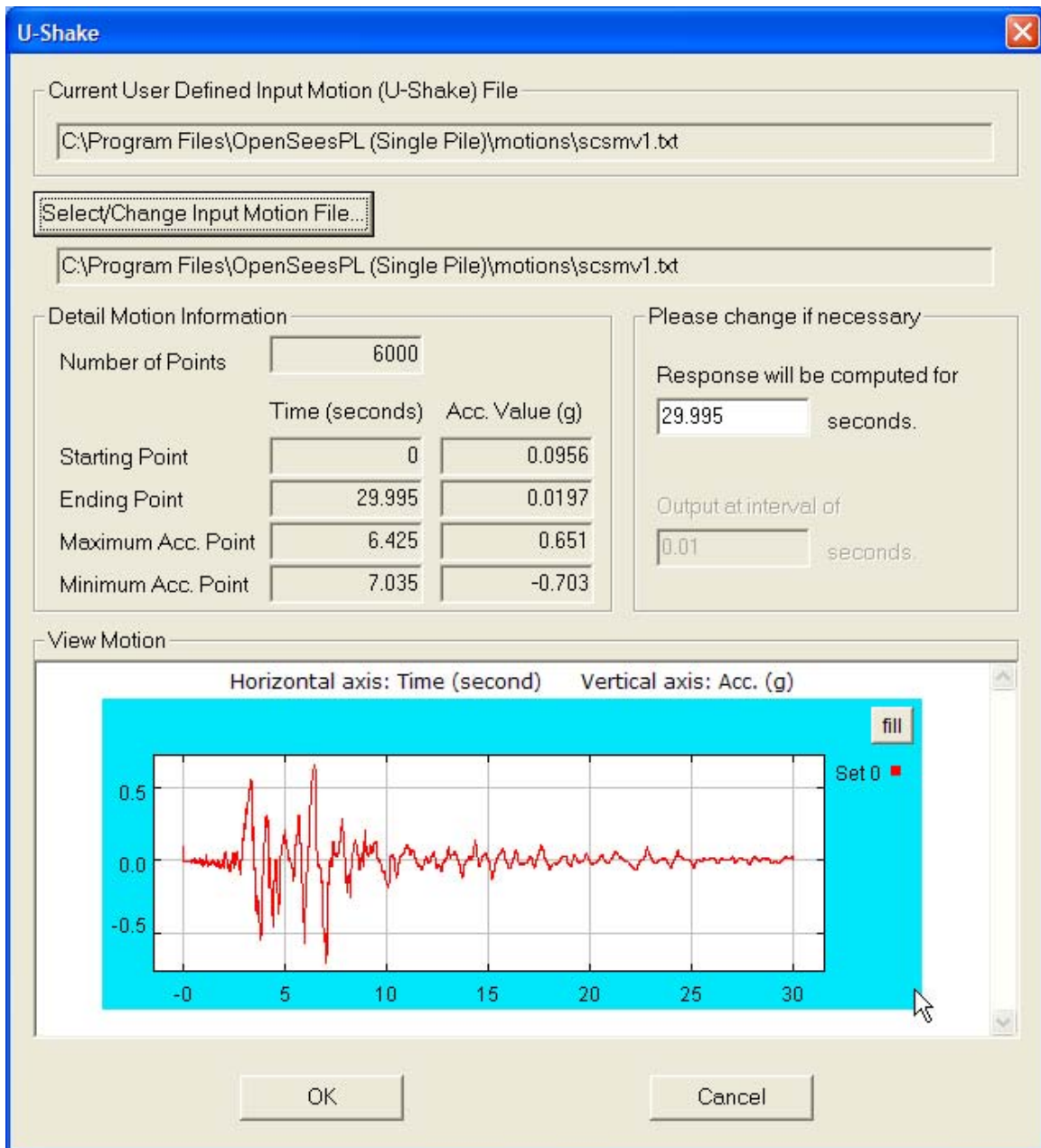


Figure 7.3: User-defined input motion (U-Shake).

7.1.3 Model Inclination

Inclined models can be defined by the following parameters (Figure 2.1):

Ground Surface Inclination Angle along Longitudinal Direction The inclination angle of the ground surface along the longitudinal direction (in degrees) (zero degree represents level ground surface).

Whole Model Inclination Angle along Longitudinal Direction The inclination angle in degrees of the whole model (zero degree represents level ground). For mildly-inclined infinite-slopes, suggested values are from 0 to 10 degrees.

7.2 Time History Output

7.2.1 Soil Response Time Histories

To view the soil response time histories, click **Soil Response Histories** in Menu **Display**.

The figures show the response time histories of the soil domain from the ground surface till the bottom, at a number of locations which are along the longitudinal direction crossing the pile center.

The following types of response time histories are available:

- Longitudinal acceleration time histories
- Longitudinal displacement (rel. to base) time histories
- Transvers acceleration time histories
- Transverse displacement (rel. to base) time histories
- Vertical acceleration time histories
- Vertical displacement time histories
- Excess pore pressure time histories
- Shear stress (xy) vs. strain & eff. confinement
- Shear stress (yz) vs. strain & eff. confinement
- Shear stress (zx) vs. strain & eff. confinement
- Longitudinal normal stress time histories
- Transverse normal stress time histories
- Effective vertical normal stress time histories
- Shear stress (xy) time histories
- Shear stress (yz) time histories
- Shear stress (zx) time histories
- Longitudinal normal strain time histories
- Transverse normal strain time histories
- Vertical normal strain time histories
- Shear strain (xy) time histories
- Shear strain (yz) time histories
- Shear strain (zx) time histories

Pile response and deformed mesh output are also available in a base shaking analysis. Please refer to Section 6.1.4.

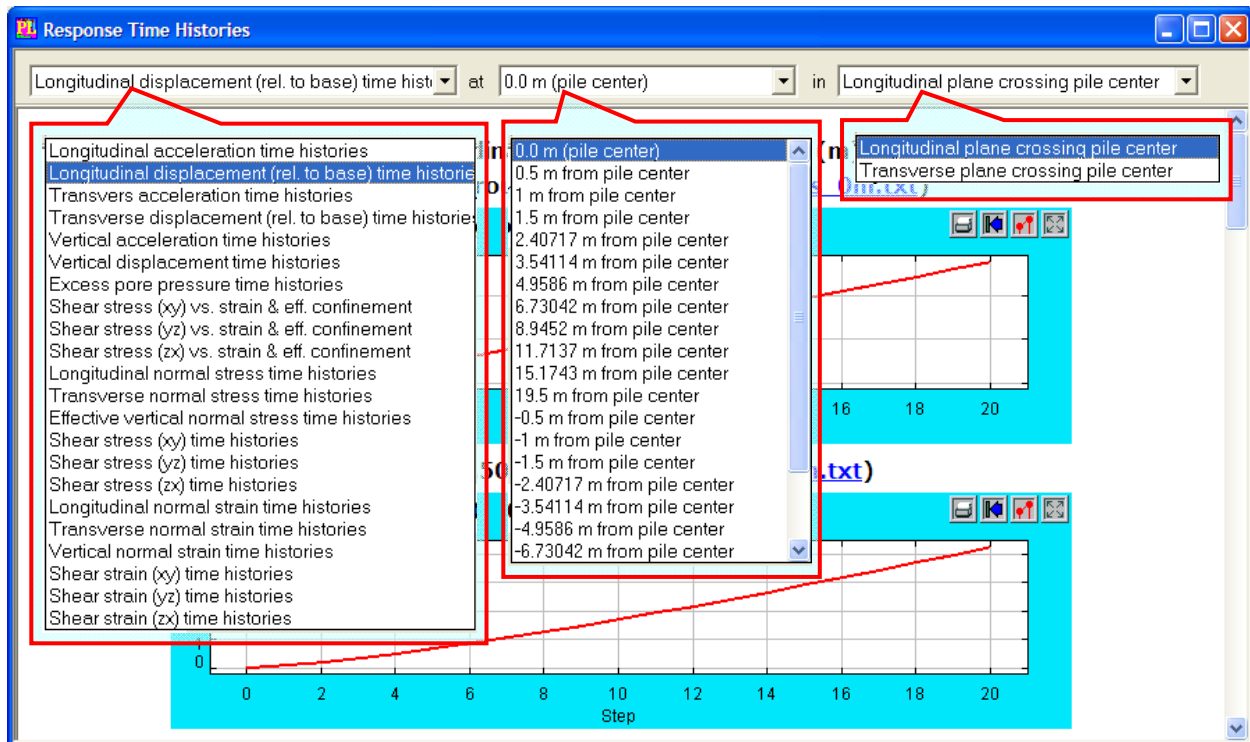


Figure 7.4: Response time histories window.

8. Pile Group

8.1 Pile Group Parameters

To activate pile group, check **Pile Group**. The pile group is defined by the following parameters (Figure 8.1):

Number of Piles The number of piles along X-direction (longitudinal) and Y-direction (transverse). Note that both numbers do not have to be the same. Therefore, one can easily build a m by n pile group model in OpenSeesPL. If “1” is entered for both, single pile will be considered.

Spacing The spacing (specified as a factor of the pile diameter) between pile centers along X-direction (longitudinal) and Y-direction (transverse). Obviously, the spacing must be greater than 1.

If **Fixed** is chosen for the pile head, a rigid pile cap will be employed. If **Free/Pinned** is chosen, the pinned connection is considered for the pile heads of the pile group.

Pile

Pile Type: Circular

Diameter/Side Length (D): 1 [m]

Total Pile Length: 12 [m]

Pile Length above Surface: 6 [m]

Pile Head: Fixed (selected), Free/Pinned

Pile Head Mass: 0 [ton]

Axial Load: 0 [kN]

☒ Pile Group

	X-Dir.	Y-Dir.
Number of Piles	3	3
Spacing (xD)	3	3

Linear Beam Properties

☒ Linear Beam Element

Young's Modulus: 30000000 [kPa]

Mass Density: 0 [ton/m3]

Moment of Inertia: 0.0490873 [m4]

Re-Calculate

☐ Nonlinear Beam Element - Aggregator Section

Modify...

☐ Nonlinear Beam Element - Fiber Section

Modify...

OK Cancel

Figure 8.1: Pile group definition.

8.2 Pile Group Meshing

To define the finite element mesh for a pile group model, click **Mesh Parameters** button in the **Model Input** window (Figure 5.1). And click **Pile Group** in the **Horizontal Meshing** tab to define the controlling parameters in the horizontal directions (Figure 8.2).

For **General Definition** and **Vertical Meshing** Tabs, please refer to Chapter 5. Figure 8.3 shows a sample mesh of a 3 x 3 pile group model (half mesh configuration).

The screenshot shows the 'Mesh' dialog box with the 'Pile Group' tab selected. The left sidebar shows a tree view with 'General Definition', 'Horizontal Meshing', 'Single Pile', 'Pile Group' (selected), 'Vertical Meshing', and 'Mesh Scaling'. The main area contains the following settings:

Longitudinal (X) Transverse (Y)

Number of Mesh Layers Between Piles: 2 2

Ratio of Adjacent Element Width over Distant: 1 1

Longitudinal

Mesh Layer # (after Pile Group)	Length [m]	# of Mesh Layers	Uniform Meshing?	Ratio of Element Length over Next
1st Layer after Interface	1	2	<input checked="" type="checkbox"/>	1
2nd Layer	10	2	<input type="checkbox"/>	0.5
3rd Layer	0	1	<input checked="" type="checkbox"/>	1
4th Layer	0	1	<input checked="" type="checkbox"/>	1
5th Layer	0	1	<input checked="" type="checkbox"/>	1

☒ Use Longitudinal Parameters for Transverse Direction

Transverse

Mesh Layer # (after Pile Group)	Length [m]	# of Mesh Layers	Uniform Meshing?	Ratio of Element Length over Next
1st Layer after Interface	1	2	<input checked="" type="checkbox"/>	1
2nd Layer	10	2	<input type="checkbox"/>	0.5
3rd Layer	0	1	<input checked="" type="checkbox"/>	1
4th Layer	0	1	<input checked="" type="checkbox"/>	1
5th Layer	0	1	<input checked="" type="checkbox"/>	1

Buttons: OK, Cancel, Apply

Figure 8.2: Pile group horizontal meshing.

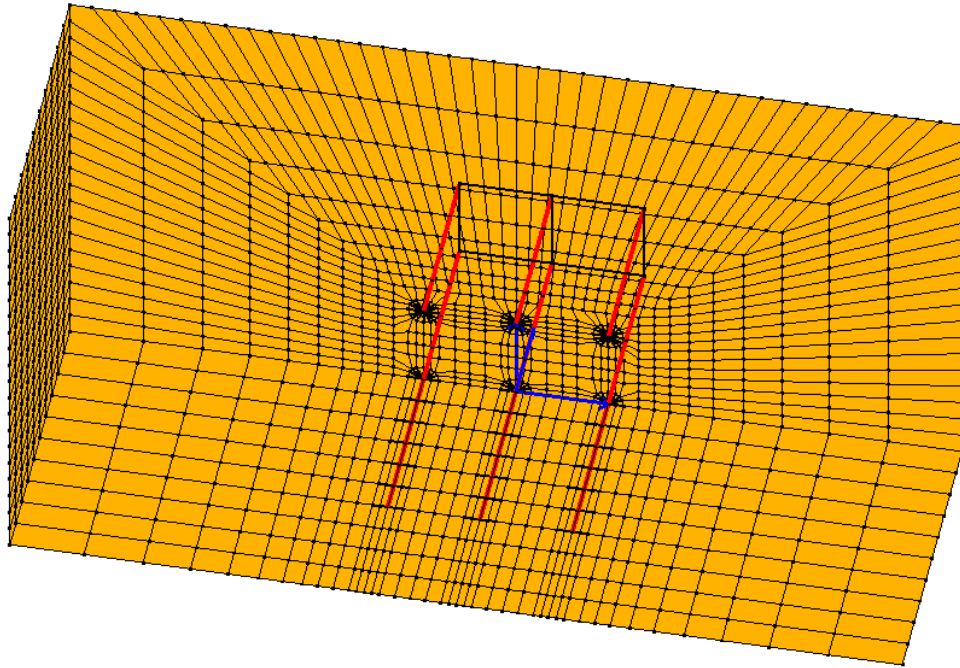


Figure 8.3: Sample mesh of a 3 by 3 pile group model (half mesh configuration).

8.3 Output for a Pile Group Model

In a pile group analysis, output is available for the responses of each pile (Figures 8.4-8.8).

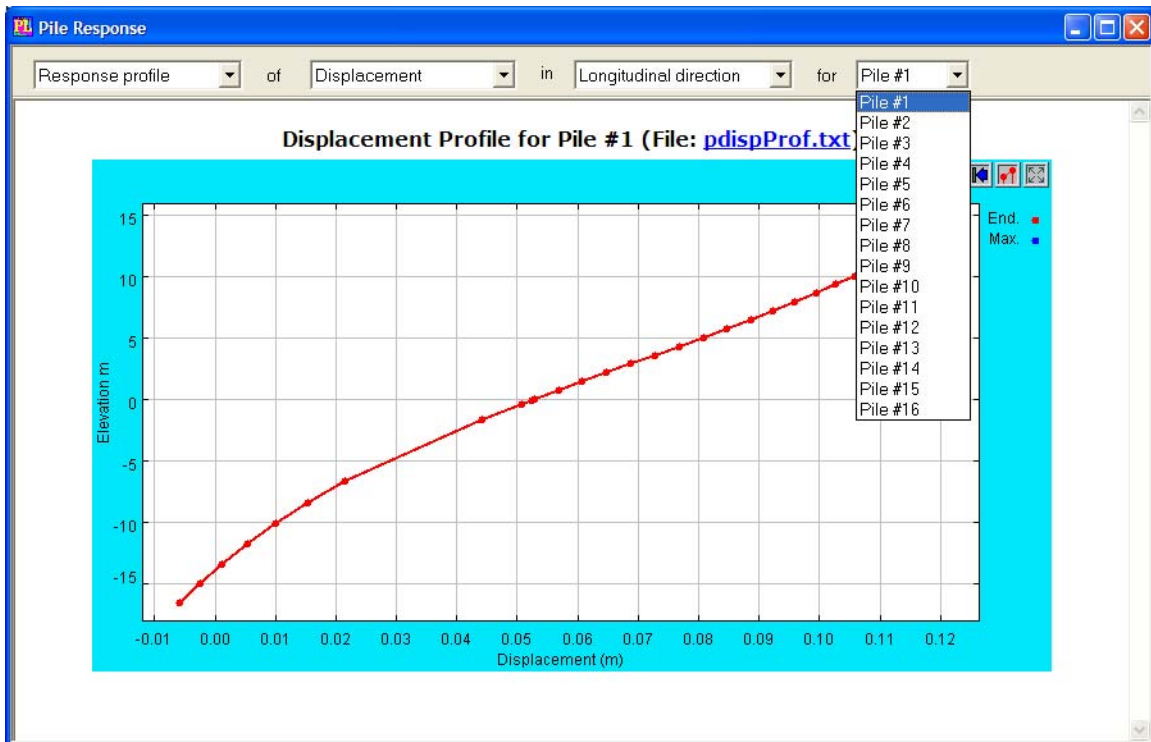


Figure 8.4: Pile response profiles for a pile group model.

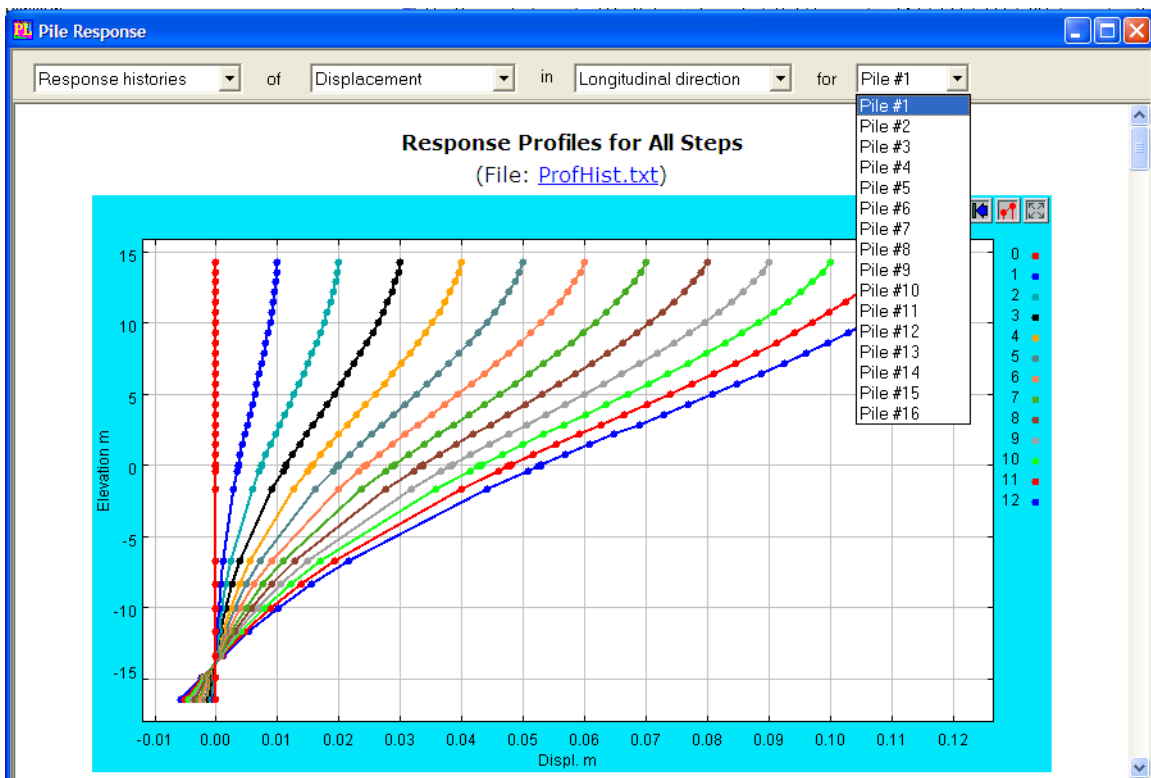


Figure 8.5: Pile response time histories for a pile group model.

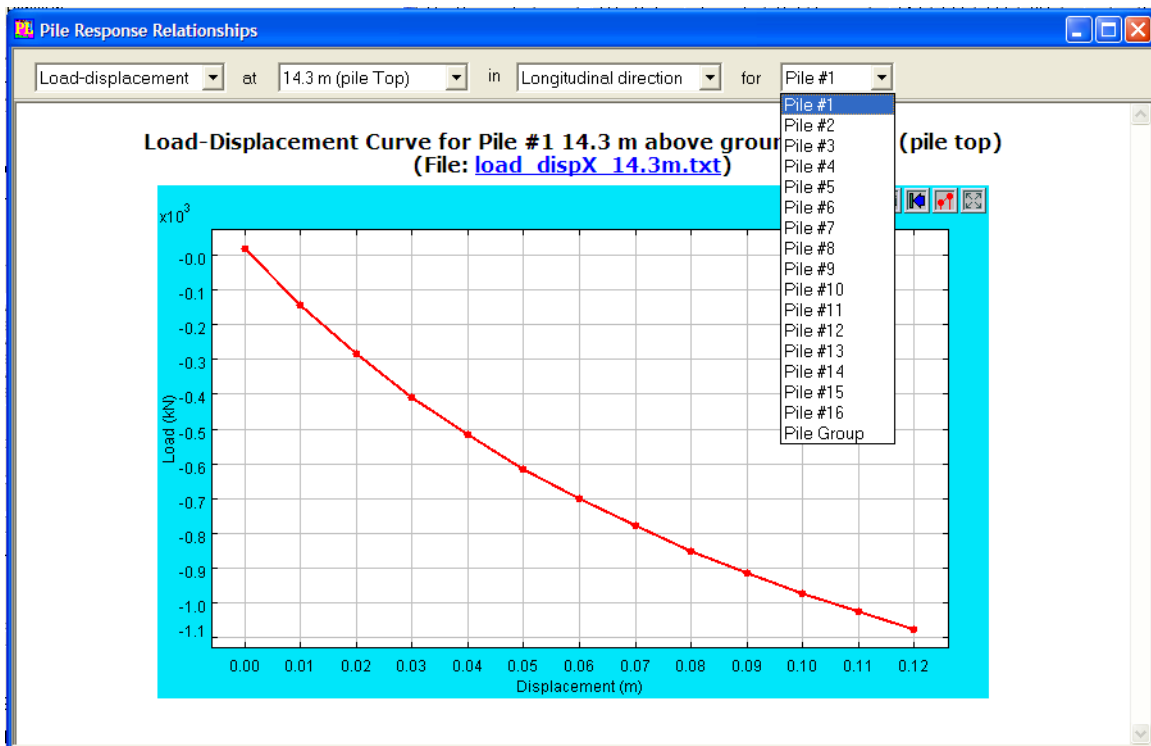


Figure 8.6: Pile response relationships for a pile group model.

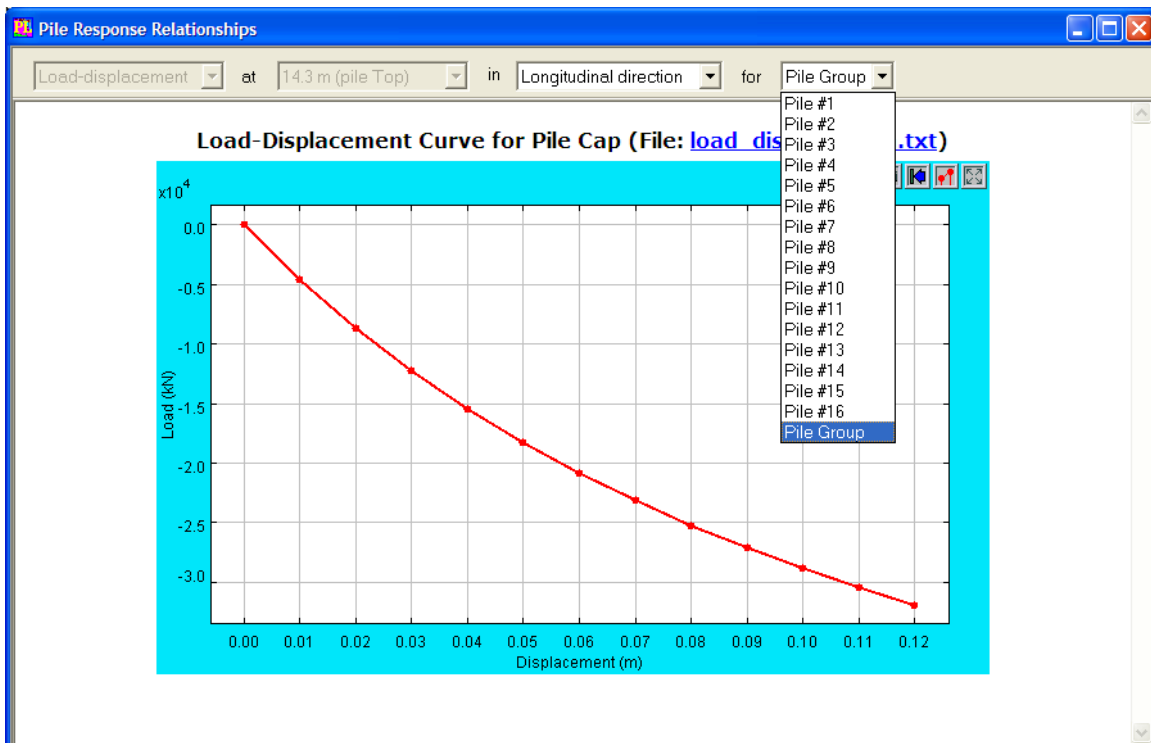


Figure 8.7: Pile response relationships at the pile cap for a pile group model.

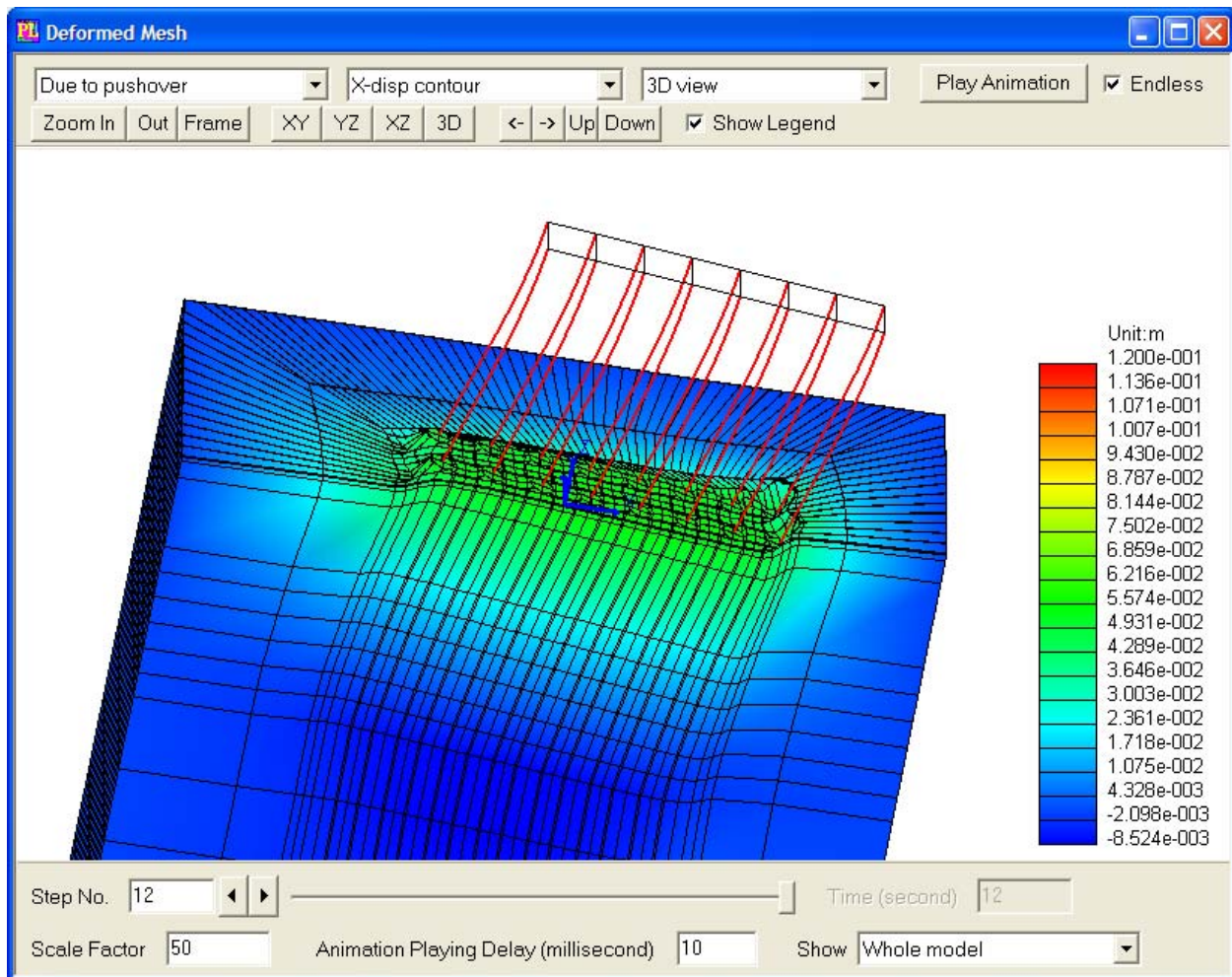


Figure 8.8: Deformed mesh of a pile group model.

Appendix A Mesh

How to Define the Soil Finite Element

Step 1

In the user interface, click **Pile Parameters**. With reference to Figure 3.1, define the following parameters according to your preference:

Diameter: The pile outer diameter.

Total Pile Length: Starting from the pile head all the way to the pile tip.

Pile Length above Surface: from pile head to mud-line (ground surface).

Soil Parameters: make sure at least the total “**Thickness**” of soil layers is defined: This is the total thickness of the ground stratum from the ground surface all the way down to the base of the soil mesh. Make sure that the pile tip is within the defined soil domain depth.

Note: Earthquake input motion is imparted along the base of the soil mesh. This base is assumed to represent rigid bedrock. As such, this input earthquake excitation constitutes total motion imparted at this Bedrock level.

Step 2

Click **Mesh Parameters** to define additional meshing parameters (please refer to Chapter 5 and Figure 5.1).

The finite element mesh created with the above default values is shown in Figure A.1. Examples of mesh generation are shown in Figures A.2-A.4.

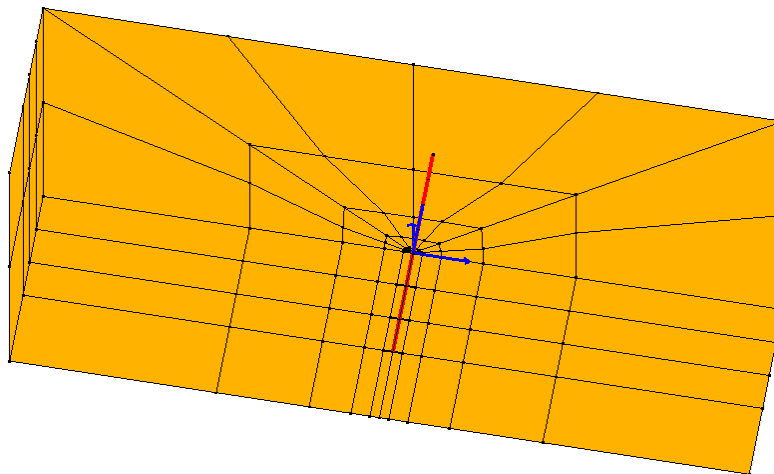
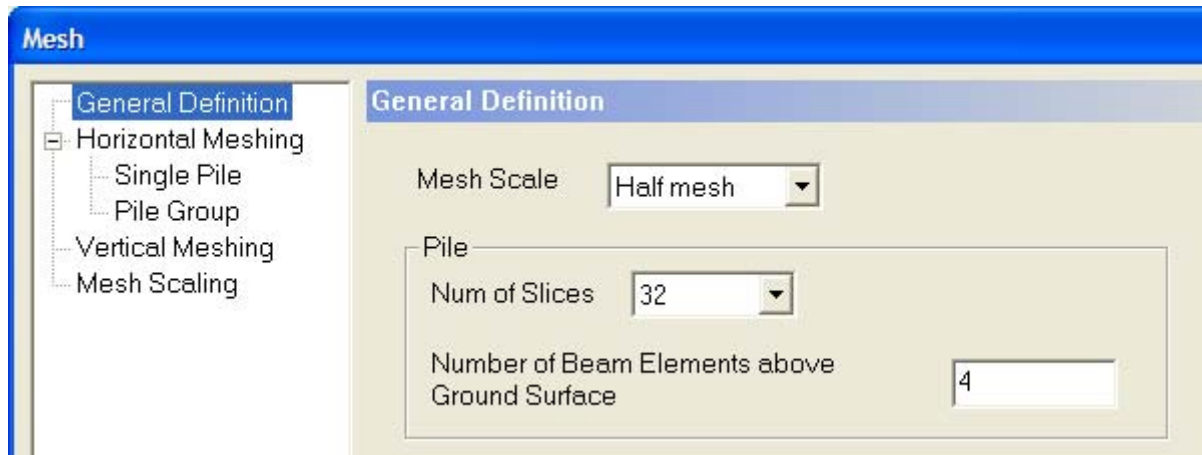
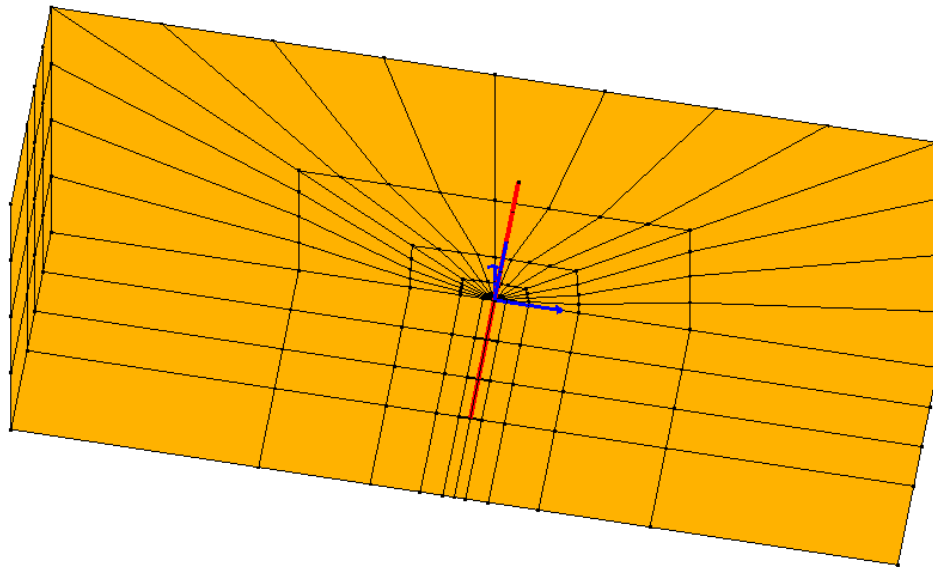


Figure A.1: Finite element mesh created with default values.



a)



b)

Figure A.2: Mesh refinement example 1: a) Change “Num of Slices” to 32; b) the resulting mesh

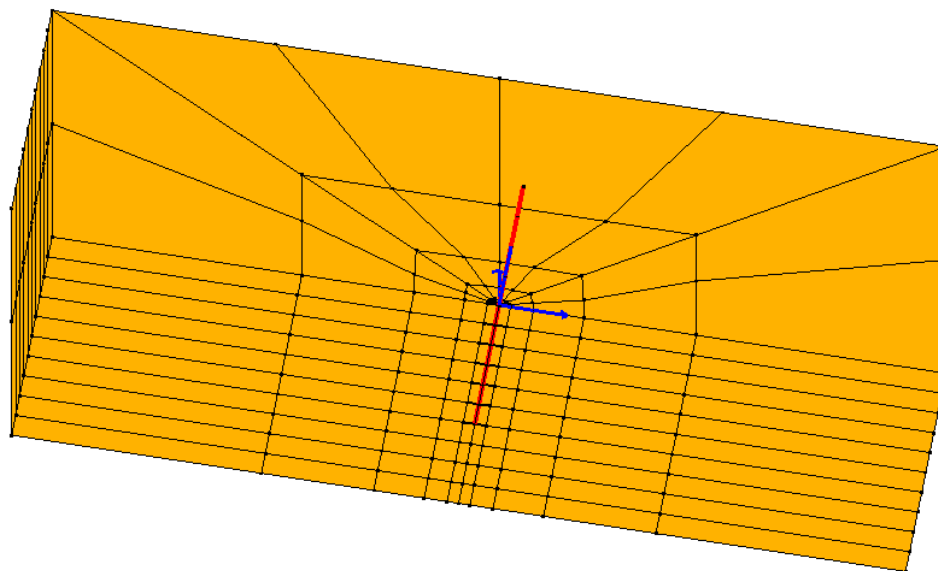
Mesh

- General Definition
- Horizontal Meshing
- Single Pile
- Pile Group
- Vertical Meshing
- Mesh Scaling

Vertical Meshing

Mesh Layer # (From Topdown)	Height [m]	Number of Mesh Layers	Uniform Meshing?	Ratio of Top Element Height over Bottom
1:	6	6	<input checked="" type="checkbox"/>	1
2:	4	4	<input checked="" type="checkbox"/>	1
3:	0	1	<input checked="" type="checkbox"/>	1
4:	0	1	<input checked="" type="checkbox"/>	1
5:	0	1	<input checked="" type="checkbox"/>	1
6:	0	1	<input checked="" type="checkbox"/>	1
7:	0	1	<input checked="" type="checkbox"/>	1
8:	0	1	<input checked="" type="checkbox"/>	1
9:	0	1	<input checked="" type="checkbox"/>	1
10:	0	1	<input checked="" type="checkbox"/>	1
11:	0	1	<input checked="" type="checkbox"/>	1

a)



b)

Figure A.3: Mesh refinement example 2: a) Change “Number of Mesh Layers” in the vertical direction; b) the resulting mesh

Mesh

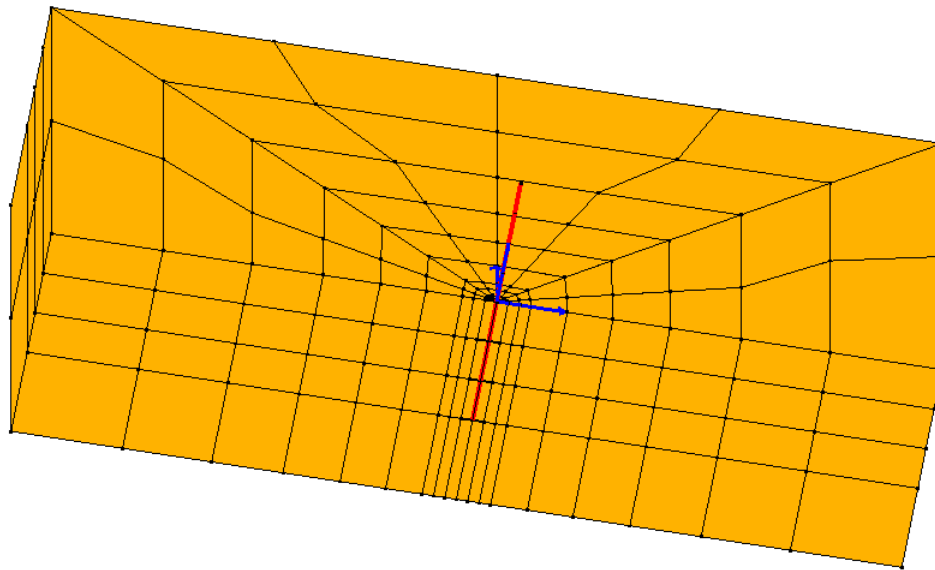
- General Definition
 - Horizontal Meshing
 - Single Pile**
 - Pile Group
 - Vertical Meshing
 - Mesh Scaling

Single Pile

Mesh Layer # (From Pile Center)	Length [m]	# of Mesh Layers	Uniform Meshing?	Ratio of Element Length over Next
Pile Radius	0.5	1	<input checked="" type="checkbox"/>	1
1st Layer after Interface	1	2	<input checked="" type="checkbox"/>	1
2nd Layer	18	6	<input type="checkbox"/>	0.8
3rd Layer	0	1	<input checked="" type="checkbox"/>	1
4th Layer	0	1	<input checked="" type="checkbox"/>	1
5th Layer	0	1	<input checked="" type="checkbox"/>	1
6th Layer	0	1	<input checked="" type="checkbox"/>	1
Outermost Zone	1	1	<input checked="" type="checkbox"/>	1

Note: Definitions following a 0-length section will be ignored, e.g., if you do not need the 3rd layer and beyond, enter 0 for the length of the 3rd layer.

a)



b)

Figure A.4: Mesh refinement example 3: a) Change meshing controlling parameters in the horizontal direction; b) the resulting mesh

Appendix B Own Weight Application with Dry and Saturated Soil Cases

Boundary Conditions:

The boundary conditions available in OpenSeesPL include Shear Beam, Rigid Box, and Periodic Boundary.

1) Shear Beam

In this case, the front and back nodes at any depth move together (horizontal and vertical directions). The Shear Beam boundary condition, if it's chosen, is enforced for all runs.

Rollers are used for lateral and base boundaries for all gravity runs. The base nodes are fixed after the first run.

If **Fixed Vert** is checked, all nodes at lateral boundaries will be fixed in vertical direction before the dynamic run.

2) Rigid Box

In gravity runs, lateral boundaries are fixed in both horizontal directions and free in vertical direction. Rollers are used for base nodes, which will be fixed after the first run.

If **Fixed Vert** is checked, all nodes at lateral boundaries will be fixed in vertical direction before the dynamic run.

3) Periodic Boundary

In this case, each node on the front boundary moves the same as the analogous node on the back boundary (horizontal and vertical directions). The Periodic boundary condition, if it's chosen, is enforced for all runs.

For gravity runs, rollers are used for lateral and base boundaries. The base nodes are fixed after the first run.

If **Fixed Vert** is checked, all nodes at lateral boundaries will be fixed in vertical direction before the dynamic run.

Dry soil case with level ground

1) Application of soil own weight with elastic soil properties

At first the defined soil properties are used to set up the soil constitutive model. A static solver is used and own weight is applied in one step with elastic soil properties. Default is global elastic modulus (600,000 kPa by default) and global initial lateral/vertical confinement ratio ($K_0 = 0.9$)

by default) for the entire soil domain. These elastic soil properties are used to define an elastic stiffness matrix (Kmatrix1). A default convergence tolerance of 0.0001 is used (displacement norm), which the user can specify in the **OpeSees Parameters** section (from **Analysis Options**).

Boundary conditions (BC1):

Lateral boundaries: Rollers are used on the lateral boundaries to prevent lateral deformation and vertical displacement is allowed.

Base: Rollers are used to prevent vertical displacement, but lateral deformation is allowed.

2) Switching from elastic soil properties to nonlinear soil properties

The actual defined soil properties in every part of the mesh are activated, and nonlinear (if specified) properties are activated as well.

The static solver is used, and Kmatrix1 is used for convergence. A convergence tolerance of 0.0001 is used (displacement norm). The boundary conditions for this step remain those of BC1.

3) Including the beam column elements and their own weight

A new mass and stiffness matrix is built based on the latest tangent soil stress-strain state, and the linear properties of the beam column elements. A convergence tolerance of 0.0001 is used (displacement norm). The load is applied in 20 steps by default (the user can modify this value in the **OpeSees Parameters** section (from **Analysis Options**)). The stiffness matrix is not updated. The boundary conditions for this step remain those of BC1.

4) Solution phase

Solution is started with a stiffness matrix based on the latest soil and beam column stress-strain state. Four different analysis scenarios are possible:

Static Push-over analysis

The static solver is used with a convergence tolerance of 0.0001 that the user can modify in the **OpeSees Parameters** section (from **Analysis Options**) (displacement norm).

Boundary conditions for this case are: Default is fixed boundaries everywhere, but the user can change that to Shear Beam or Periodic Boundary.

Dynamic push-over analysis

In this case, a dynamic solver is used (modified Newton-Raphson) with the time integration parameters $\gamma = 0.6$ and $\beta = 0.3025$, and the actual user specified time step. Note that the user can also modify the Rayleigh mass and stiffness proportional viscous damping parameters (which are set by default to 2% at the frequencies of 1 Hz and 6 Hz).

After the dynamic load has been applied, analysis can proceed for a user specified number of seconds so that the “free vibration response” can be assessed if so desired.

Boundary conditions for this case are: Default is fixed boundaries everywhere, but the user can change that to Shear Beam or Periodic Boundary.

Dynamic Base (earthquake) excitation:

In this case, a dynamic solver is used (modified Newton-Raphson) with the time integration parameters $\gamma = 0.6$ and $\beta = 0.3025$, and the actual user specified time step. The convergence tolerance of 0.0001 is the default but the user can modify this value in the **OpeSees Parameters** section (from **Analysis Options**) (displacement norm). Note that the user can also modify the Rayleigh mass and stiffness proportional viscous damping parameters which are set by default to 2% at the frequencies of 1 Hz and 6 Hz).

After the dynamic load has been applied, analysis can proceed for a user specified number of seconds so that the “free vibration response” can be assessed if so desired.

Boundary conditions for this case are: Default is fixed boundaries everywhere, with the base moving according to the applied base excitation. The user might wish to activate alternate boundary conditions along the lateral boundaries in the form of Shear beam boundary conditions where the front and back nodes at any depth move together, or a periodic boundary condition where each node on the front boundary moves the same as the analogous node on the back boundary (and the vertical is free, but can be fixed by the user).

Eigenvalue analysis:

In this step the mass and stiffness matrices corresponding to the latest stress-strain state (after application of own weight of the beam-column elements) are used to compute natural frequencies and mode shapes (using the static solver).

Boundary conditions for this case are: Default is fixed boundaries everywhere, with the base moving according to the applied base excitation. The user might wish to activate alternate boundary conditions along the lateral boundaries in the form of Shear beam boundary conditions where the front and back nodes at any depth move together, or a periodic boundary condition where each node on the front boundary moves the same as the analogous node on the back boundary (and the vertical is free, but can be fixed by the user).

Dry soil case with mildly inclined ground and soil with water table specified

1) Application of soil own weight with elastic soil properties

A dynamic solver is used and own weight is applied in 5 steps (time step is set to 50,000 secs and gamma γ and beta β parameters are set to 1.5 and 1 in order to obtain a static solution) with

elastic soil properties (elastic modulus = 600,000 kPa and initial lateral/vertical confinement ratio $K_0 = 0.9$ by default) and a default global very large permeability coefficient (100 m/s by default; the permeability will be changed to the user-specified value before the dynamic run).

Default is global elastic modulus (600,000 kPa by default) and global initial lateral/vertical confinement ratio ($K_0 = 0.9$ by default) for the entire soil domain. These specified global values will be used for the top soil layer. For all other soil layers including the pile zone and the interfacing zone, the elastic modulus employed is equal to the above global value (600,000 kPa by default) times the ratio of the mass density of the current soil layer over the top soil layer.

These elastic soil properties are used to define an elastic stiffness matrix (Kmatrix1). A default convergence tolerance of 0.0001 is used (displacement norm), which the user can specify in the **OpeSees Parameters** section (from **Analysis Options**).

Boundary conditions (BC1):

Lateral boundaries: Rollers are used on the lateral boundaries to prevent lateral deformation and vertical displacement is allowed.

Base: Rollers are used to prevent vertical displacement, but lateral deformation is allowed.

2) Model inclination

If the model is inclined, an extra run for applying the horizontal gravity factor is added. The horizontal gravity factor is applied at the based nodes as acceleration input (the base nodes have to be fixed before this run). The vertical gravity factor is applied at the first run (through the soil element body force factor).

3) Switching from elastic soil properties to nonlinear soil properties

The actual defined soil properties in every part of the mesh are activated, and nonlinear (if specified) properties are activated as well.

The dynamic solver is used (similar to item 1 above), and Kmatrix1 is used for convergence. Own weight is applied in 5 steps (time step is set to 50,000 secs). A convergence tolerance of 0.0001 is used (displacement norm). The boundary conditions for this step remain those of BC1.

4) Including the beam column elements and their own weight

A new mass and stiffness matrix is built based on the latest tangent soil stress-strain state, and the linear properties of the beam column elements. A convergence tolerance of 0.0001 is used (displacement norm). The load is applied in 20 steps by default (the user can modify this value in the the **OpeSees Parameters** section (from **Analysis Options**). The stiff matrix is not updated.

The dynamic solver is used (similar to Section 2, and 5 time steps are allowed with no additional input excitation to ensure convergence to a stable static solution). The boundary conditions for this step remain those of BC1.

5) Solution Phase

Solution is started with a stiffness matrix based on the latest soil and beam column stress-strain state. Four different analysis scenarios are possible:

Static Push-over analysis:

The dynamic solver is used (similar to item 1 above) with a convergence tolerance of 0.0001 (displacement norm) that the user can modify in the **OpeSees Parameters** section (from **Analysis Options**).

Boundary conditions for this case are: Default is fixed boundaries everywhere, but the user can change that to Shear Beam or Periodic Boundary.

Dynamic push-over analysis:

In this case, a dynamic solver is used (modified Newton-Raphson) with the time integration parameters $\gamma = 0.6$ and $\beta = 0.3025$, and the actual user specified time step. Note that the user can also modify the Rayleigh mass and stiffness proportional viscous damping parameters (which are set by default to 2% at the frequencies of 1 Hz and 6 Hz).

After the dynamic load has been applied, analysis can proceed for a user specified number of seconds so that the “free vibration response” can be assessed if so desired.

Boundary conditions for this case are: Default is fixed boundaries everywhere, but the user can change that to Shear Beam or Periodic Boundary.

Dynamic Base (earthquake) excitation:

In this case, a dynamic solver is used (modified Newton-Raphson) with the time integration parameters $\gamma = 0.6$ and $\beta = 0.3025$, and the actual user specified time step. The convergence tolerance of 0.0001 is the default but the user can modify this value (displacement norm) in the **OpeSees Parameters** section (from **Analysis Options**). Note that the user can also modify the Rayleigh mass and stiffness proportional viscous damping parameters which are set by default to 2% at the frequencies of 1 Hz and 6 Hz).

After the dynamic load has been applied, analysis can proceed for a user specified number of seconds so that the “free vibration response” can be assessed if so desired.

Boundary conditions for this case are: Default is fixed boundaries everywhere, with the base moving according to the applied base excitation. The user might wish to activate alternate boundary conditions along the lateral boundaries in the form of Shear beam boundary conditions where the front and back nodes at any depth move together, or a periodic boundary condition where each node on the front boundary moves the same as the analogous node on the back

boundary (and the vertical is free, but can be fixed by the user).

Eigenvalue analysis:

In this step the mass and stiffness matrices corresponding to the latest stress-strain state (after application of own weight of the beam-column elements) are used to compute natural frequencies and mode shapes (using a dynamic solver).

Boundary conditions for this case are: Default is fixed boundaries everywhere, with the base moving according to the applied base excitation. The user might wish to activate alternate boundary conditions along the lateral boundaries in the form of Shear beam boundary conditions where the front and back nodes at any depth move together, or a periodic boundary condition where each node on the front boundary moves the same as the analogous node on the back boundary (and the vertical is free, but can be fixed by the user).

Appendix C Benchmark Linear Finite Element Analysis of Laterally Loaded Single Pile Using OpenSees & Comparison with Analytical Solution

Introduction

In this study:

- I) The response of a laterally loaded pile obtained using the OpenSeesPL interface is compared with the analytical elastic solution proposed by Abedzadeh and Pak (2004). Detailed information about the analytical elastic solution is provided in Appendix C-I (please see this end of Appendix C).
- II) Based on the linear analysis presented below, nonlinear soil response is addressed in Appendix C-II (please see this end of Appendix C).

Laterally Loaded Pile

Pile Data

The pile employed in the OpenSees simulation is circular with a diameter of 16" (radius $a = 8"$) while the one for the analytical elastic solution is a cylindrical pipe pile of the same radius and a wall thickness $h = 0.1a$. Both cases have the same pile length $l = 33.3$ ft ($l/a = 50$). The cross-sectional moment of inertia of the pipe pile $I = \pi a^3 h = 1286.8$ in⁴, which will be used for the circular pile in the OpenSees simulation.

In summary, the geometric and elastic material properties of the pile are listed below:

Radius $a = 8"$

Pile length $l = 33.3$ ft

Young's Modulus of Pile $E_p = 29000$ ksi

Moment of Inertia of Pile $I = 1286.8$ in⁴

Soil Domain

The pile is assumed to be fully embedded in a homogeneous, isotropic, linearly elastic half-space. The elastic properties of the soil are assumed constant along the depth (in order to compare with the analytical elastic solution) and are listed below:

Shear Modulus of Soil $G_s = 7.98$ ksi

Bulk Modulus of Soil $B = 13.288$ ksi (i.e., Poisson's ratio $\nu_s = 0.25$)

Submerged Unit Weight $\gamma' = 62.8$ pcf

The ratio of Young's Modulus of Pile (E_p) to the Shear Modulus of Soil (G_s):
 $E_p/G_s = 3634$ (which will be used later to obtain the analytical elastic solution by

interpolation).

Lateral Load

The pile head (free head condition), which is located at the ground surface, is subjected to a horizontal load (H) of 31.5 kips.

Finite Element Simulation

In view of symmetry, a half-mesh is studied as shown in Figure C.1. For comparison, both 8-node and 20-node elements are used (2,900 8-node brick elements, 20 beam-column elements and 189 rigid beam-column elements in total) in the OpenSeesPL simulation. Length of the mesh in the longitudinal direction is 520 ft, with 260 ft transversally (in this half-mesh configuration, resulting in a 520 ft x 520 soil domain in plan view). Layer thickness is 66 ft (the bottom of the soil domain is 32.7 ft below the pile tip, so as to mimic the analytical half-space solution).

The floating pile is modeled by beam-column elements, and rigid beam-column elements are used to model the pile size (diameter).

The following boundary conditions are enforced:

- I) The bottom of the domain is fixed in the longitudinal (x), transverse (y), and vertical (z) directions.
- II) Left, right and back planes of the mesh are fixed in x and y directions (the lateral directions) and free in z direction.
- III) Plane of symmetry is fixed in y direction and free in z and x direction (to model the full-mesh 3D solution).

The lateral load is applied at the pile head (ground level) in x (longitudinal) direction.

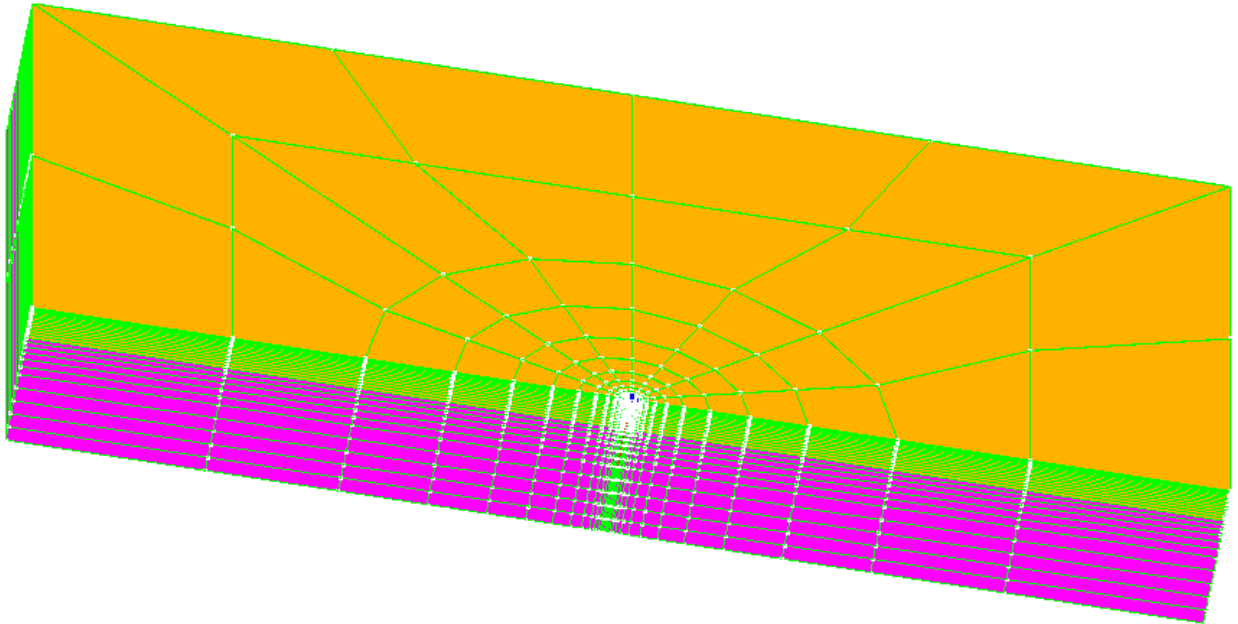
The above simulations were performed using OpenSeesPL (Lu et al., 2006).

Simulation Results and Comparison with Elastic Solution

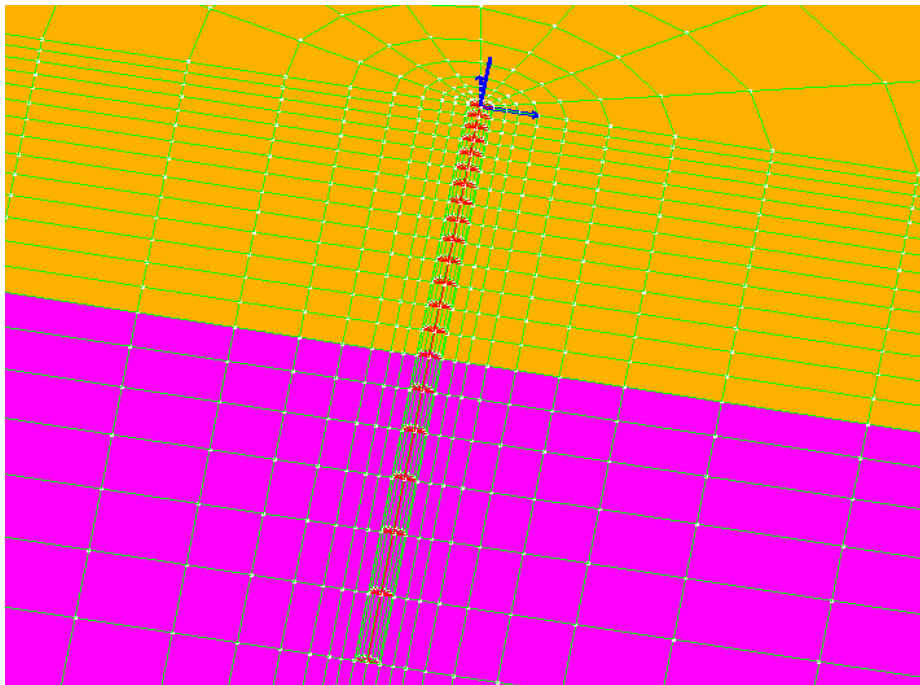
Deflection and bending moment response profiles obtained from OpenSees are shown in Figure C.2 and Figure C.3, along with the analytical elastic solution by Abedzadeh and Pak (2004) for comparison (note that the elastic solution was obtained by performing a linear interpolation of the normalized deflections and moments shown in Figure C.4 and Figure C.5 for $E_p/G_s = 3634$).

The pile head deflection and the maximum bending moment from OpenSees and the elastic solution are also listed in Table C.1. In general, the numerical results match well with the analytical elastic solution. The pile head deflection from the 20-node element mesh (0.043") is almost identical to the elastic solution (0.042").

For nonlinear run, please see Appendix C-II.



a) Isometric view



b) Pile head close-up

Figure C.1: Finite element mesh employed in this study.

Table C.1: Comparison of OpenSees results and the analytical elastic solution.

	OpenSees Results		Elastic solution by Abedzadeh and Pak (2004)
	8-node element	20-node element	
Pile head deflection (in)	0.039	0.043	0.042
Maximum moment M_{\max} (kip-ft)	30	31	27
Depth where M_{\max} occurs (ft)	2.87	2.87	2.7

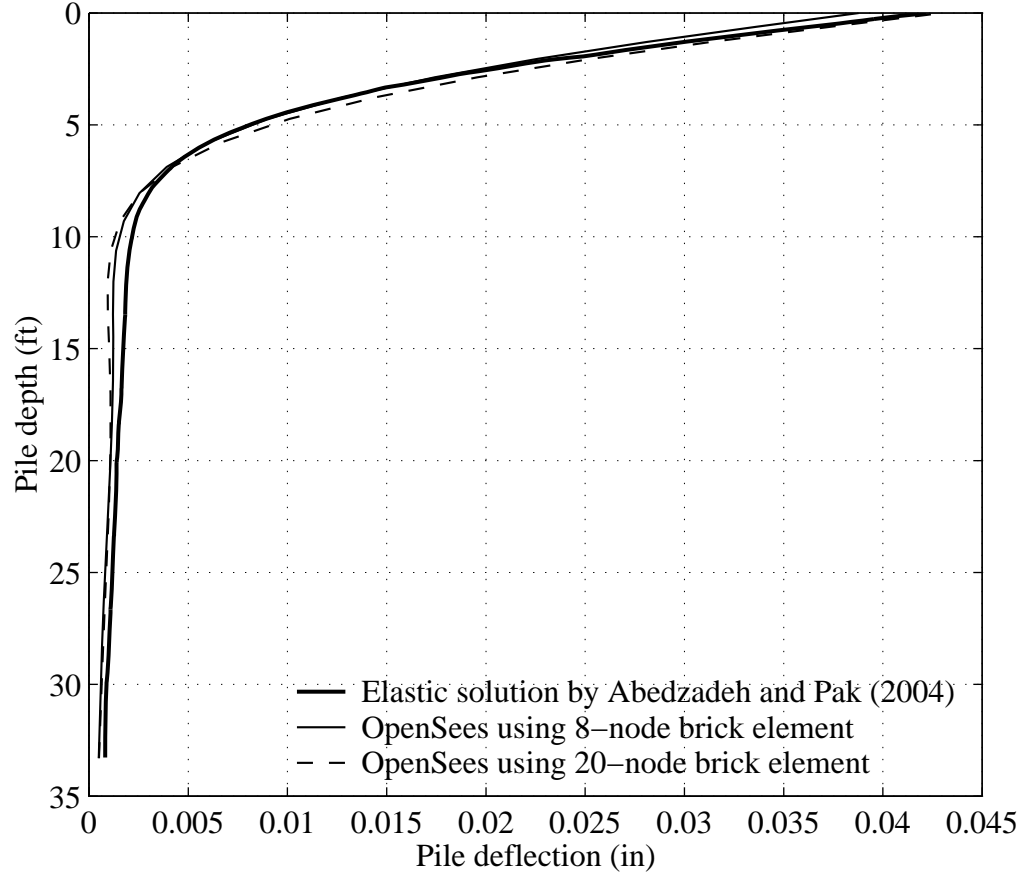


Figure C.2: Comparison of pile deflection profiles ($\nu_s=.25$, $l/a=50$).

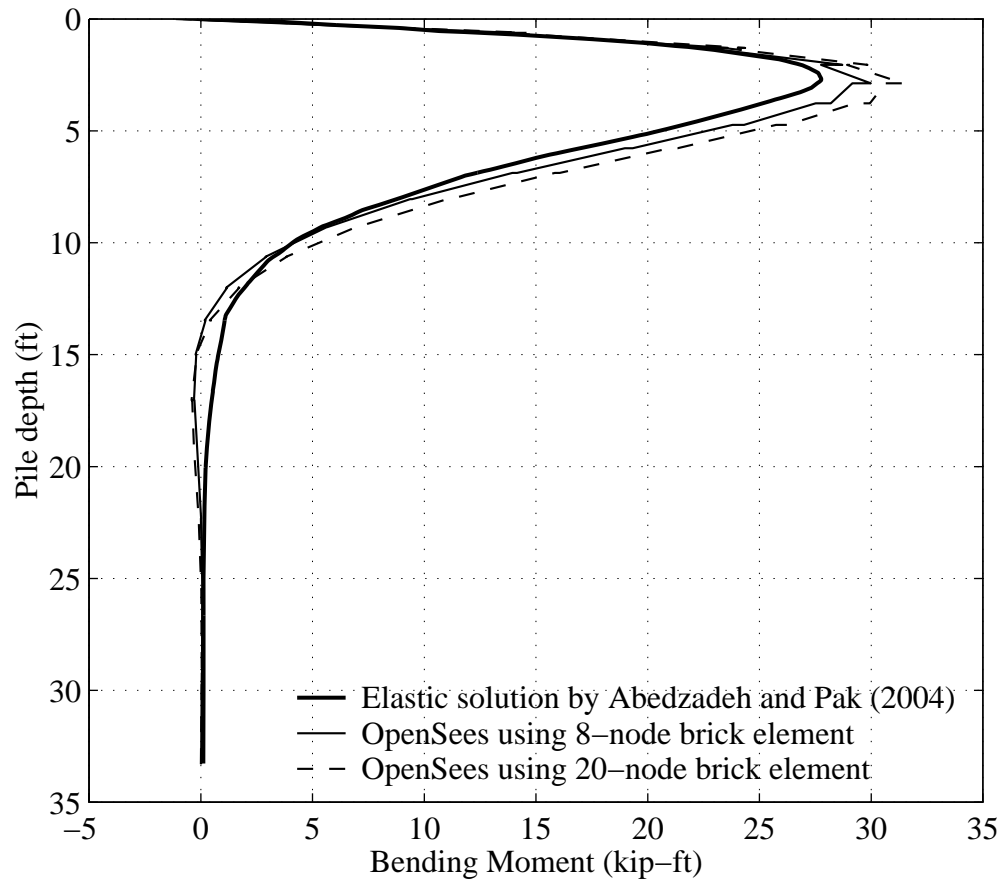


Figure C.3: Comparison of pile bending moment profiles ($v_s=.25$, $l/a=50$).

Appendix C-I: Elastic Solution of the Response of a Laterally Loaded Pile in a Semi-Infinite Soil Medium with Constant Modulus along Depth

(For details, please see: Farzad Abedzadeh and Y. S. Pak. (2004). “Continuum Mechanics of Lateral Soil–Pile Interaction”, *Journal of Engineering Mechanics*, Vol. 130, No. 11, November, pp. 1309-1318).

Consider a flexible cylindrical pipe pile of radius a , length l , a wall thickness $h \ll a$ (note that the moment of inertia $I = \pi a^3 h$). The pile is assumed to be fully embedded in a homogenous, isotropic, linearly elastic half-space with a shear modulus G_s and a Poisson’s ratio $\nu_s = 0.25$.

Using Eqs. (78)-(83) and Figure 9 of the above reference, the pile response ($h/a=0.1$, $l/a=50$) under an applied pure pile-head horizontal load is shown in Figure C.4 and Figure C.5, where,

E_p – Young’s Modulus of Pile

G_s – Shear Modulus of Soil

w – Pile deflection (in)

H – Horizontal load (kip)

z – Pile depth (ft)

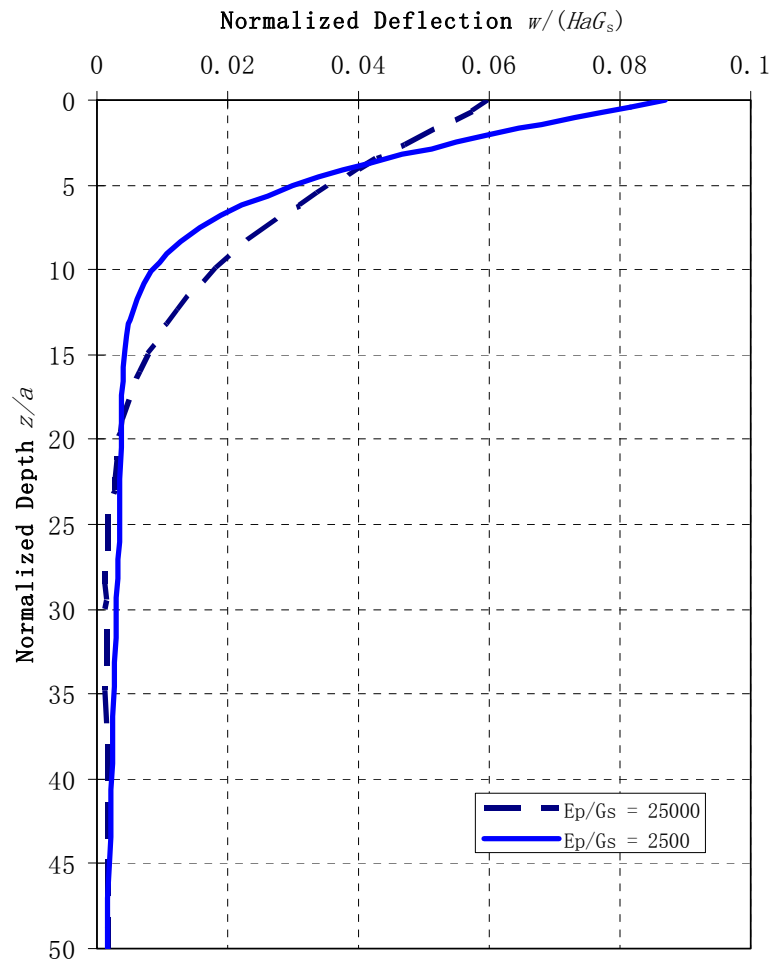


Figure C.4: Sample pile deflection ($h/a=.1$, $l/a=50$) under an applied pure pile-head horizontal load (Abedzadeh and Pak, 2004).

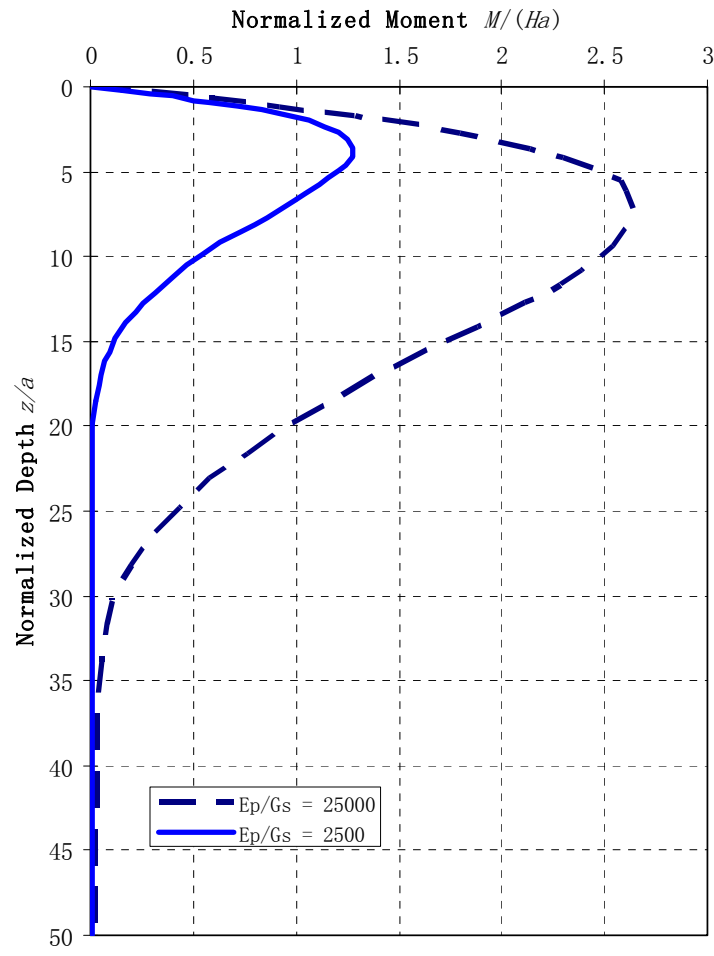


Figure C.5: Sample pile bending moment ($h/a=.1$, $l/a=50$) under an applied pure pile-head horizontal load (Abedzadeh and Pak, 2004).

Appendix C-II: Nonlinear Response of the Single Pile Model

In the nonlinear run, the same material properties of the linear run are employed except the soil now assumed to be a clay material with a maximum shear strength or cohesion = 5.1 psi, in the range of a Medium Clay. This maximum shear strength is achieved at a specified strain $\gamma_{\max} = 10\%$.

The lateral load (H) is applied at an increment of 0.7875 kips and the final load is 94.5 kips (= 3 x 31.5 kips). The 8-node brick element mesh is employed in this nonlinear analysis (Figure C.1).

Simulation Results

Figure C.6 shows the load-deflection curve for the nonlinear run, along with the linear result (for the 8-node brick element mesh; the final lateral load is also extended to 94.5 kips) as described in the previous sections for comparison. It is seen from Figure C.6 that nearly linear behavior is exhibited in the nonlinear run for only low levels of applied lateral load (less than 10 kips).

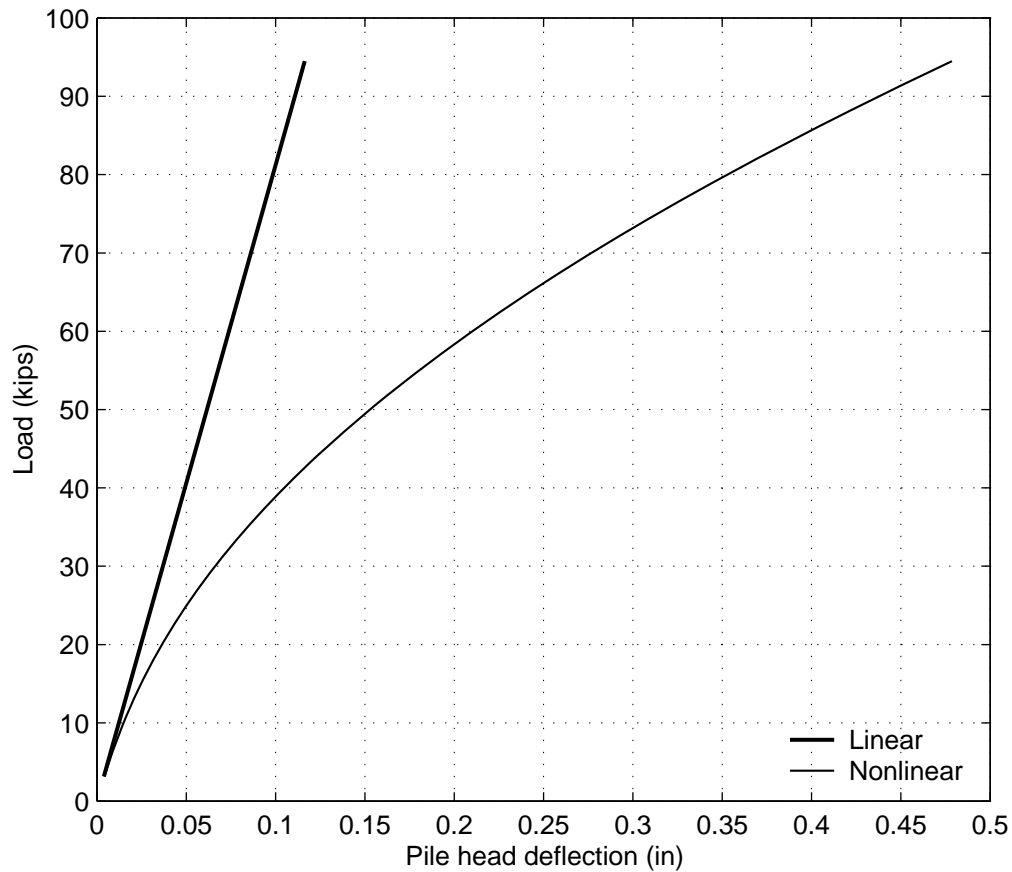
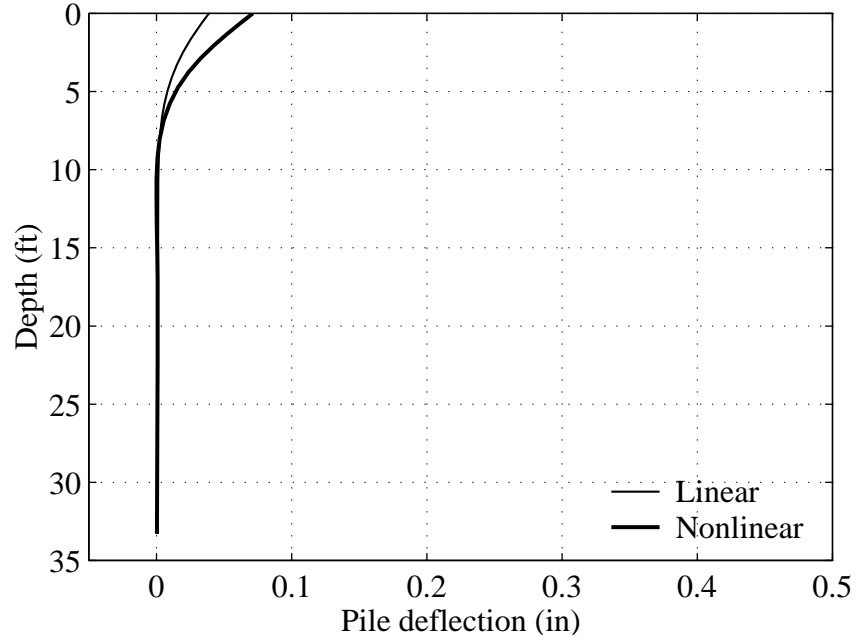
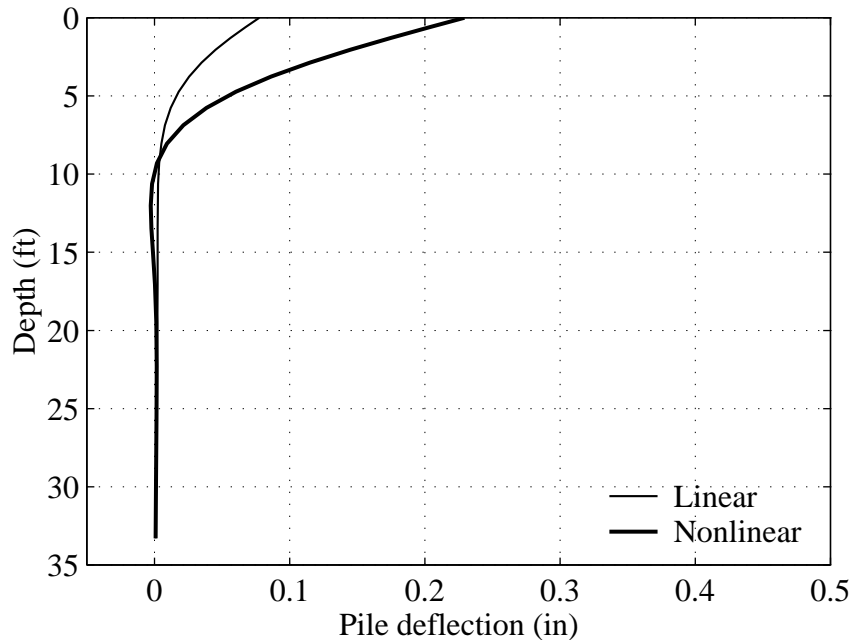


Figure C.6: Comparison of the load-deflection curves for the linear and nonlinear runs.

The pile deflection profiles for both linear and nonlinear cases are displayed in Figure 7. For comparison, the linear and nonlinear responses at the lateral load of 31.5 kips, 63 kips ($= 2 \times 31.5$), and 94.5 kips ($= 3 \times 31.5$) are shown (Figure C.7). The bending moment profiles for the 3 load levels are shown in Figure C.8a-c.

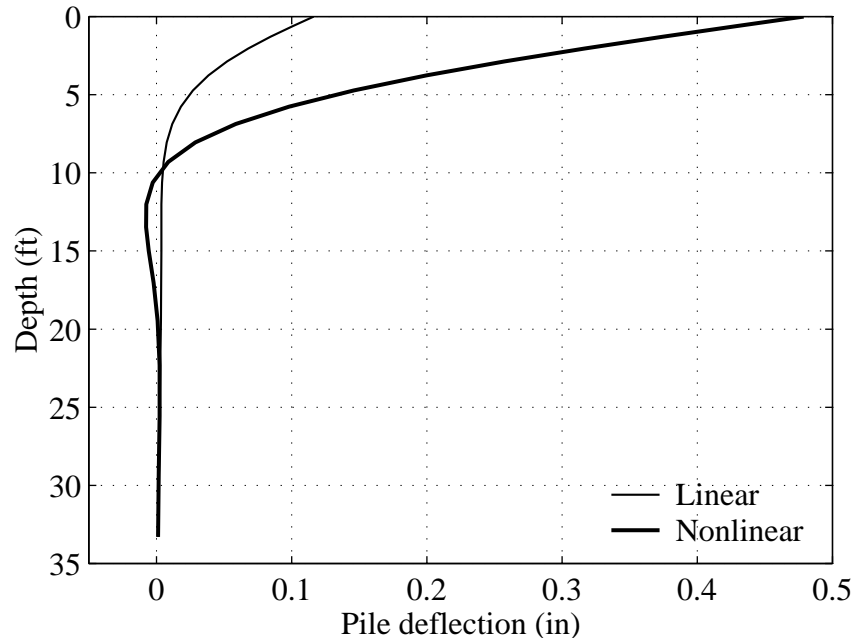


a) $H = 31.5$ kips



b) $H = 63$ kips

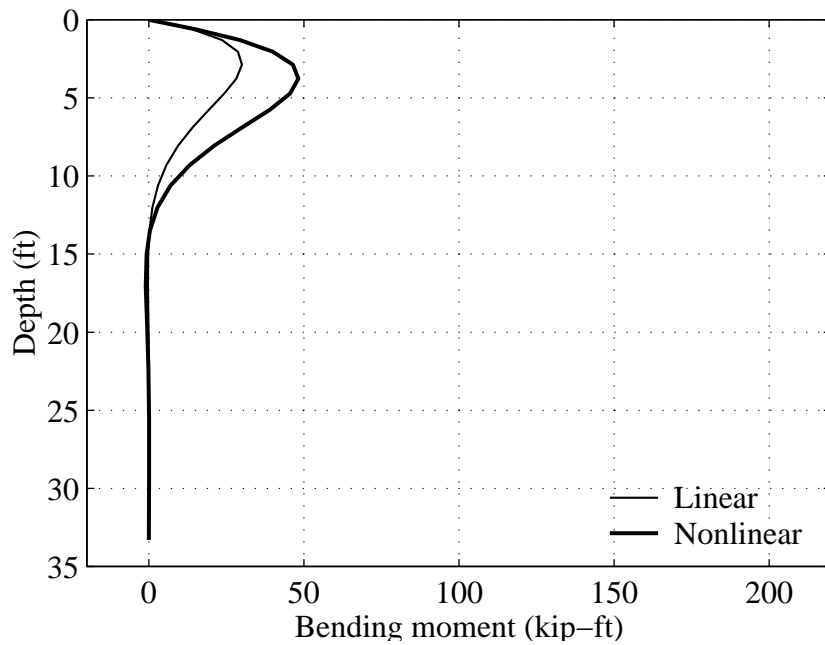
Figure C.7: Comparison of the pile deflection profiles for the linear and nonlinear runs.



c) $H = 94.5$ kips

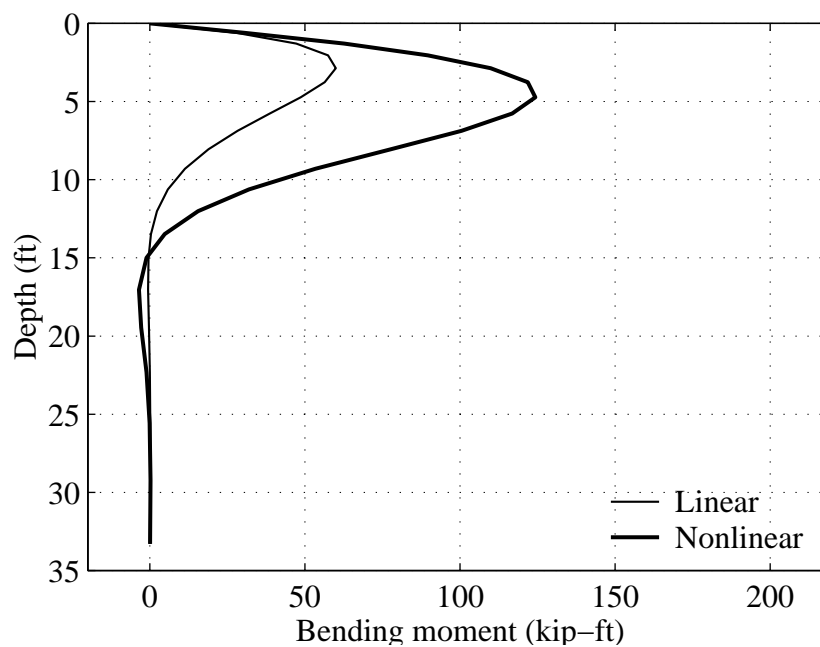
Figure C.7: (continued).

The pile head deflections and the maximum bending moments for both linear and nonlinear analyses are listed in Table C.2. The stress ratio contour fill of the nonlinear run is displayed in Figure C.9.

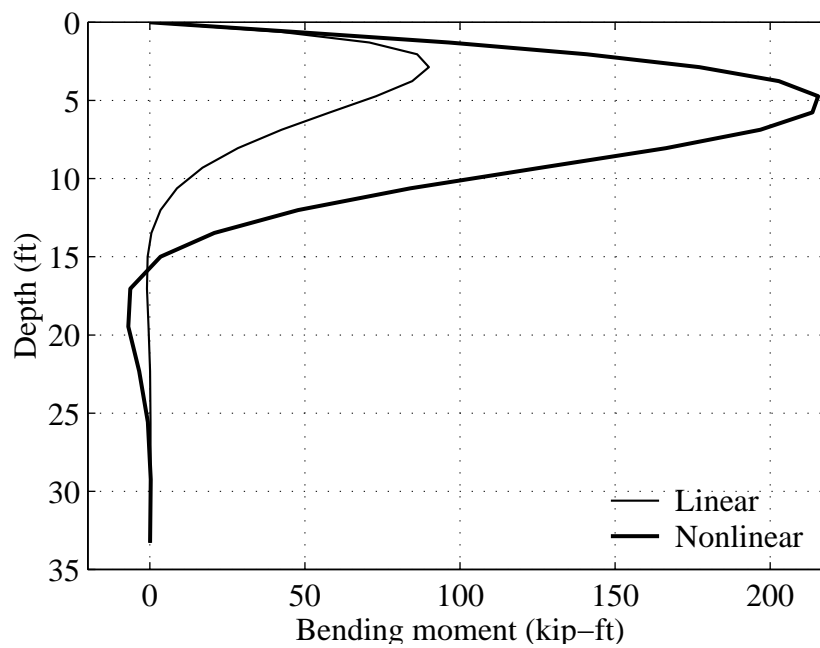


a) $H = 31.5$ kips

Figure C.8: Comparison of the pile bending moment profiles for the linear and nonlinear runs.



b) $H = 63$ kips



c) $H = 94.5$ kips

Figure C.8: (continued).

Table C.2: OpenSees simulation results for the linear and nonlinear runs.

	$H = 31.5$ kips		$H = 63$ kips		$H = 94.5$ kips	
	Linear	Nonlinear	Linear	Nonlinear	Linear	Nonlinear
Pile head deflection (in)	0.039	0.07	0.078	0.23	0.12	0.48
Maximum moment M_{\max} (kip-ft)	30	48.2	60	124.3	90	215.5
Depth where M_{\max} occurs (ft)	2.9	3.8	2.9	4.7	2.9	4.7

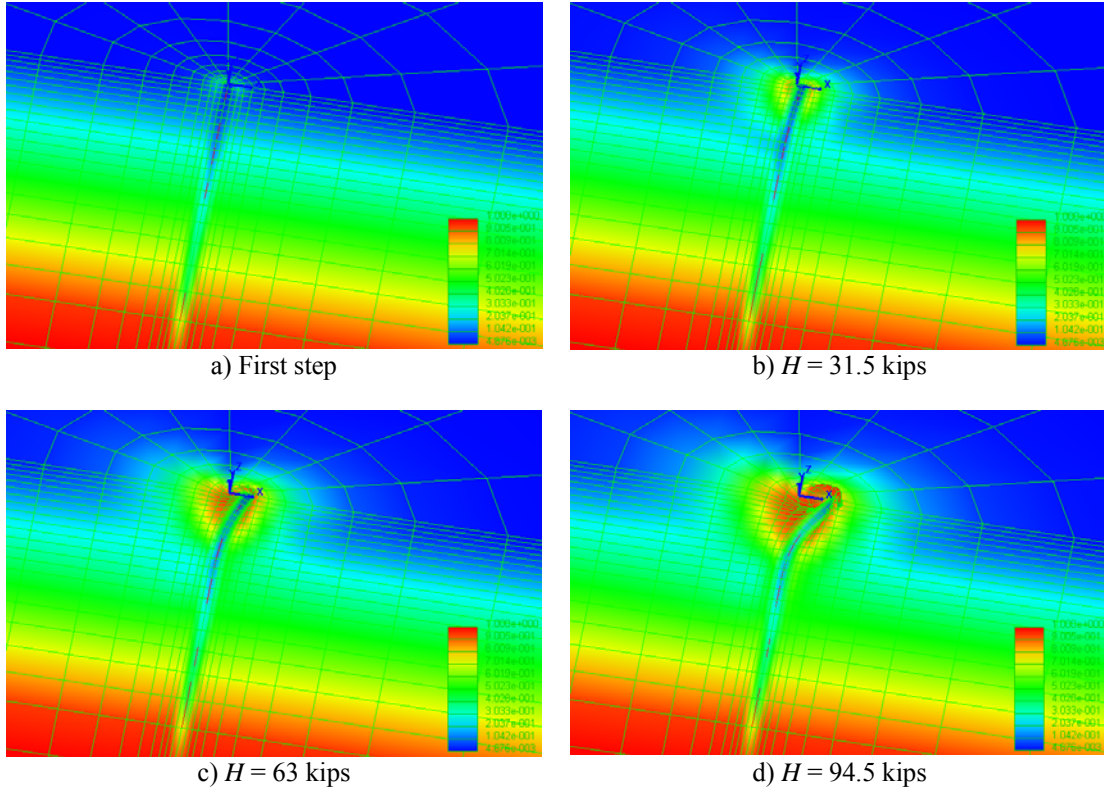


Figure C.9: Stress ratio contour fill of the nonlinear run at different load levels (red color shows yielded soil elements).

Appendix D Finite Element Analysis of Arkansas Test Series Pile #2 Using Opensees (with LPILE Comparison)

Introduction

In this study, we conduct a finite element simulation of Pile No. 2 of the Arkansas test series (Alizadeh and Davisson 1970) using the OpenSeesPL interface. This pipe pile is subjected to lateral loads. Comparison with LPILE is also included in Appendix D-I (please see the end of Appendix D).

Laterally Loaded Pile

Pile Data

The pile employed in the OpenSees simulation is circular with a diameter of 16" (radius $a = 8"$) while the one for the experimental test is a cylindrical pipe pile of the same radius and a wall thickness $h = 0.312"$. The cross-sectional moment of inertia of the pipe pile $I = 838.2 \text{ in}^4$ (Bowles 1988, pages 777-778), which will be used for the circular pile in the OpenSees simulation.

The geometric and elastic material properties of the pile are listed below (Bowles 1988):

Diameter = 16" or Radius $a = 8"$

Pile length $l = 52.9 \text{ ft}$

Young's Modulus of Pile $E_p = 29000 \text{ ksi}$

Moment of Inertia of Pile $I = 838.2 \text{ in}^4$

Soil Domain

In this section, the pile is embedded in a uniform soil layer (pile top is 0.1' above the ground line). Linear and nonlinear soil responses are investigated. The Medium density (relative) granular soil type (Lu et al. 2006) is selected in this initial attempt. The material properties of the soil are listed below:

At the reference confinement of 80 kPa (or 11.6 psi), the Shear Modulus of Soil $G_s = 10.88 \text{ ksi}$ and the Bulk Modulus of Soil $B = 29 \text{ ksi}$ (i.e., Poisson's ratio $\nu_s = 0.33$), see Lu et al. 2006.

Submerged Unit Weight $\gamma' = 62.8 \text{ pcf}$ (Bowles 1988)

For nonlinear analysis, the Friction Angle $\phi = 32^\circ$ (Bowles 1988) and the peak shear stress occurs at a shear strain $\gamma_{\max} = 10\%$ (at the 11.6 psi confinement)

Lateral Load

The pile head (with a free head condition), which is 0.1' above the ground surface, is subjected to horizontal loads (H) of 21 kips, 31.5 kips and 43 kips (Bowles 1988).

Finite Element Simulation

In view of symmetry, a half-mesh (2,900 8-node brick elements, 23 beam-column elements and 207 rigid beam-column elements in total) is studied as shown in Figure D.1. Length of the mesh in the longitudinal direction is 520 ft, with 260 ft transversally (in this half-mesh configuration, resulting in a 520 ft x 520 soil domain in plan view). Layer thickness is 80 ft (the bottom of the soil domain is 27.2 ft below the pile tip, so as to mimic the analytical half-space solution).

The floating pile is modeled by beam-column elements, and rigid beam-column elements are used to model the pile size (diameter).

The following boundary conditions are enforced:

- I) The bottom of the domain is fixed in the longitudinal (x), transverse (y), and vertical (z) directions.
- II) Left, right and back planes of the mesh are fixed in x and y directions (the lateral directions) and free in z direction.
- III) Plane of symmetry is fixed in y direction and free in z and x direction (to model the full-mesh 3D solution).

The lateral load is applied at the pile head (ground level) in x (longitudinal) direction.

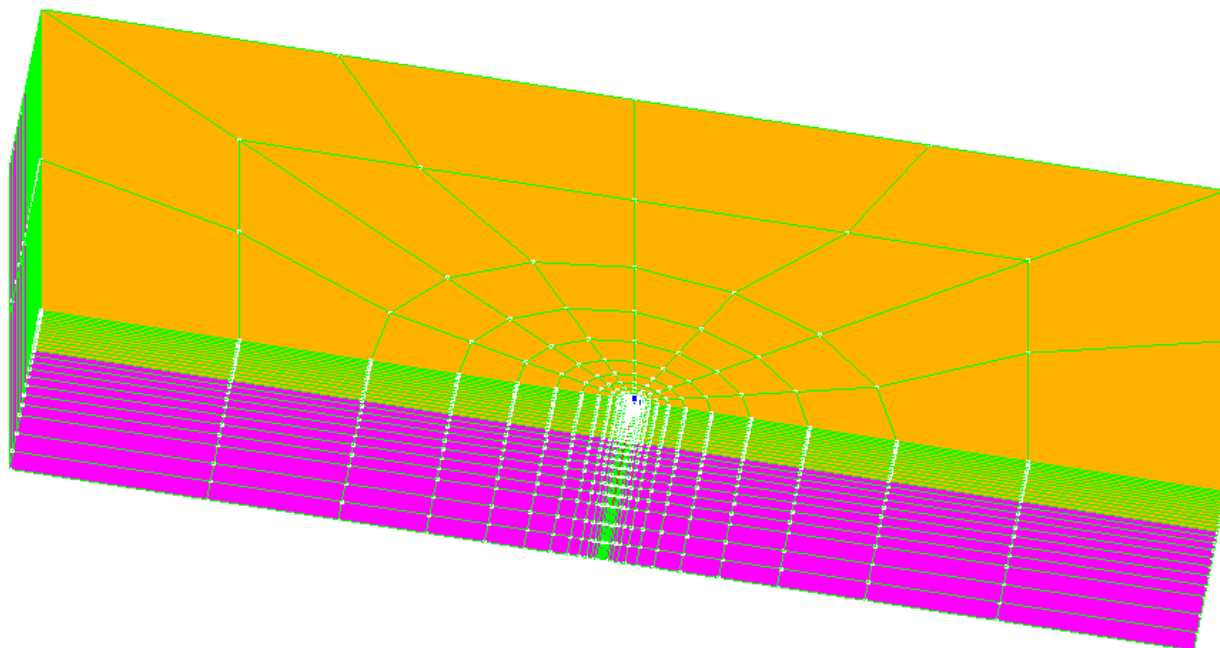
The above simulations were performed using OpenSeesPL (Lu et al. 2006).

Simulation Results

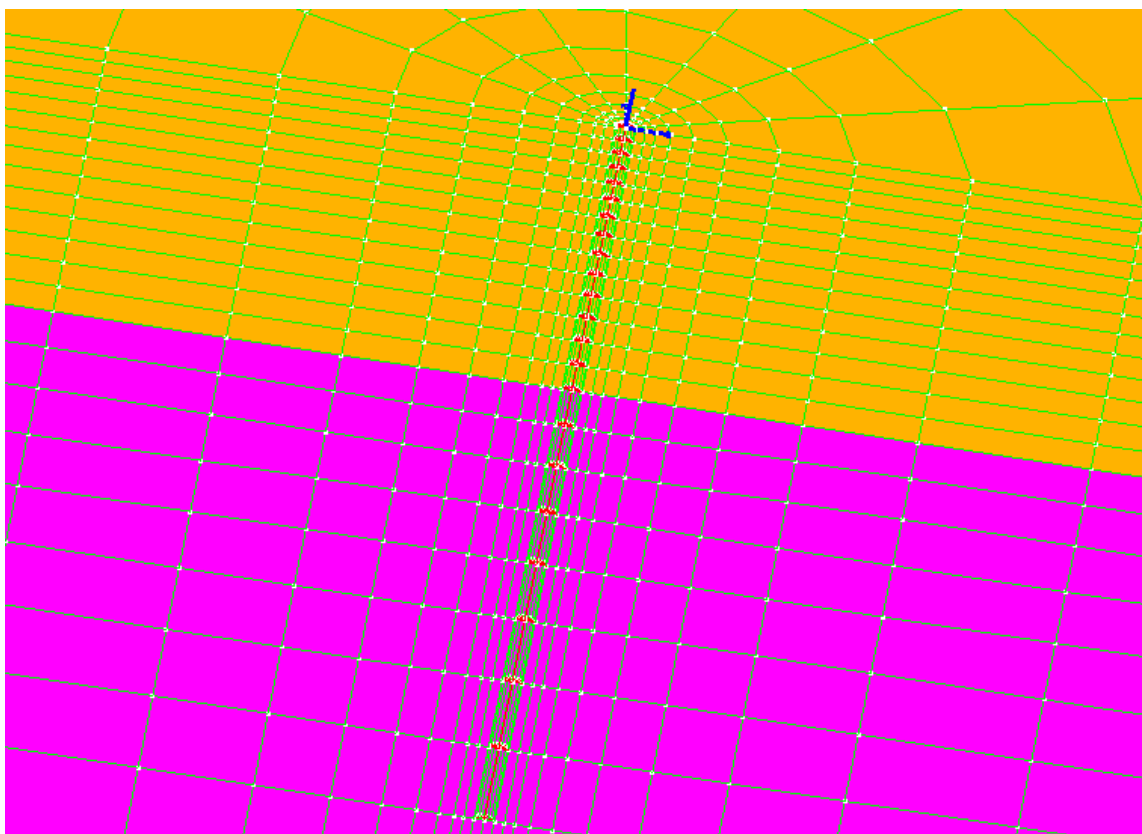
The pile deflections at the ground line and the maximum bending moments for the linear and nonlinear analyses are listed in Table D.1, along with the experimental measurements for comparison (Alizadeh and Davisson 1970; Bowles 1988).

Figure D.2 shows the load-deflection curve for the linear and nonlinear runs. Comparison of the pile deflection profiles for the linear and nonlinear analyses are displayed in Figure D.3a-c. The bending moment profiles for the 3 load levels are shown in Figure D.4a-c, along with the observed for comparison (Alizadeh and Davisson 1970). The stress ratio contour fill of the nonlinear run is displayed in Figure D.5.

Comparison with LPILE is included in Appendix D-I.



(a) Isometric view



(b) Pile head close-up

Figure D.1: Finite element mesh employed in this study.

Table D.1: OpenSees Simulation Results and Experimental Measurements.

	Analysis type	Pile deflection at ground line (in)	Max. bending moment M_{\max} (kip-ft)	M_{\max} depth (ft)	Profile displays
H = 21 kips					
Experimental		0.17	62	4	Figures 3a & 4a
Case 1	Linear soil	0.085	35.1	3.1	
Case 2	Nonlinear soil	0.31	70.5	6.8	
H = 31.5 kips					
Experimental		0.26	85	5	Figures 3b & 4b
Case 3	Linear soil	0.13	52.6	3.1	
Case 4	Nonlinear soil	0.56	115.5	6.8	
H = 43 kips					
Experimental		0.4	120	5	Figures 3c & 4c
Case 5	Linear soil	0.17	70.1	3.1	
Case 6	Nonlinear soil	0.89	164.7	6.8	

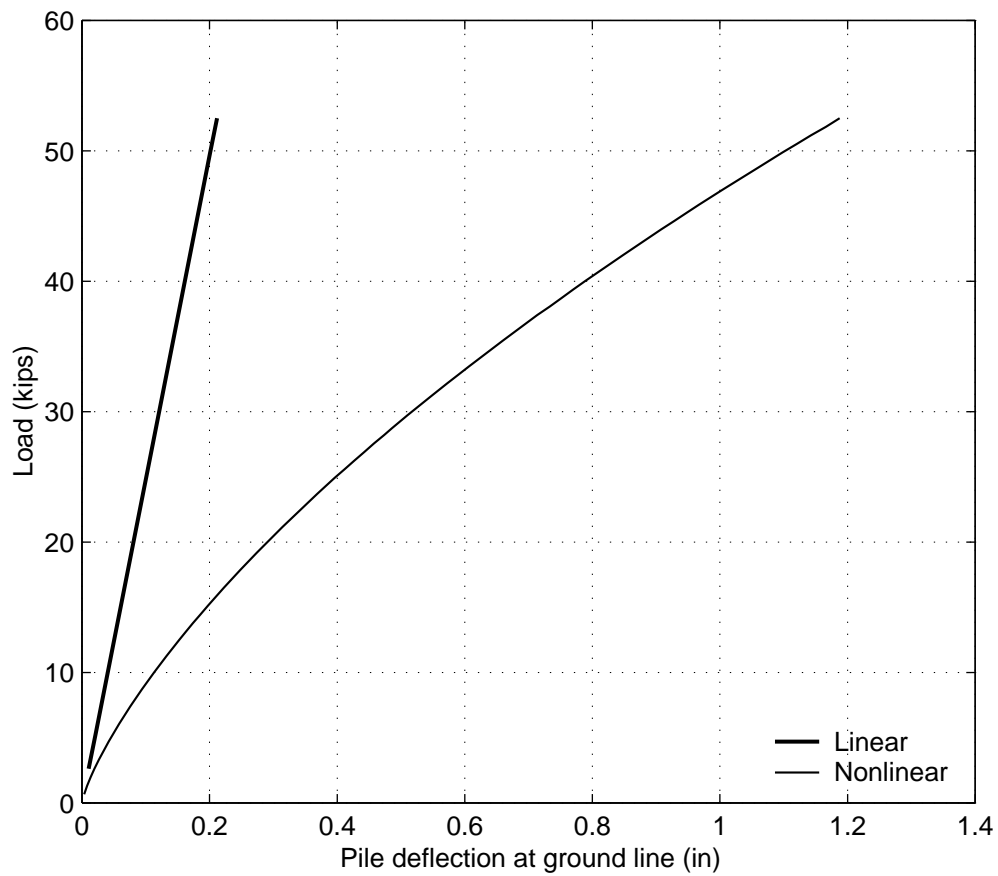
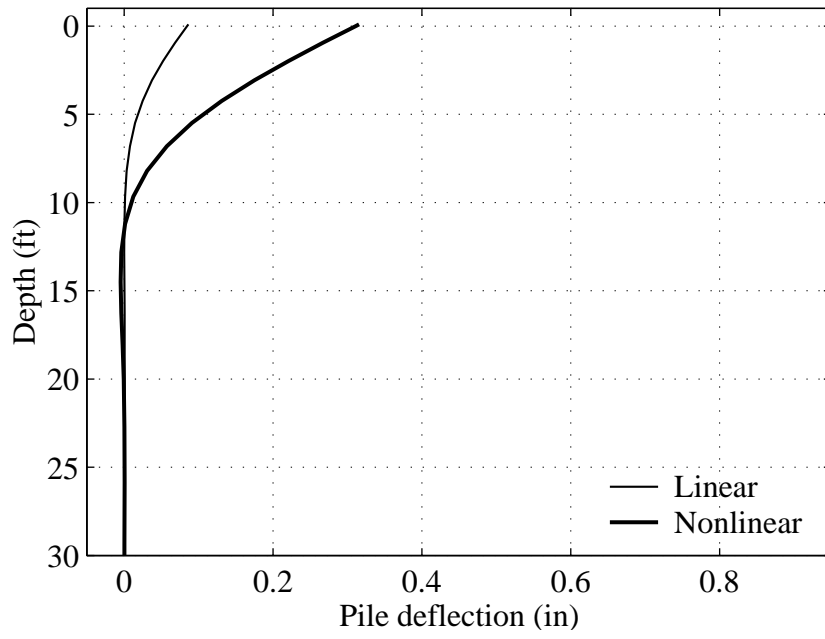
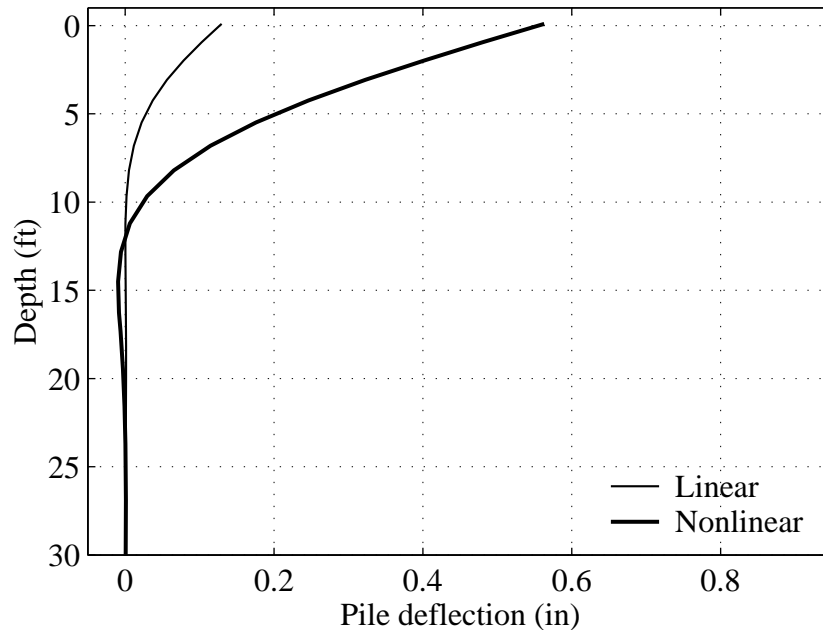


Figure D.2: Comparison of the load-deflection curves for the linear and nonlinear runs.

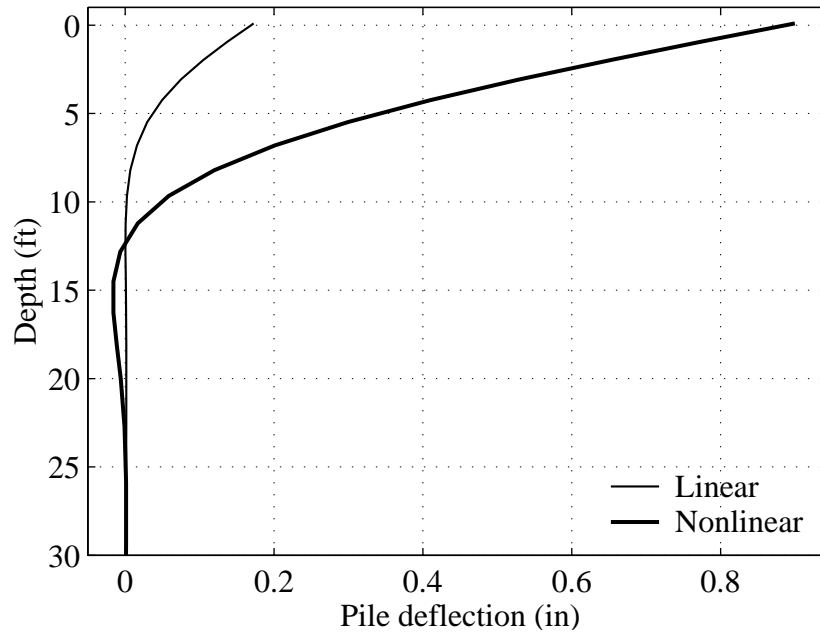


d) $H = 21$ kips



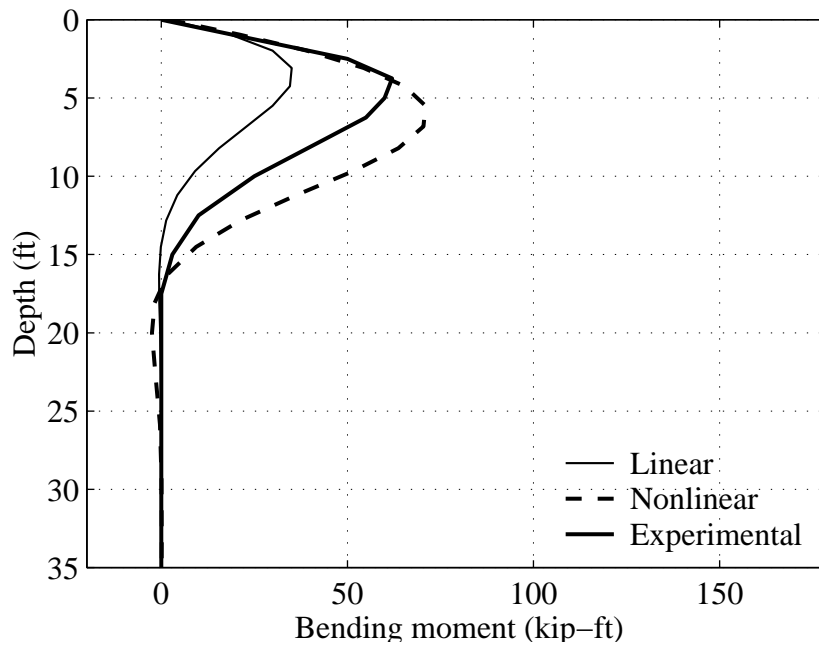
e) $H = 31.5$ kips

Figure D.3: Comparison of the pile deflection profiles for the linear and nonlinear runs.



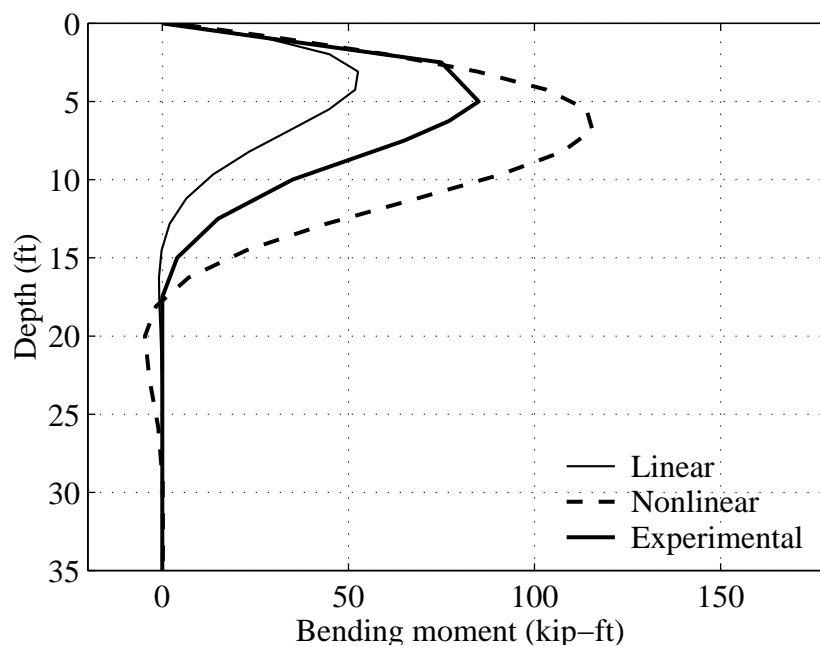
f) $H = 43$ kips

Figure D.3: (continued).

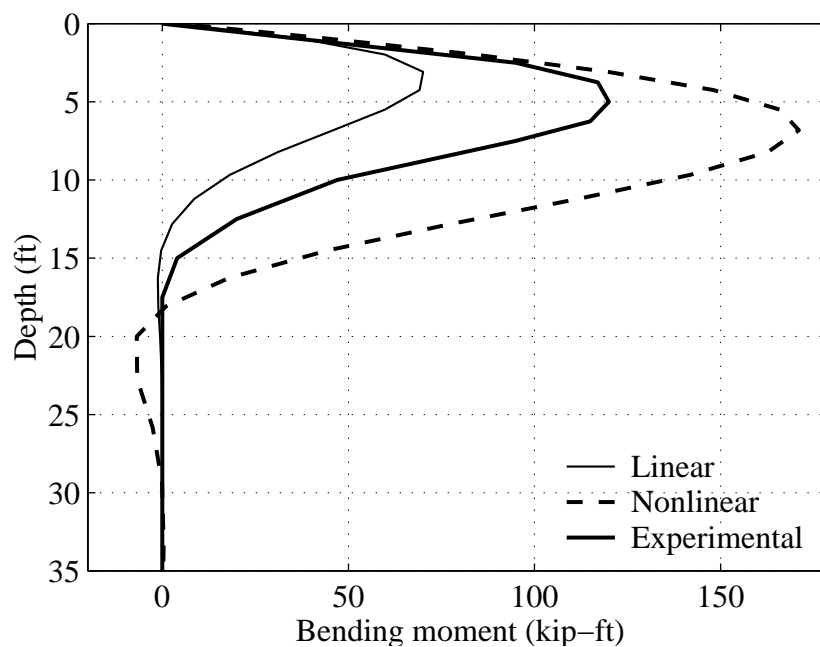


a) $H = 21$ kips

Figure D.4: Comparison of the pile bending moment profiles for the linear and nonlinear runs.



b) $H = 31.5$ kips



c) $H = 43$ kips

Figure D.4: (continued).

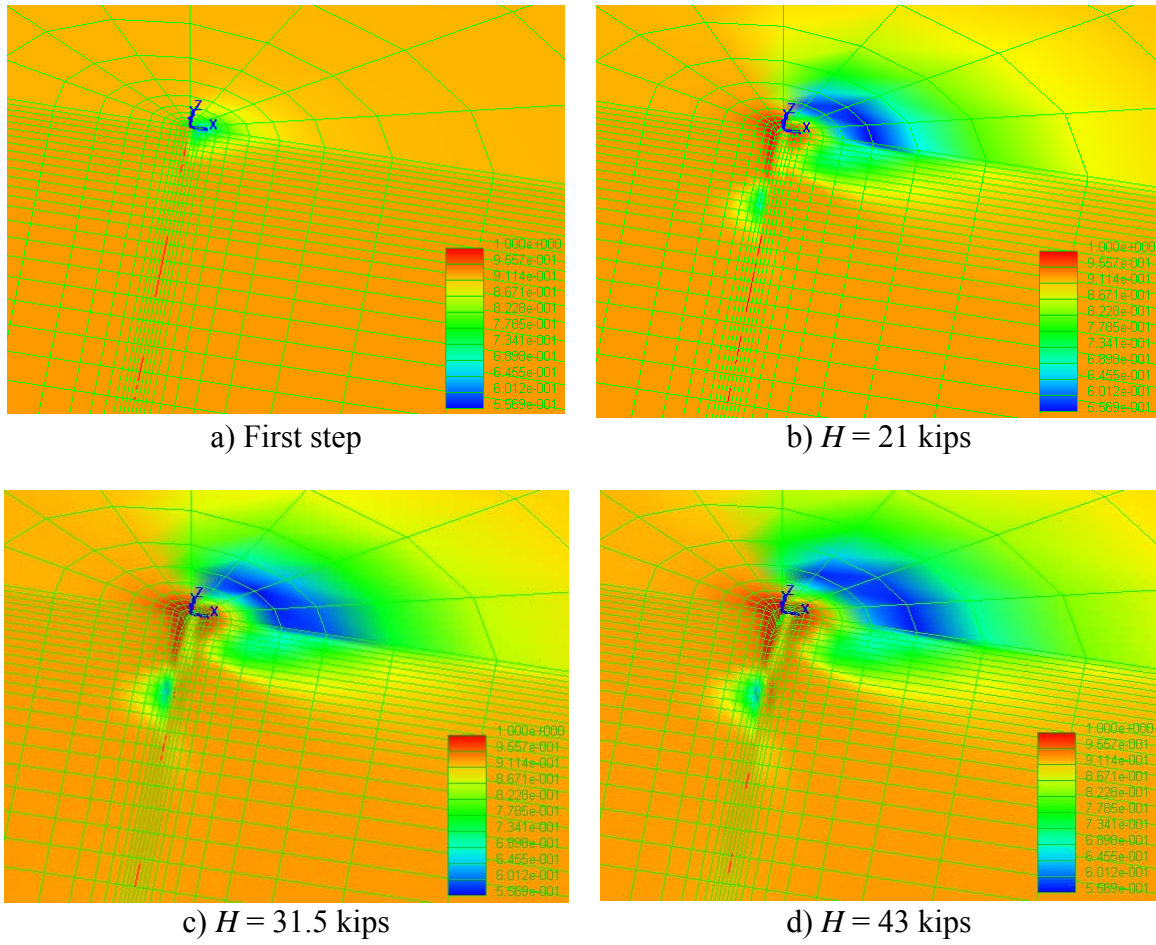
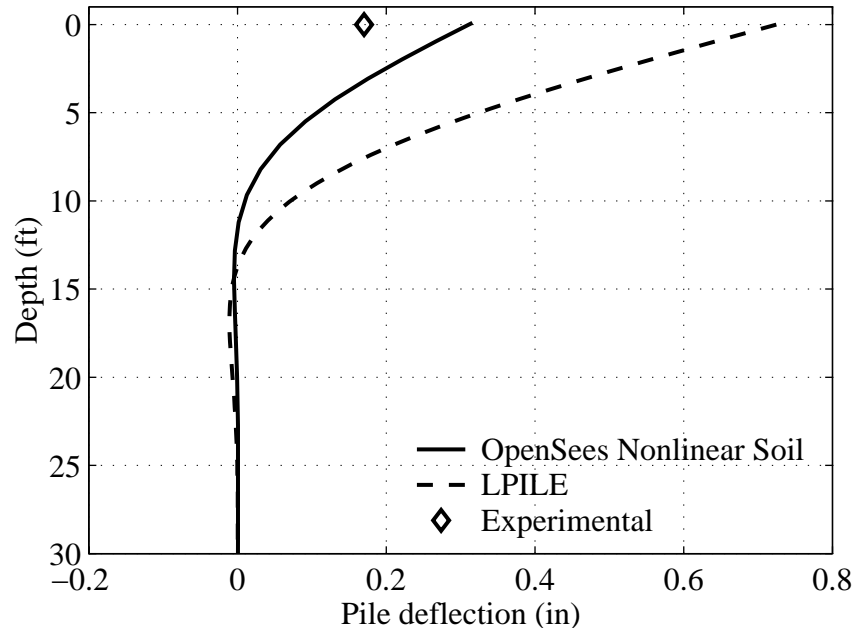


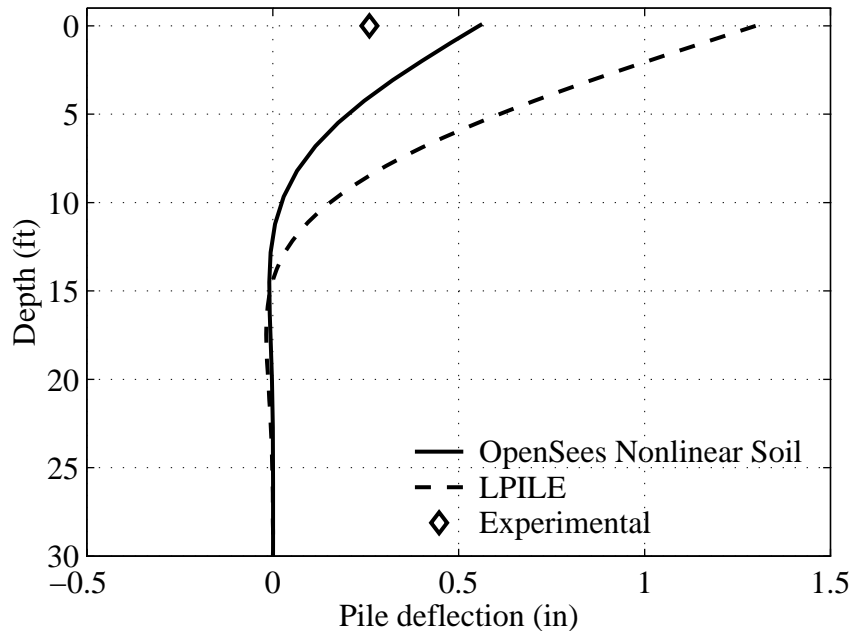
Figure D.5: Stress ratio contour fill of the nonlinear run at different load levels (red color shows yielded soil elements).

Appendix D-I: Comparison with LPILE

In the LPILE run, a p-y modulus of 90 psi is employed (p-y multiplier = 1.0). All other properties are the same as described earlier.

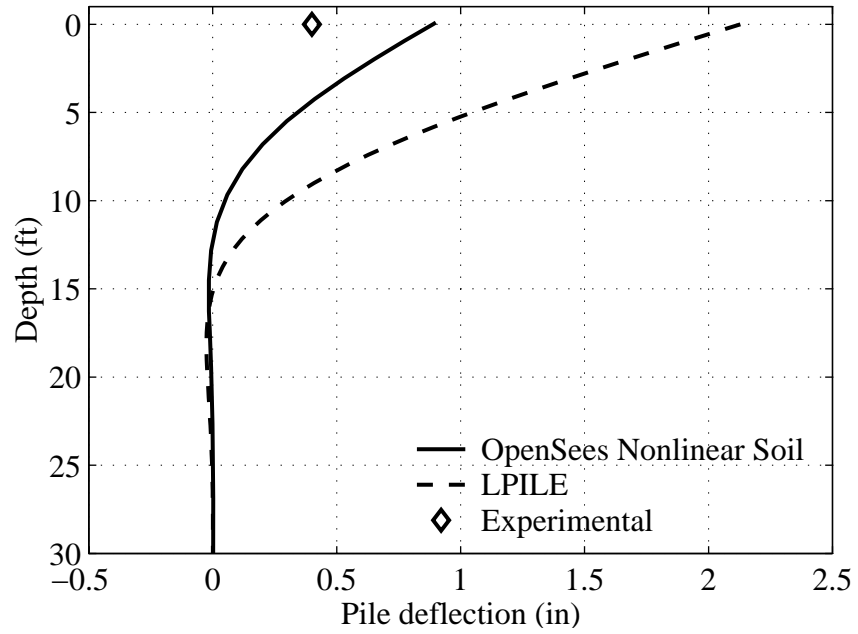


a) $H = 21$ kips



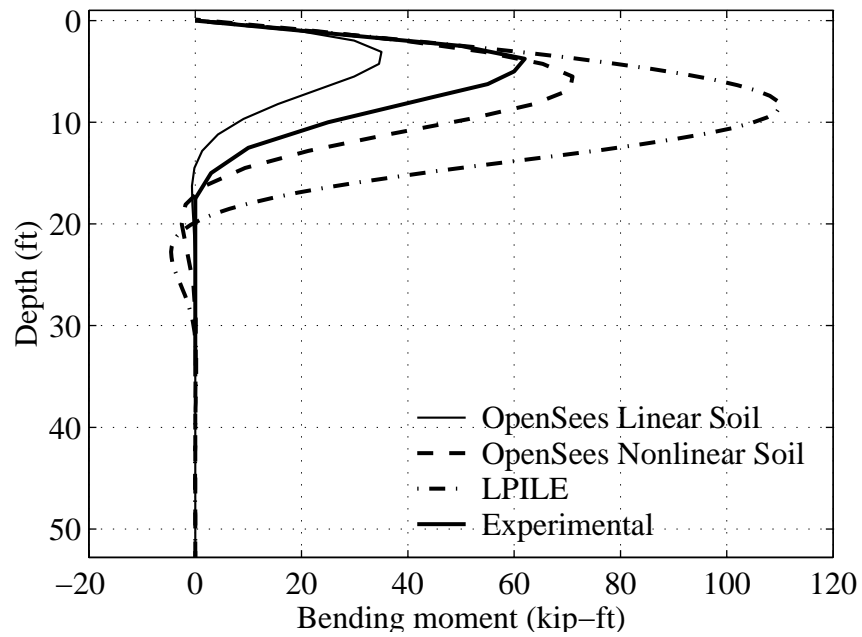
b) $H = 31.5$ kips

Figure D.6: Comparison of the pile deflection profiles for the linear and nonlinear runs.



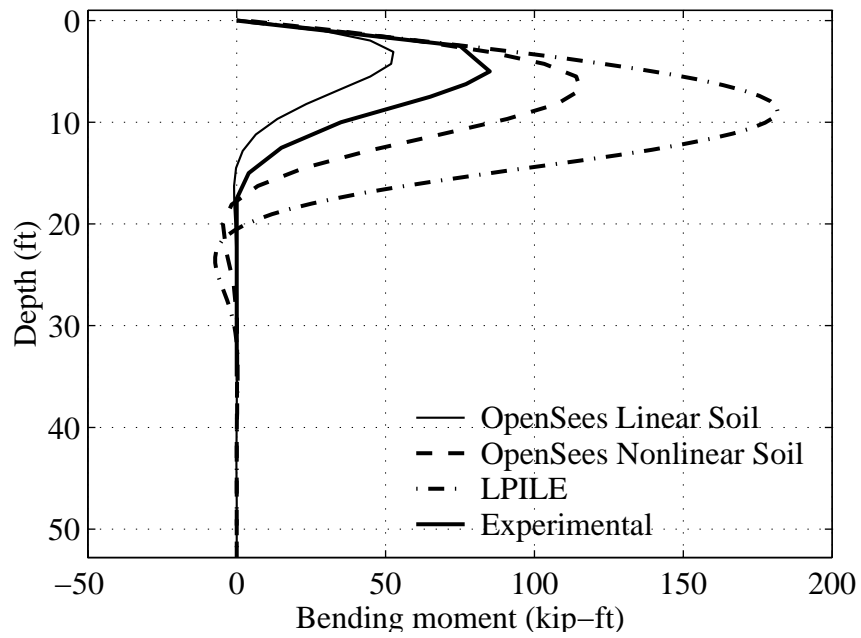
c) $H = 43$ kips

Figure D.6: (continued).

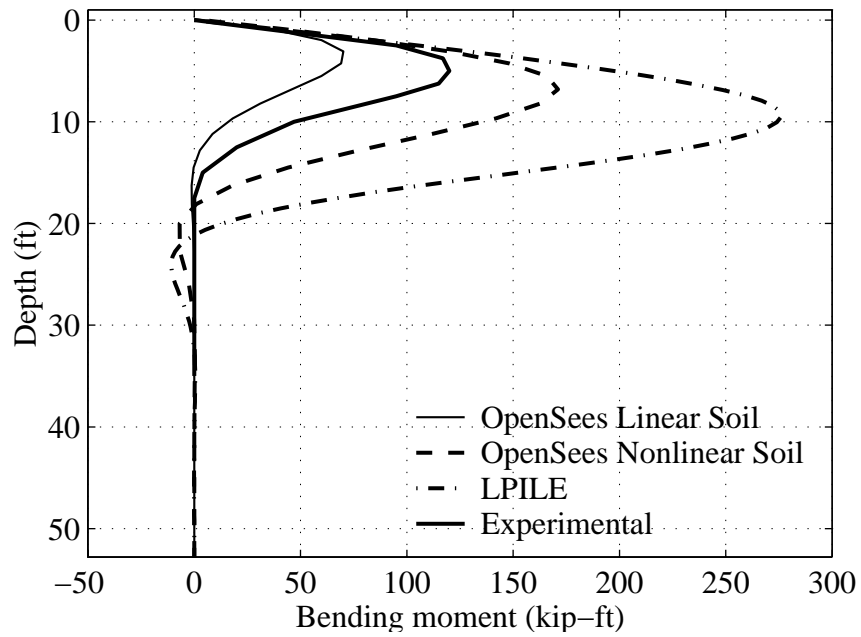


a) $H = 21$ kips

Figure D.7: Comparison of the pile bending moment profiles for the linear and nonlinear runs.



b) $H = 31.5$ kips



c) $H = 43$ kips

Figure D.7: (continued).

Appendix E Finite Element Analysis of Standard CalTrans 16" CIDH Pile Using Openssees for General Comparison with LPILE (with Default P-Y Multiplier = 1.0)

Introduction

In this study, we conduct a finite element simulation of the standard Caltran 16" CIDH pile using the 3D OpenSeesPL interface. The simulated pile responses are compared with LPILE results.

Laterally Loaded Pile

Pile Data

The geometric and elastic material properties of the pile are listed below:

Diameter $D = 16"$

Pile length $l = 35$ ft

Moment of Inertia of Pile $I = 850$ in⁴

Young's Modulus of Pile $E_c = 4030$ ksi

In this initial study, the pile was modeled to remain linear (also in view of the applied load levels).

Soil Domain

Linear and nonlinear soil responses are investigated. The Medium relative-density granular soil type (Lu et al. 2006) is selected in the analyses. The material properties of the soil are listed below:

At the reference confinement of 80 kPa (or 11.6 psi), the Shear Modulus of Soil $G_s = 10.88$ ksi and the Bulk Modulus of Soil $B = 29$ ksi (i.e., Poisson's ratio $\nu_s = 0.33$), see Lu et al. 2006.

Effective Unit Weight $\gamma' = 110$ pcf (given by CalTrans)

For nonlinear analysis, the Friction Angle $\phi = 33^\circ$ (given by CalTrans) and the peak shear stress occurs at a shear strain $\gamma_{\max} = 10\%$ (at the 11.6 psi confinement). The parameter γ_{\max} along with the shear modulus define the nonlinear soil stress-strain curve. Other values of γ_{\max} should be explored in the future.

Lateral Load

Two load cases (Table 1) are studied. The loads are applied at the pile head.

Table E.1: Load cases for the study.

	Shear (kips)	Moment (kip-ft)	Axial load (kips)
Load case 1*	16	0	52
Load case 2**	19.8	-100	52

* Fixed pile head connection

** Apply moment in opposite direction of shear.

Finite Element Simulation

In view of symmetry, a half-mesh (2,900 8-node brick elements, 19 beam-column elements and 180 rigid beam-column elements in total) is studied as shown in Figure E.1. Length of the mesh in the longitudinal direction is 520 ft, with 260 ft transversally (in this half-mesh configuration, resulting in a 520 ft x 520 soil domain in plan view). Layer thickness is 60 ft (the bottom of the soil domain is 25 ft below the pile tip, so as to mimic the analytical half-space solution).

The floating pile is modeled by beam-column elements (Mazzoni et al. 2006), and rigid beam-column elements are used to model the pile size (diameter).

The following boundary conditions are enforced:

- I) The bottom of the domain is fixed in the longitudinal (x), transverse (y), and vertical (z) directions.
- II) Left, right and back planes of the mesh are fixed in x and y directions (the lateral directions) and free in z direction.
- III) Plane of symmetry is fixed in y direction and free in z and x direction (to model the full-mesh 3D solution).

The lateral load is applied at the pile head (ground level) in x (longitudinal) direction.

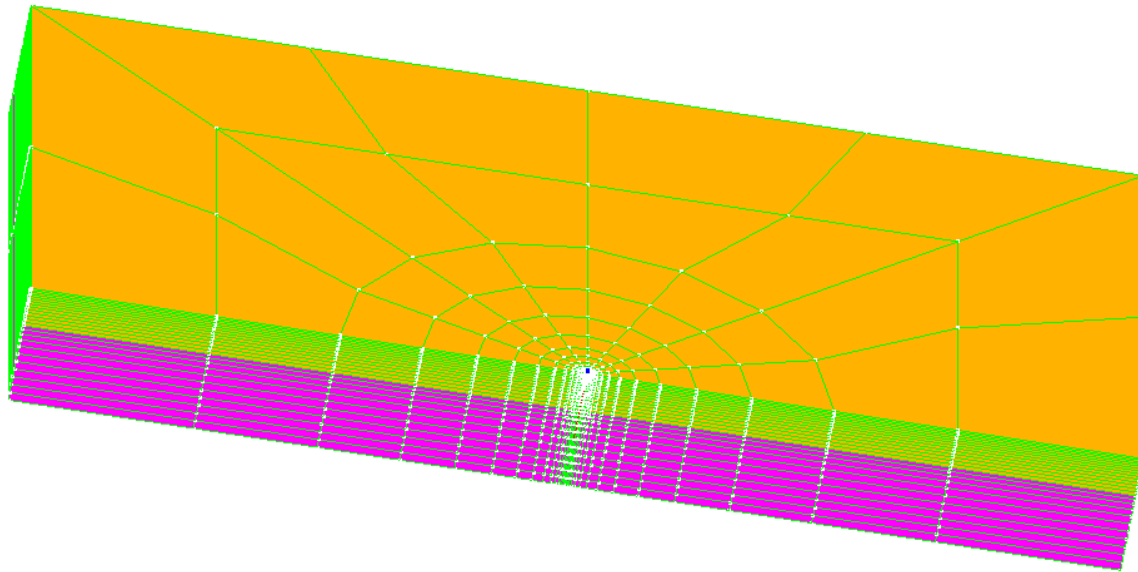
The above simulations were performed using OpenSeesPL (Lu et al. 2006).

Simulation Results

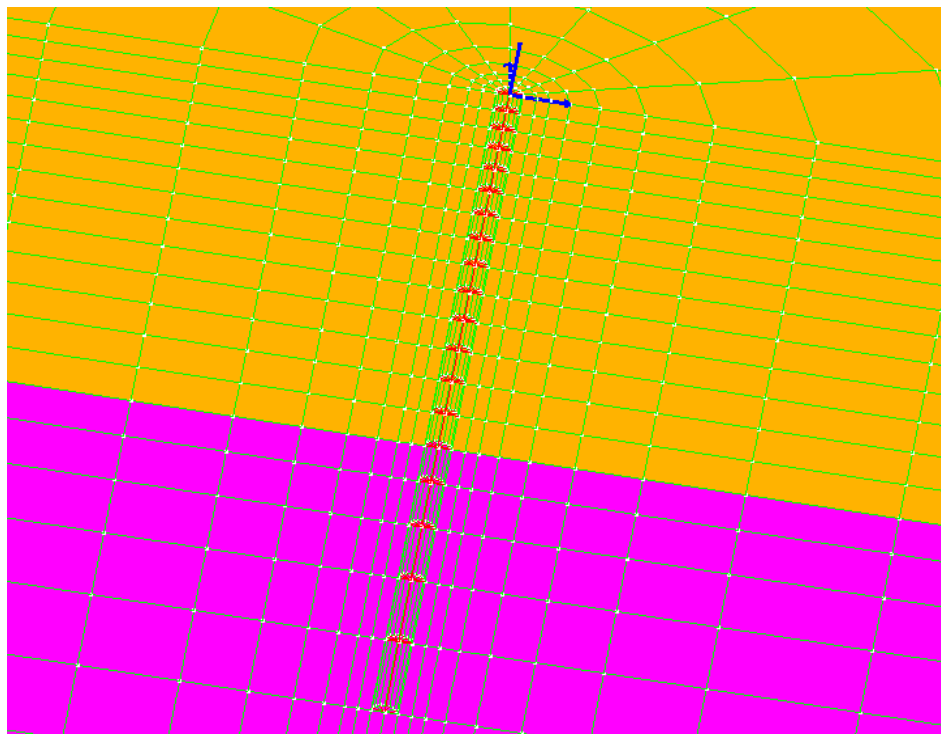
The pile head deflections and the maximum bending moments for the linear and nonlinear analyses are listed in Table 2, along with LPILE results for comparison (see Appendix for partial output of LPILE results).

Figures C.2-C.5 show comparisons of the pile deflection, rotation, bending moment and shear force profiles, respectively, for load case 1. Figures C.6-C.9 show comparisons of

the pile deflection, rotation, bending moment and shear force profiles, respectively, for load case 2. The stress ratio contour fill of the nonlinear runs for load cases 1 & 2 are displayed in Figures C.10 & C.11.



(a) Isometric view



(b) Pile head close-up

Figure E.1: Finite element mesh employed in this study.

Table E.2: CalTrans CIDH Pile OpenSees Simulation and LPILE Results.

	Analysis type	Pile head deflection (in)	Max. bending moment M_{\max} (kip-ft)	M_{\max} depth (ft)	Profile displays
Load Case 1 Fixed Head H = 16 kips	LPILE	0.24	-48.2	0	Figures 2 & 4
	Linear soil	0.038	-20.8	0	
	Nonlinear soil	0.092	-32.3	0	
Load Case 2 Free Head M = -100 kip-ft applied opposite to shear	LPILE	-0.094	-100	0	Figures 6 & 8
	Linear soil	-0.06	-96.7	0	
	Nonlinear soil	-0.094	-96.9	0	

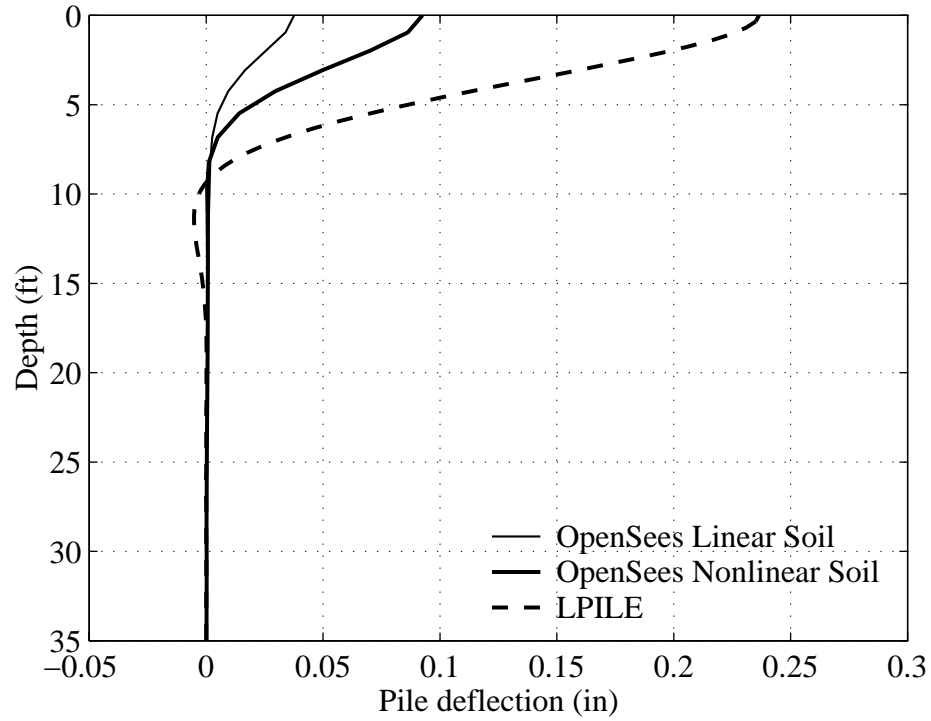


Figure E.2: Comparison of pile deflection profiles for load case 1.

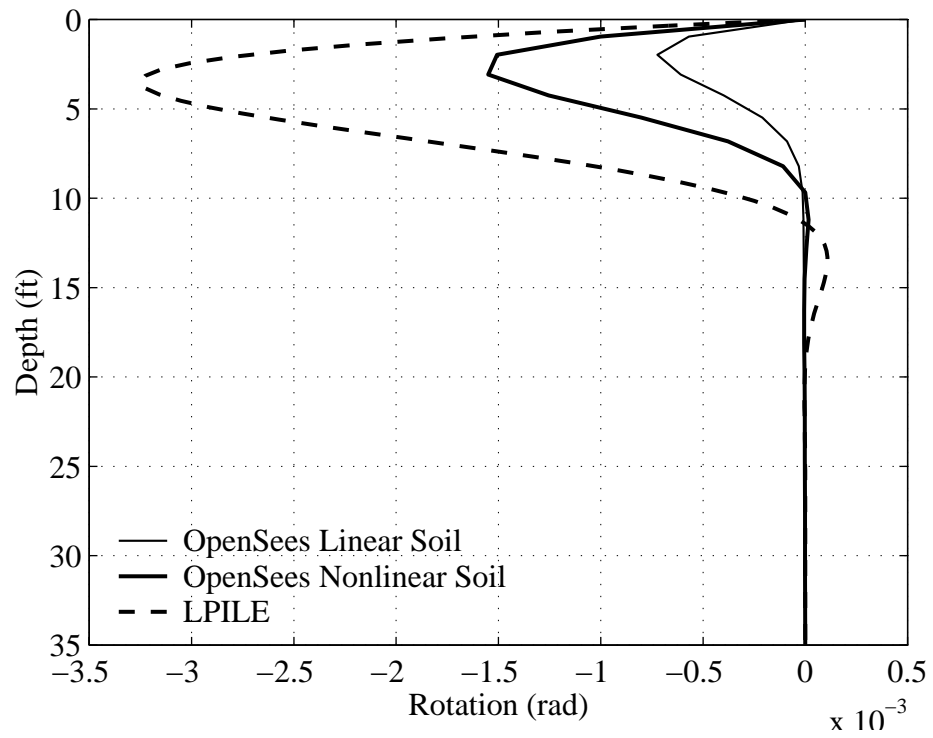


Figure E.3: Comparison of pile rotation profiles for load case 1.

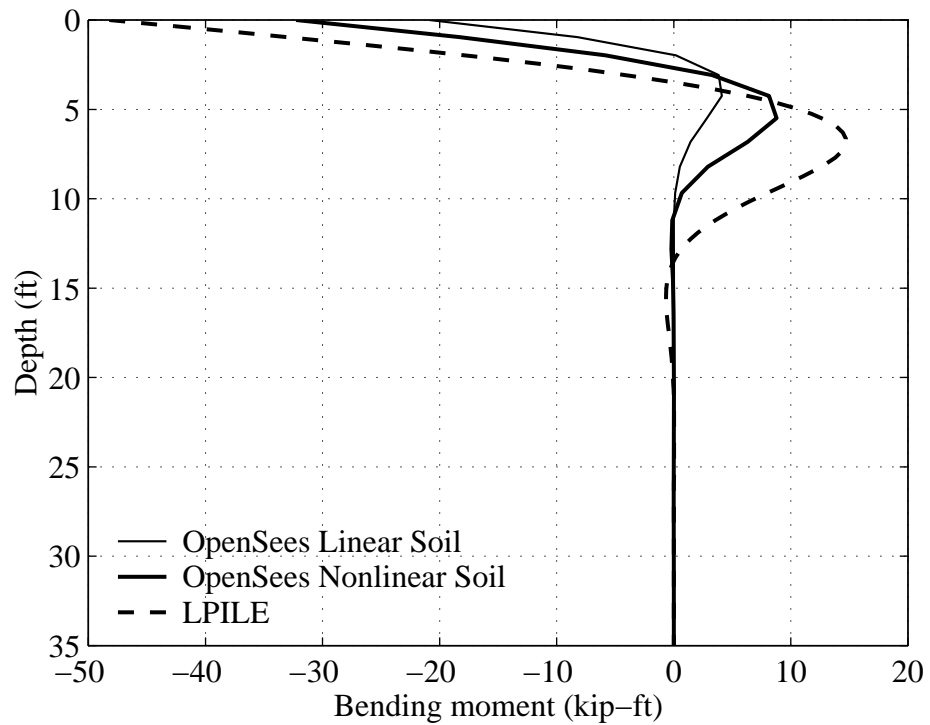


Figure E.4: Comparison of bending moment profiles for load case 1.

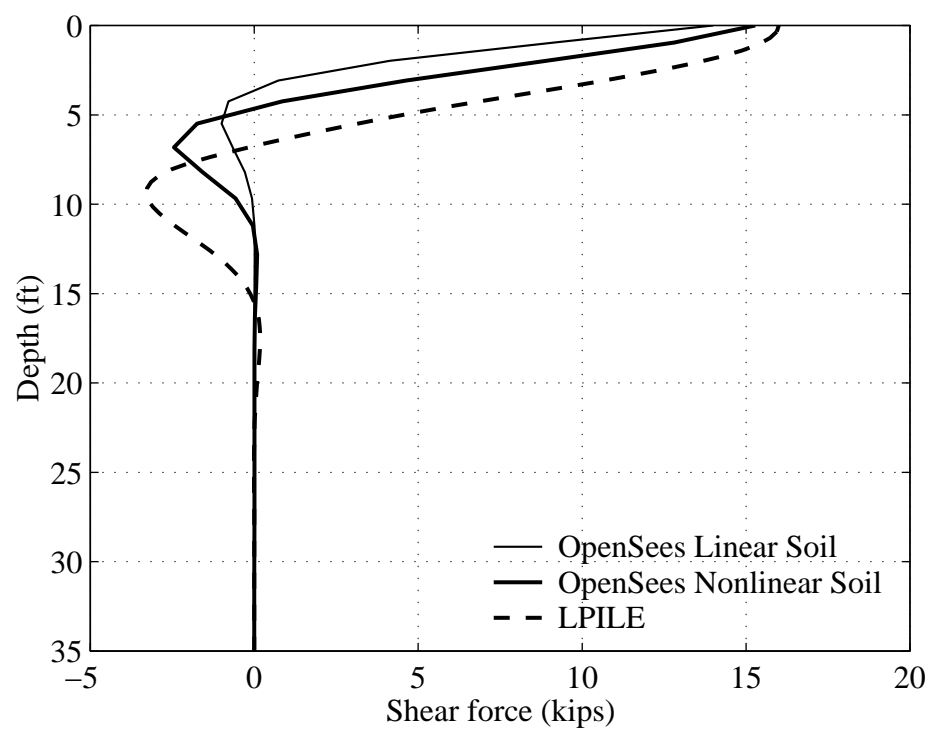


Figure E.5: Comparison of shear force profiles for load case 1.

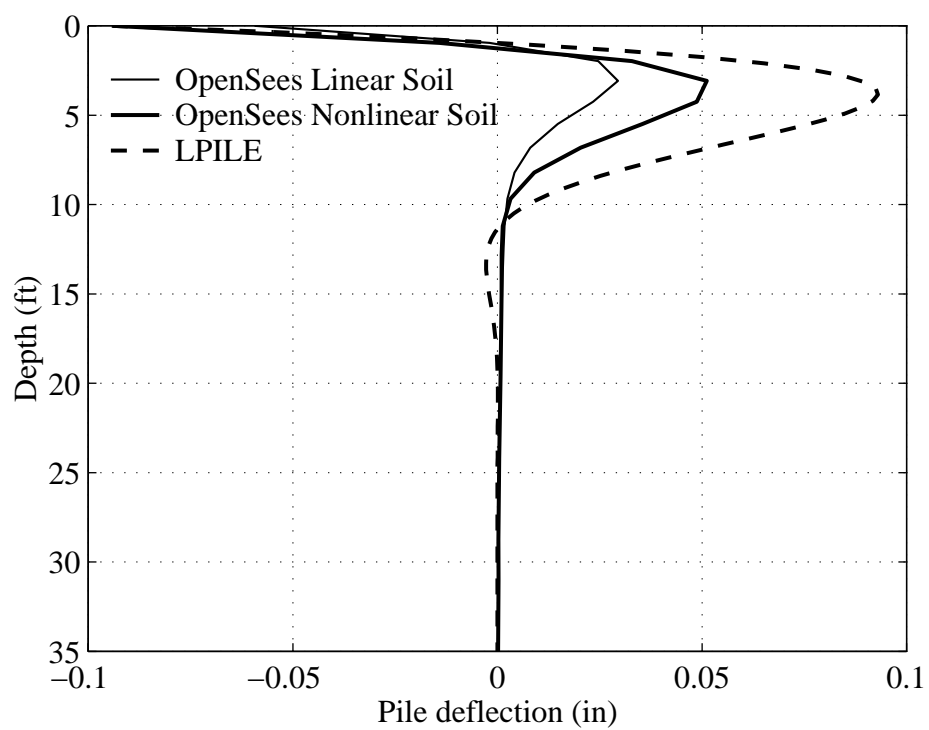


Figure E.6: Comparison of pile deflection profiles for load case 2.

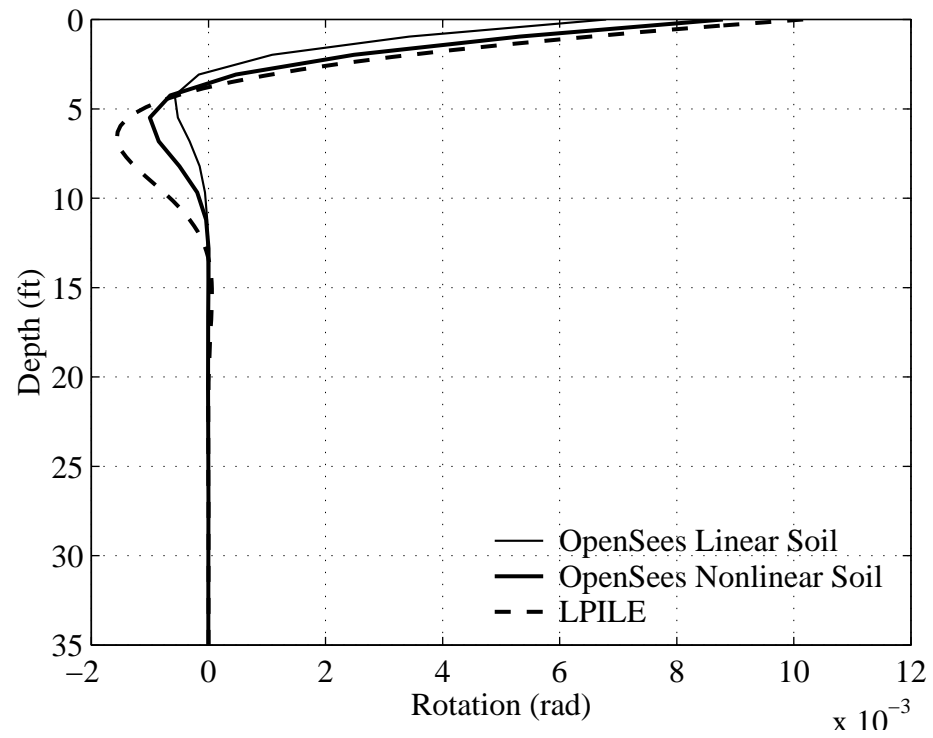


Figure E.7: Comparison of pile rotation profiles for load case 2.

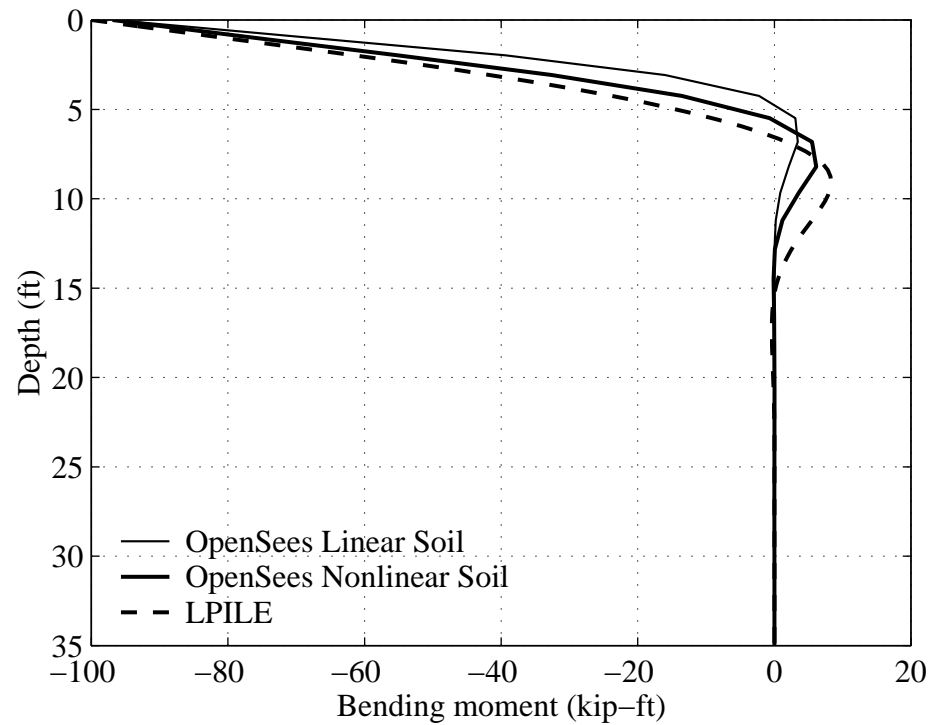


Figure E.8: Comparison of bending moment profiles for load case 2.

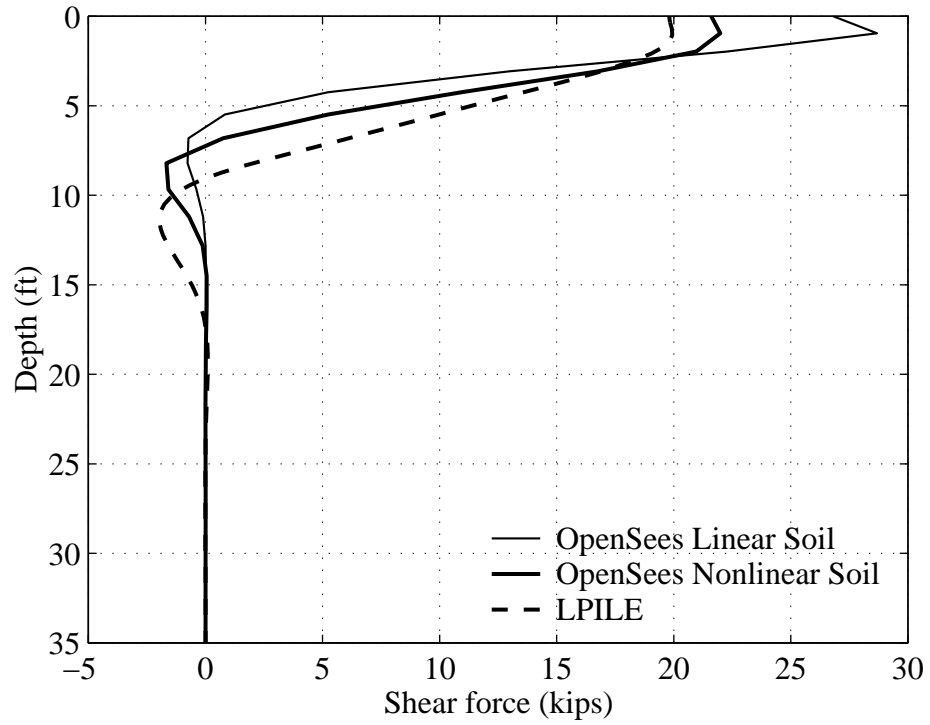


Figure E.9: Comparison of shear force profiles for load case 2.

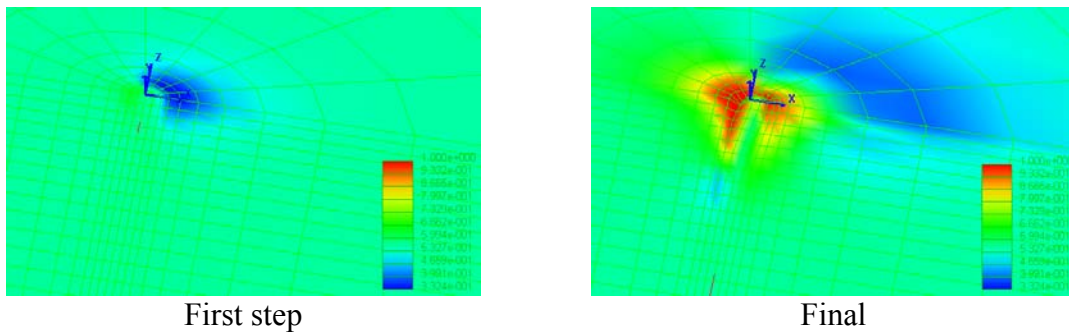


Figure E.10: Stress ratio contour fill for load case 1 (red color shows yielded soil elements).

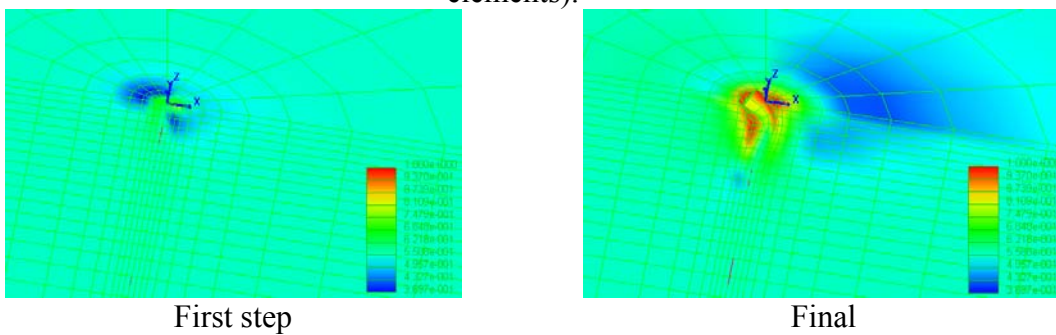


Figure E.11: Stress ratio contour fill for load case 2 (red color shows yielded soil elements).

Appendix F Finite Element Analysis of Caltrans 42" CIDH Pile Using OpenSees for General Comparison with LPILE (with Default P-Y Multiplier = 1.0)

Introduction

In this study, we conduct a finite element simulation of a CalTrans 42" CIDH pile using the 3D OpenSeesPL interface. The simulated pile responses are compared with LPILE results.

Laterally Loaded Pile

Pile Data

The geometric and elastic material properties of the pipe pile are listed below:

Diameter $D = 42"$ or radius $a = 21"$

Wall thickness $h = 0.75"$

Pile length $l = 35$ ft

Moment of Inertia of Pile $I = \pi a^3 h = 21,821$ in⁴

Young's Modulus of Pile $E_s = 29,000$ ksi

In this initial study, the pile was modeled to remain linear (also in view of the applied load levels).

Soil Domain

Linear and nonlinear soil responses are investigated. The Medium relative-density granular soil type (Lu et al. 2006) is selected in the analyses. The material properties of the soil are listed below:

At the reference confinement of 80 kPa (or 11.6 psi), the Shear Modulus of Soil $G_s = 10.88$ ksi and the Bulk Modulus of Soil $B = 29$ ksi (i.e., Poisson's ratio $\nu_s = 0.33$), see Lu et al. 2006.

Unit Weight $\gamma = 110$ pcf

For nonlinear analysis, the Friction Angle $\phi = 33^\circ$ and the peak shear stress occurs at a shear strain $\gamma_{\max} = 10\%$ (at the 11.6 psi confinement). The parameter γ_{\max} along with the shear modulus define the nonlinear soil stress-strain curve. Other values of γ_{\max} should be explored in the future.

Lateral Load

A total of six load cases (Table 1) are studied. The loads are applied at the pile head.

Table F.1: Load cases for the study.

	Pile head condition	Shear (kips)	Moment (kip-ft)
Load case 1	Fixed head	64	0
Load case 2	Fixed head	128	0
Load case 3	Fixed head	256	0
Load case 4	Free head	64	0
Load case 5	Free head	128	0
Load case 6	Free head	256	0

Finite Element Simulation

In view of symmetry, a half-mesh (2,900 8-node brick elements, 19 beam-column elements and 180 rigid beam-column elements in total) is studied as shown in Figure F.1. Length of the mesh in the longitudinal direction is 1360 ft, with 680 ft transversally (in this half-mesh configuration, resulting in a 1360 ft x 1360 soil domain in plan view). Layer thickness is 60 ft (the bottom of the soil domain is 25 ft below the pile tip, so as to mimic the analytical half-space solution).

The floating pile is modeled by beam-column elements (Mazzoni et al. 2006), and rigid beam-column elements are used to model the pile size (diameter).

The following boundary conditions are enforced:

- I) The bottom of the domain is fixed in the longitudinal (x), transverse (y), and vertical (z) directions.
- II) Left, right and back planes of the mesh are fixed in x and y directions (the lateral directions) and free in z direction.
- III) Plane of symmetry is fixed in y direction and free in z and x direction (to model the full-mesh 3D solution).

The lateral load is applied at the pile head (ground level) in x (longitudinal) direction.

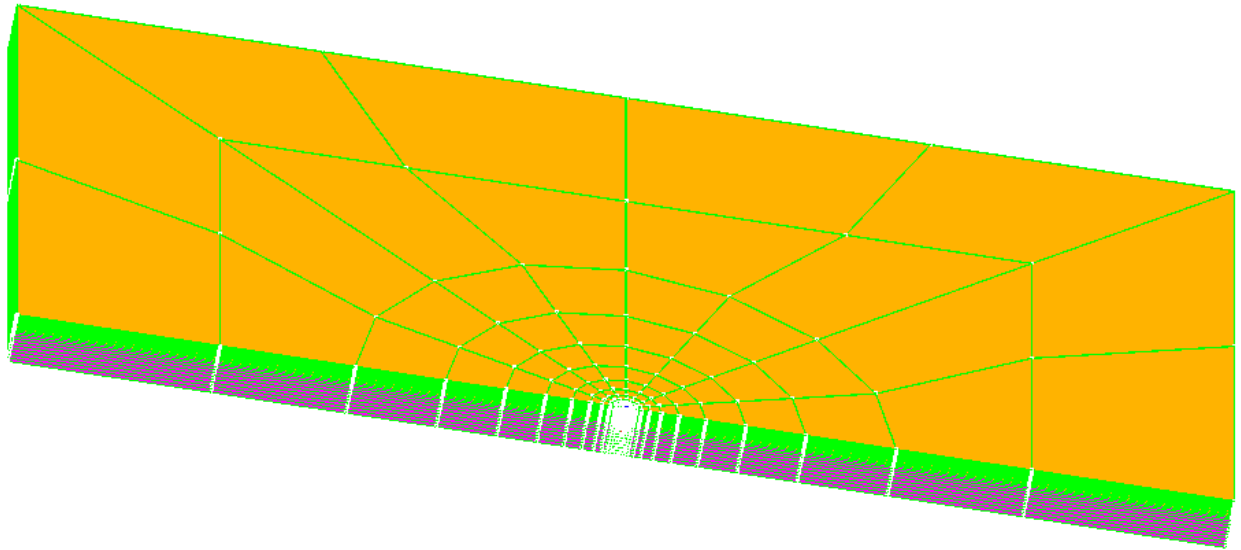
The above simulations were performed using OpenSeesPL (Lu et al. 2006).

Simulation Results

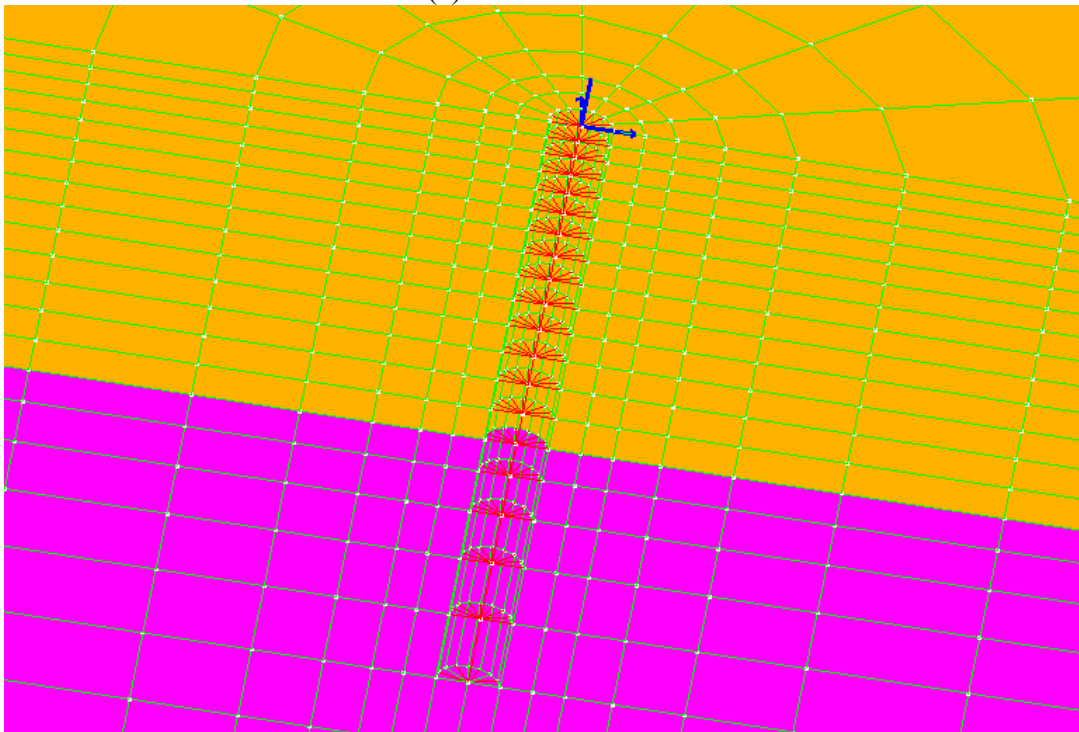
Figures D.2-D.5 show comparisons of the pile deflection, rotation, bending moment and shear force profiles, respectively, for the fixed-head condition (load cases 1, 2 & 3), along with LPILE results for comparison. Figures D.6-D.9 show comparisons of the pile deflection, rotation, bending moment and shear force profiles, respectively, for the free-head condition (load cases 4, 5 & 6), also along with LPILE results for comparison. The

stress ratio contour fill of the nonlinear runs for the fixed and free head conditions are displayed in Figures D.10 & D.11.

Comparisons of the linear and nonlinear responses using OpenSees are shown in Appendix (Figures D.12-D.19).



(a) Isometric view



(b) Pile head close-up

Figure F.1: Finite element mesh employed in this study.

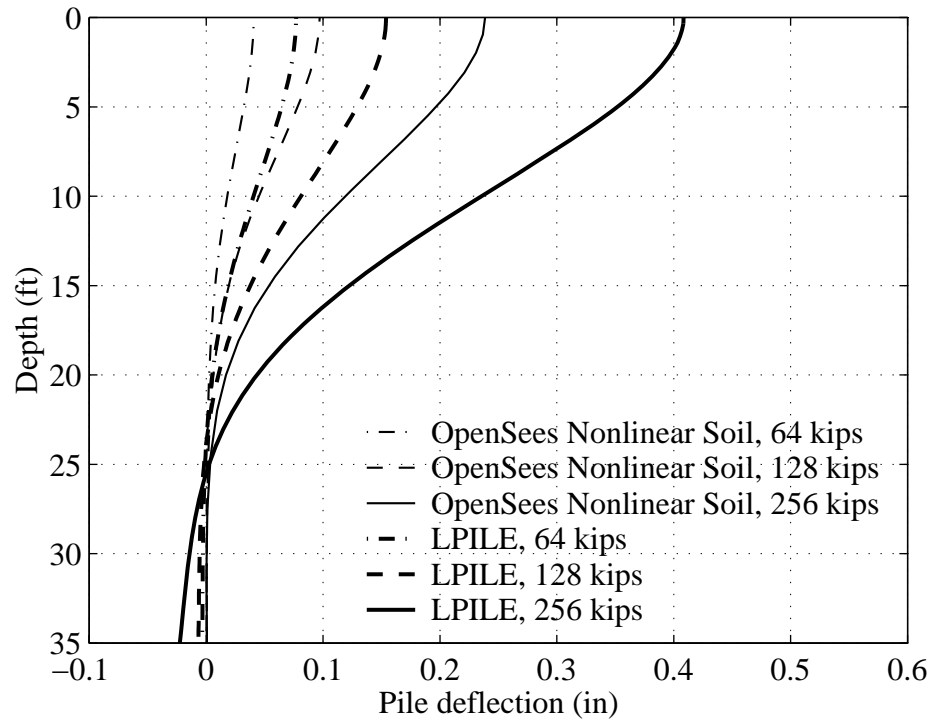


Figure F.2: Comparison of pile deflection profiles for the fixed-head condition.

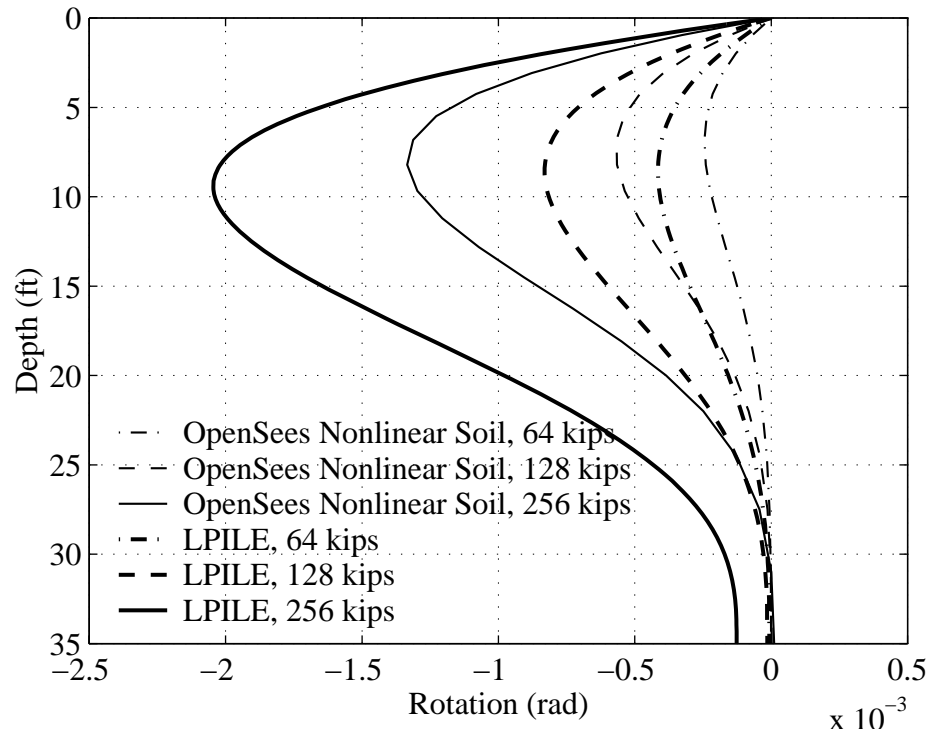


Figure F.3: Comparison of pile rotation profiles for the fixed-head condition.

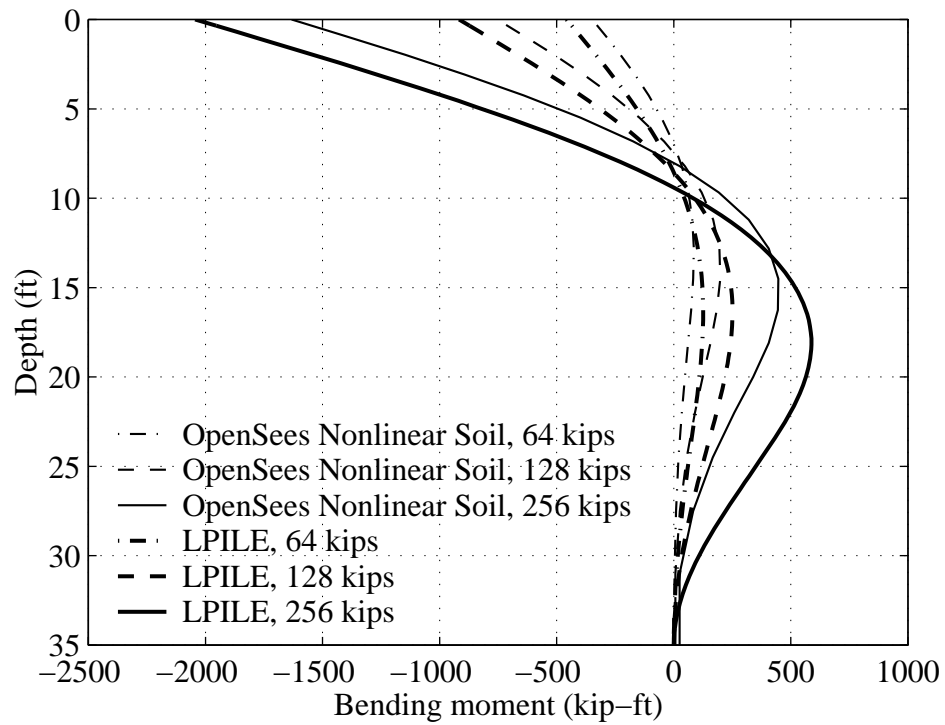


Figure F.4: Comparison of bending moment profiles for the fixed-head condition.

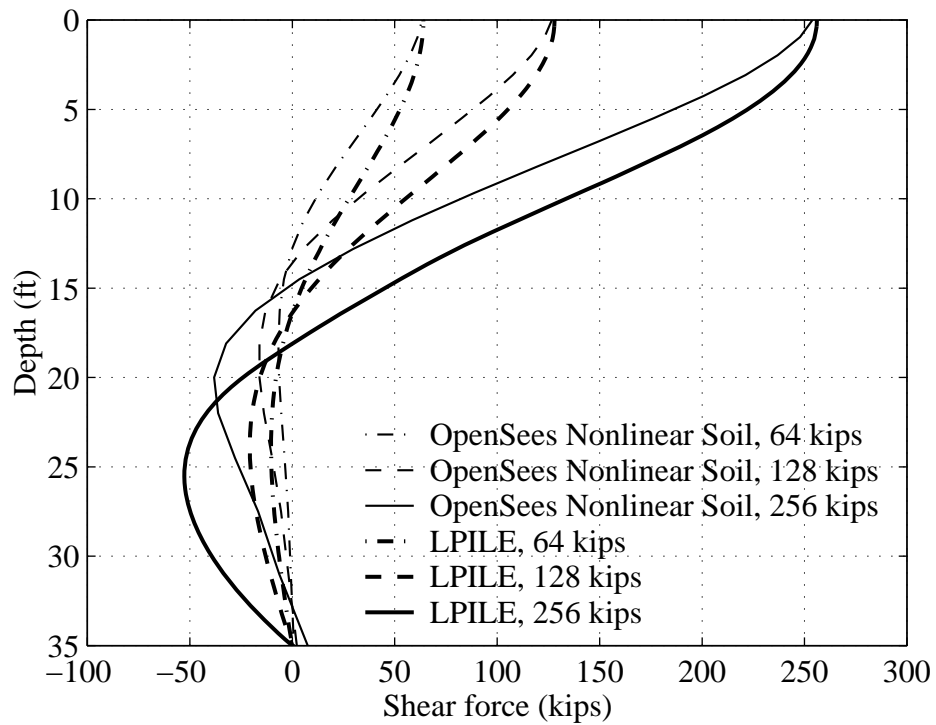


Figure F.5: Comparison of shear force profiles for the fixed-head condition.

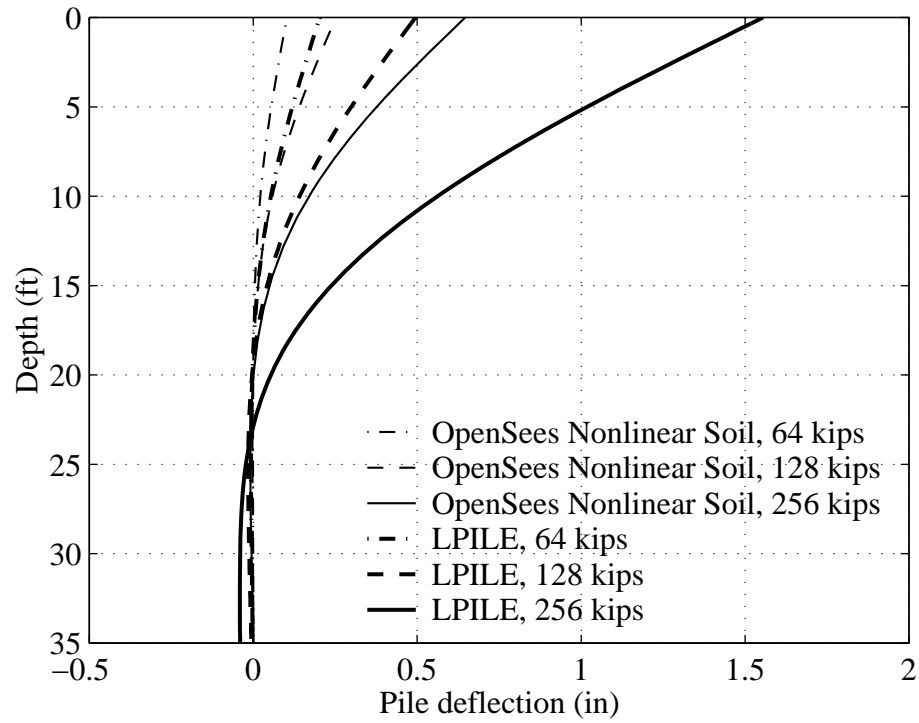


Figure F.6: Comparison of pile deflection profiles for the free-head condition.

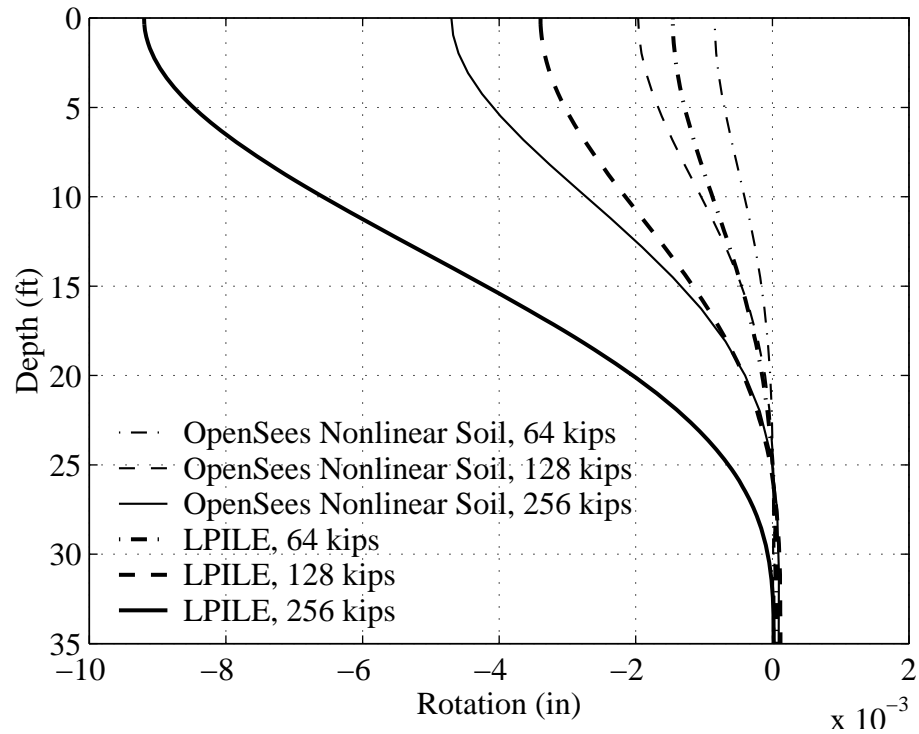


Figure F.7: Comparison of pile rotation profiles for the free-head condition.

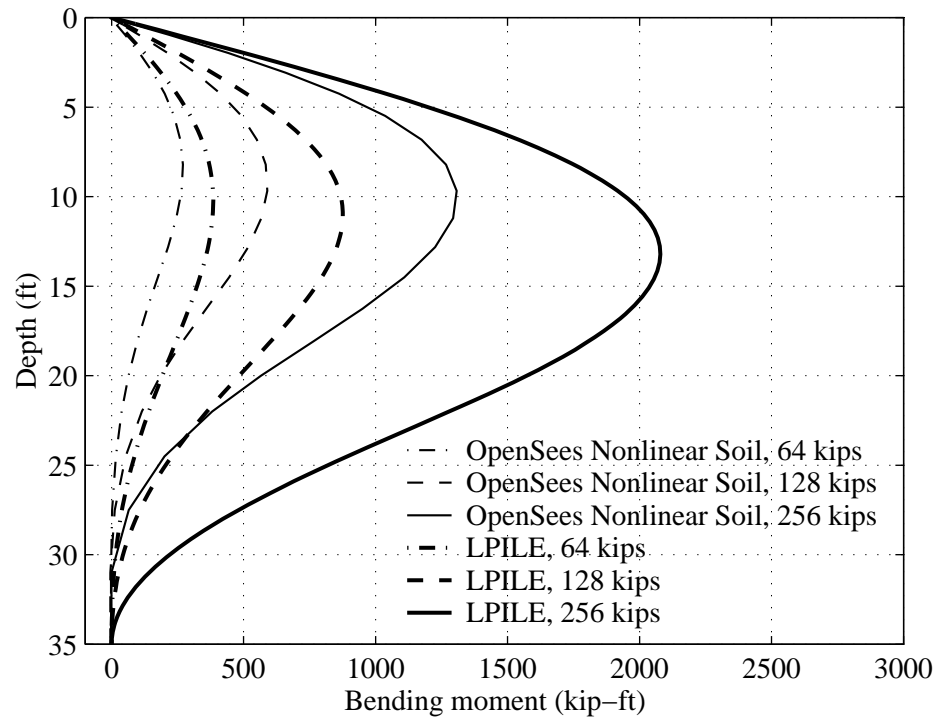


Figure F.8: Comparison of bending moment profiles for the free-head condition.

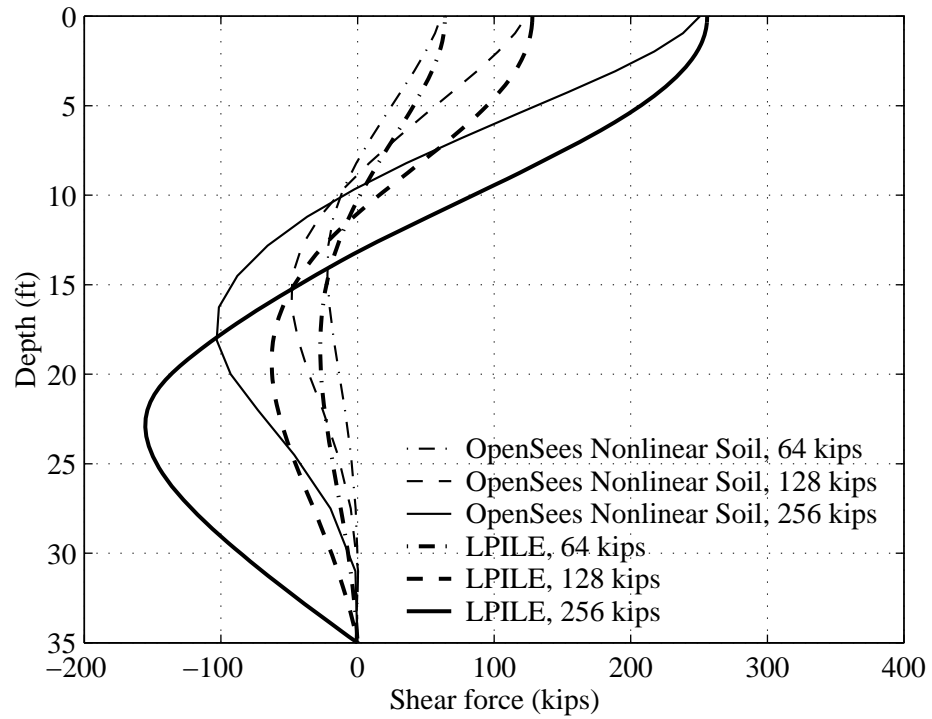
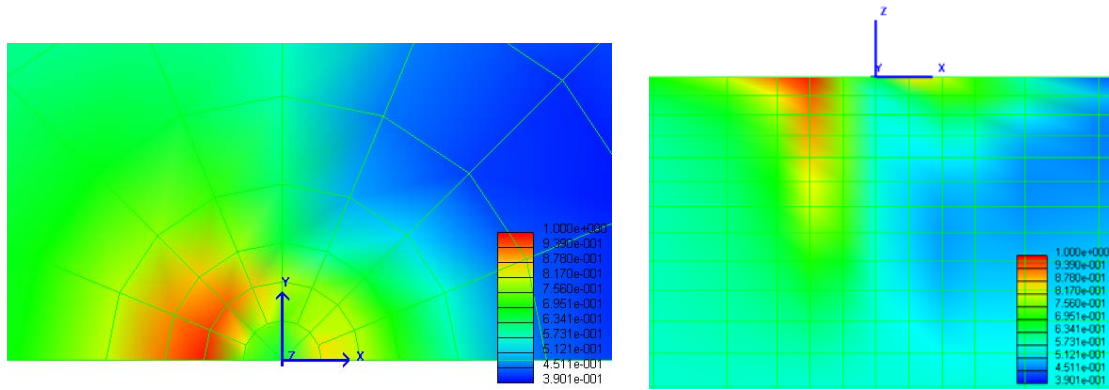
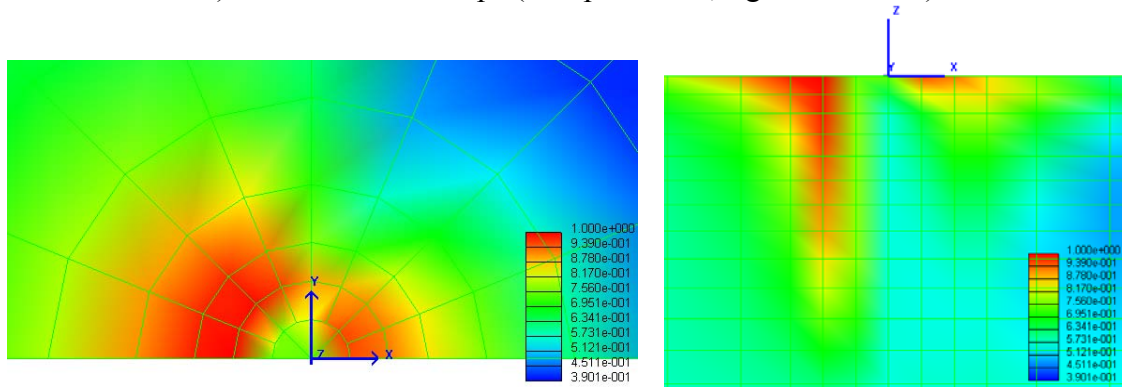


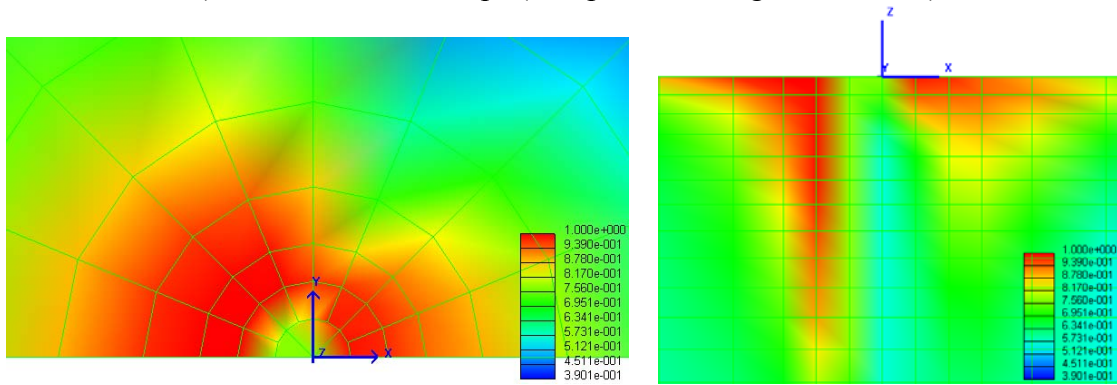
Figure F.9: Comparison of shear force profiles for the free-head condition.



a) lateral load = 64 kips (left: plan view; right: side view)

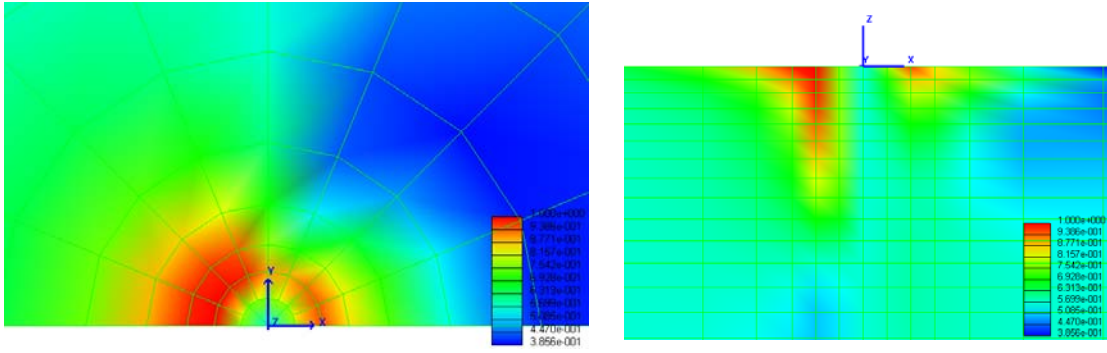


b) lateral load = 128 kips (left: plan view; right: side view)

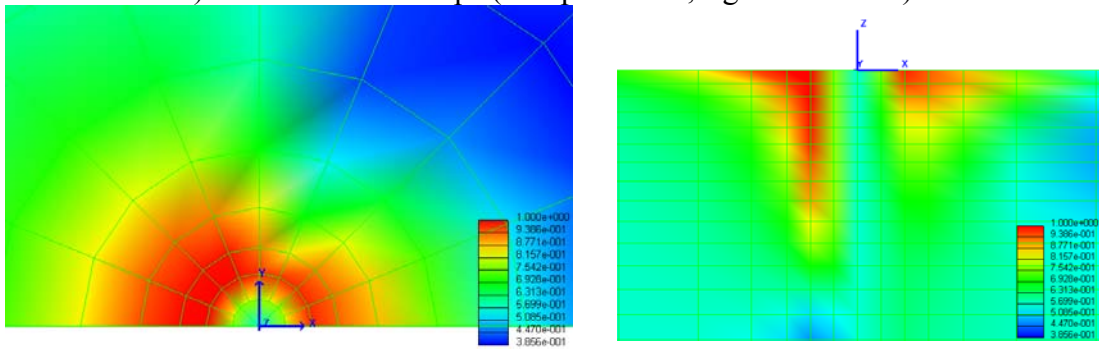


c) lateral load = 256 kips (left: plan view; right: side view)

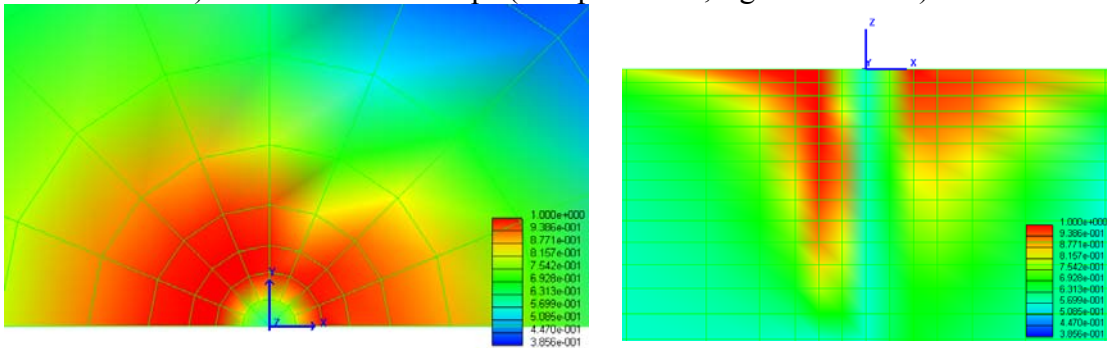
Figure F.10: Stress ratio contour fill of the nonlinear run for the fixed-head condition (red color shows yielded soil elements).



a) lateral load = 64 kips (left: plan view; right: side view)



b) lateral load = 128 kips (left: plan view; right: side view)



c) lateral load = 256 kips (left: plan view; right: side view)

Figure F.11: Stress ratio contour fill of the nonlinear run for the free-head condition (red color shows yielded soil elements).

Appendix F-I: OpenSees Simulation Results

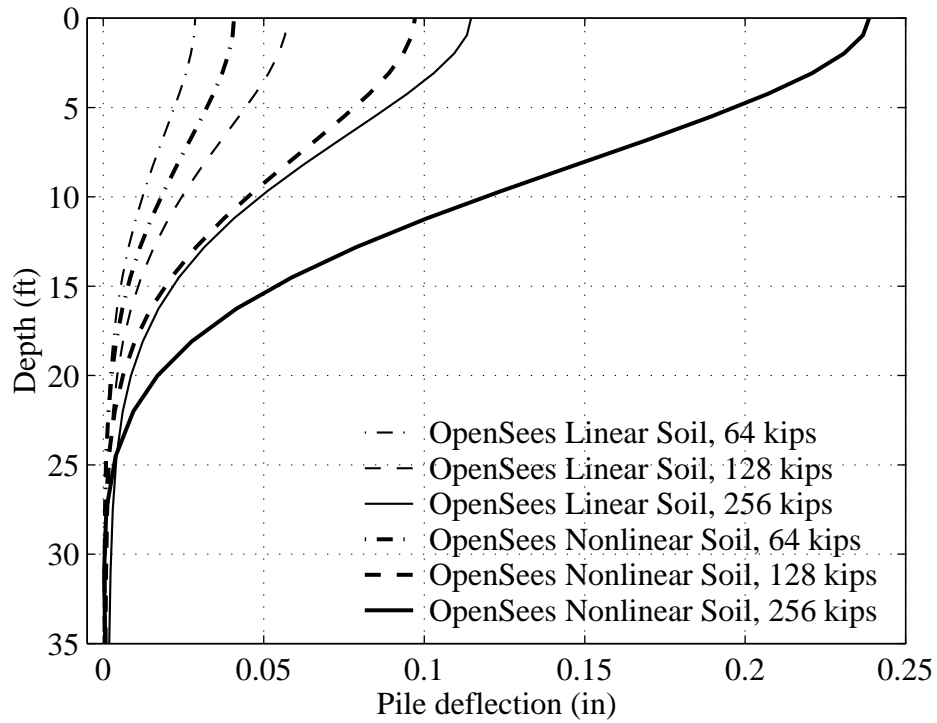


Figure F.12: Comparison of pile deflection profiles for the fixed-head condition.

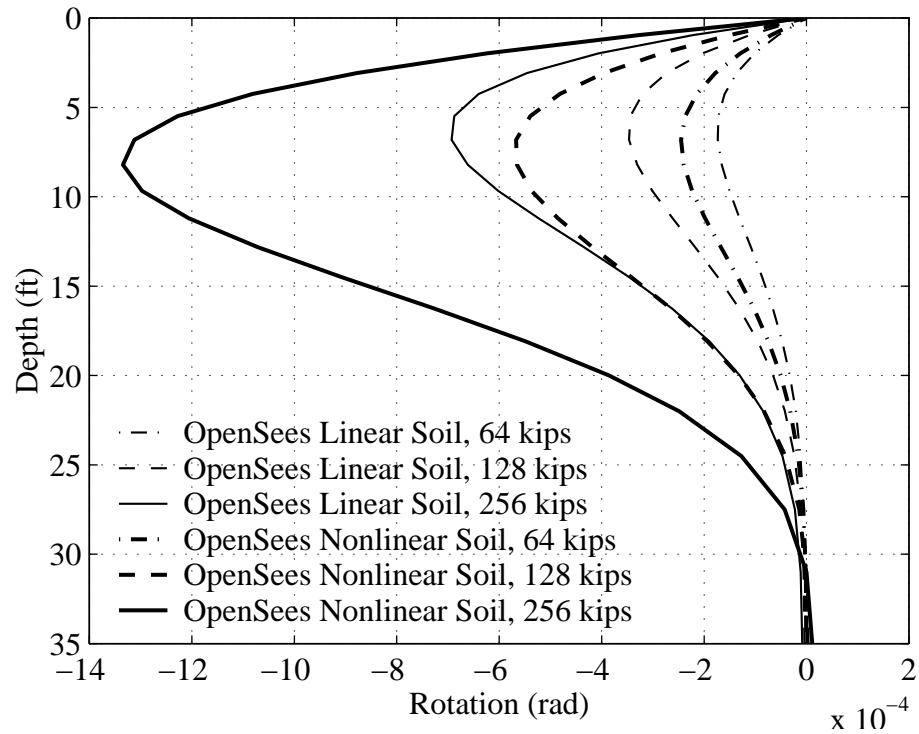


Figure F.13: Comparison of pile rotation profiles for the fixed-head condition.

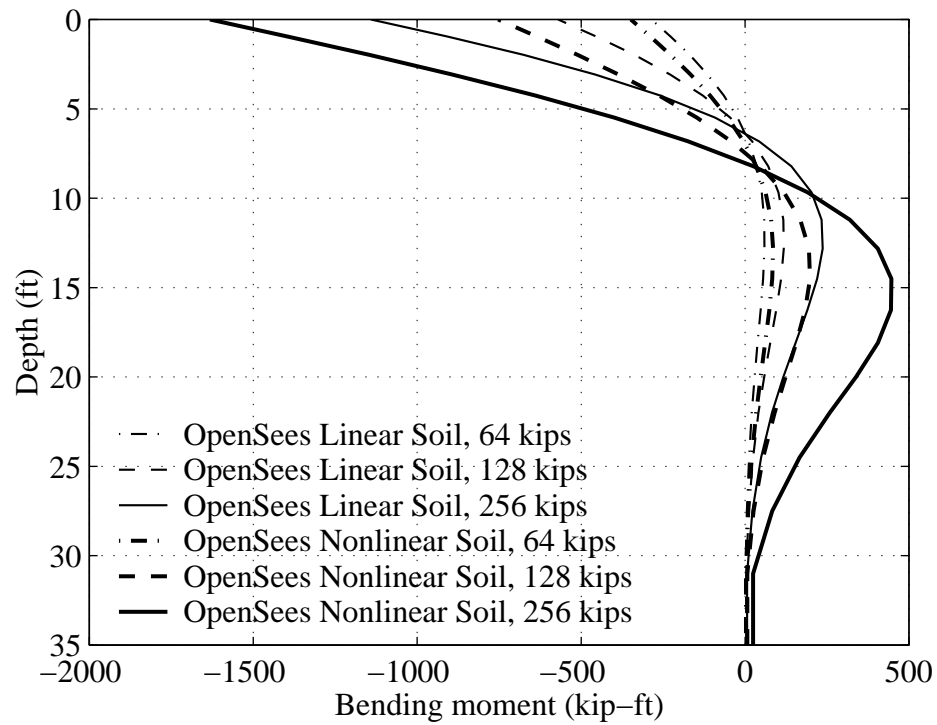


Figure F.14: Comparison of bending moment profiles for the fixed-head condition.

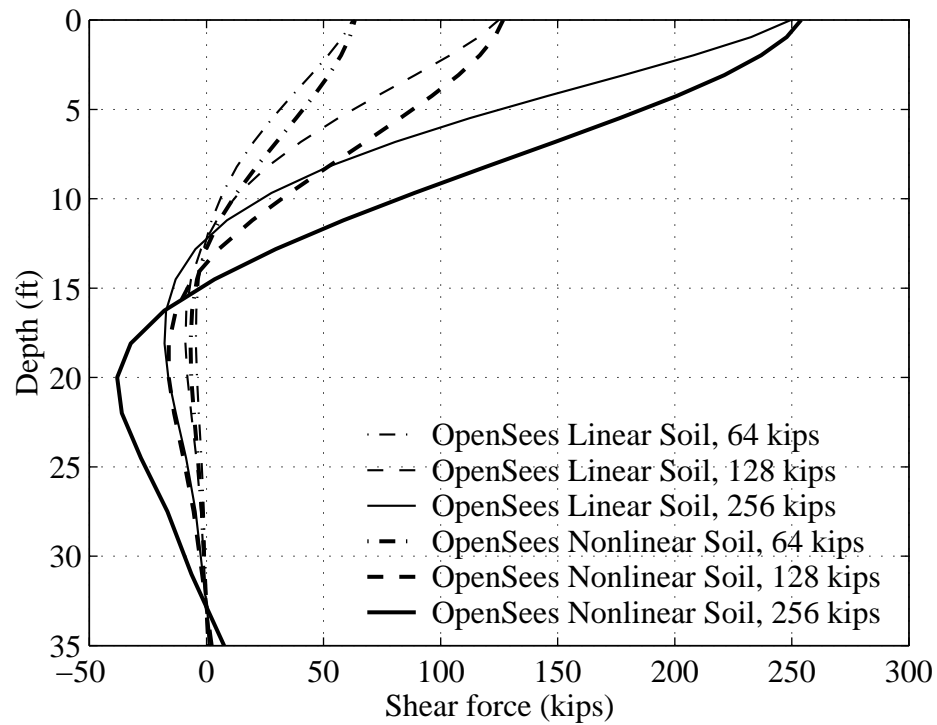


Figure F.15: Comparison of shear force profiles for the fixed-head condition.

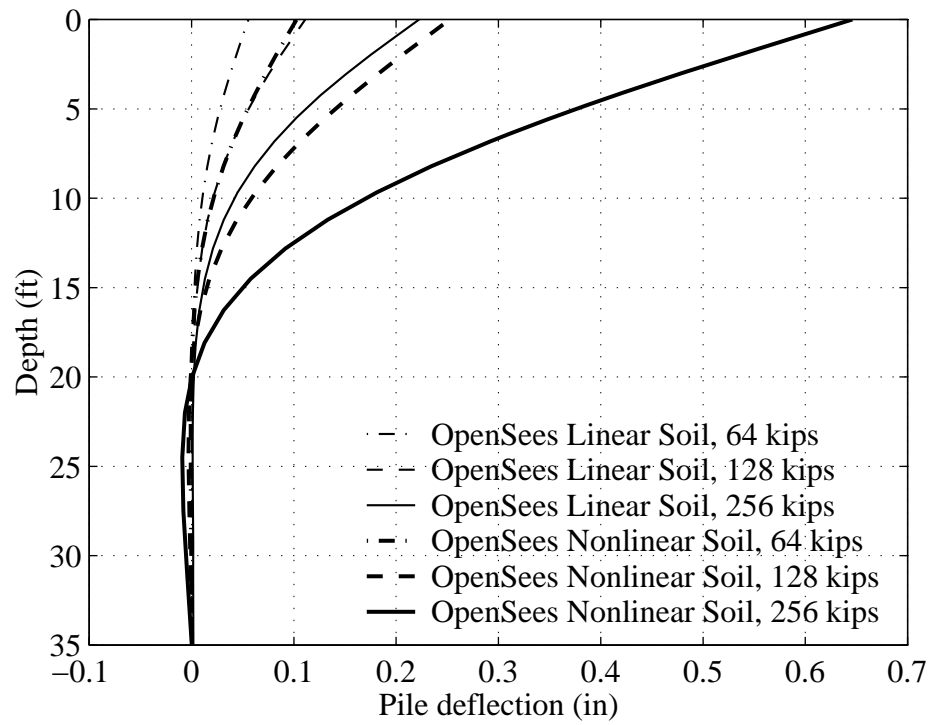


Figure F.16: Comparison of pile deflection profiles for the free-head condition.

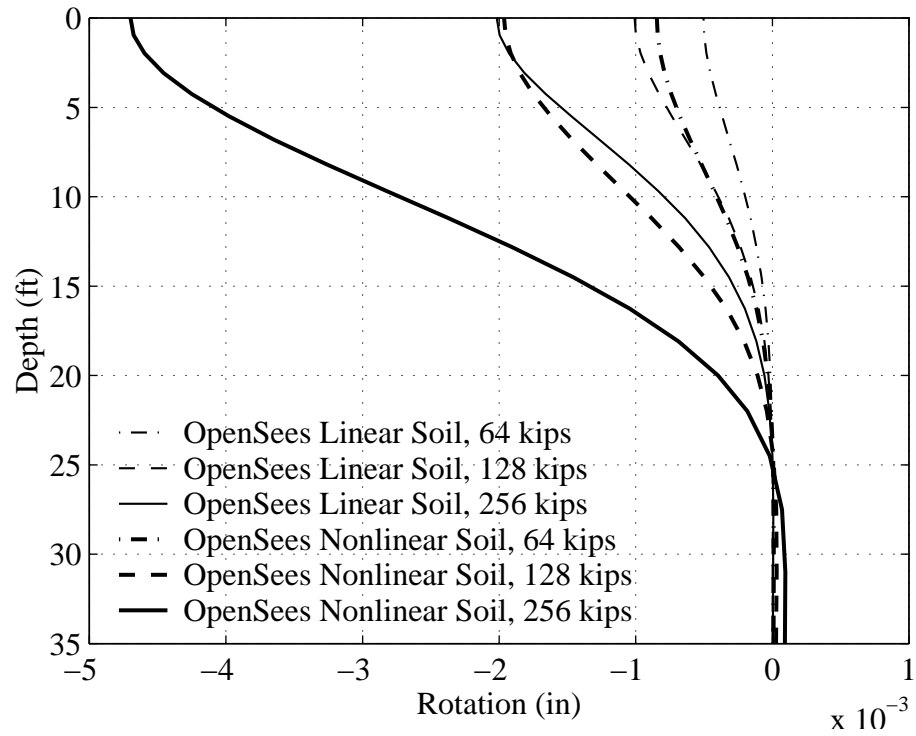


Figure F.17: Comparison of pile rotation profiles for the free-head condition.

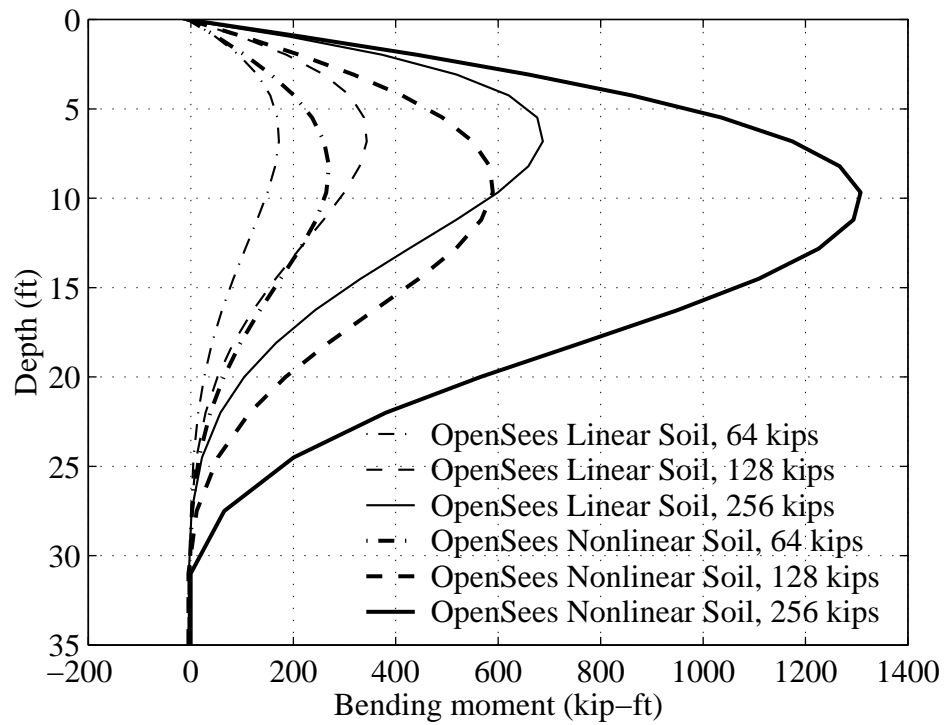


Figure F.18: Comparison of bending moment profiles for the free-head condition.

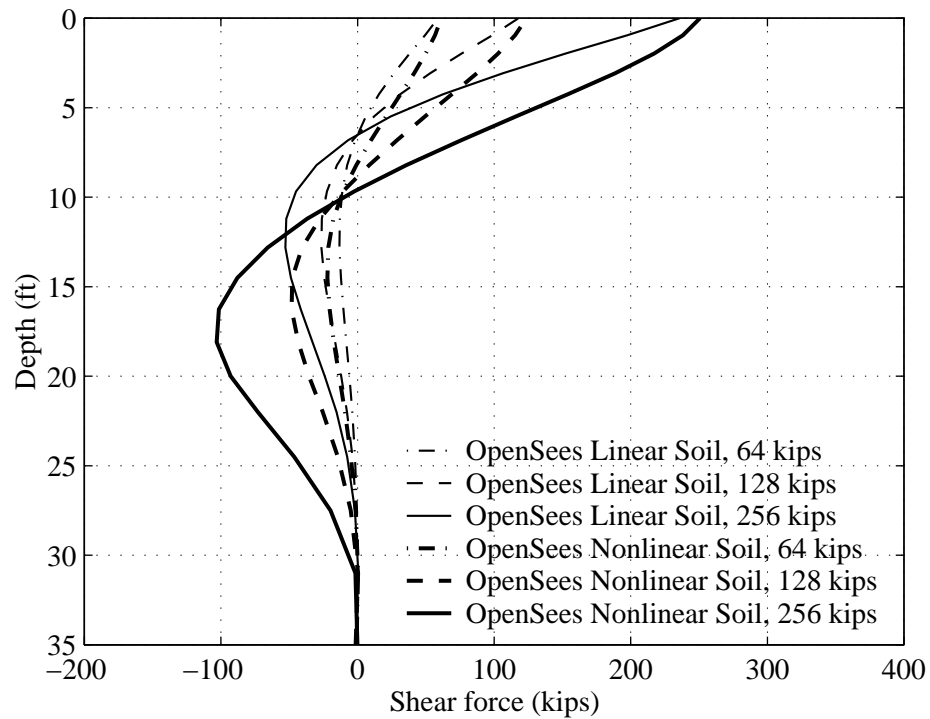


Figure F.19: Comparison of shear force profiles for the free-head condition.

Appendix G Finite Element Analysis of Standard CalTrans 16" CIDH Pile Subjected to Axial Load

Introduction

In this study, we conduct a finite element simulation of the standard Caltran 16" CIDH pile using the 3D OpenSeesPL interface. The simulated pile is subjected to axial load.

Axially Loaded Pile

Pile Data

The geometric and elastic material properties of the pile are listed below:

Diameter $D = 16"$

Pile length $l = 35$ ft

Moment of Inertia of Pile $I = 850$ in⁴

Young's Modulus of Pile $E_c = 4030$ ksi

In this initial study, the pile was modeled to remain linear (also in view of the applied load levels).

Soil Domain

Nonlinear soil response is investigated. The Medium relative-density granular soil type (Lu et al. 2006) is selected in the analyses. The material properties of the soil are listed below:

At the reference confinement of 80 kPa (or 11.6 psi), the Shear Modulus of Soil $G_s = 10.88$ ksi and the Bulk Modulus of Soil $B = 29$ ksi (i.e., Poisson's ratio $\nu_s = 0.33$), see Lu et al. 2006.

Effective Unit Weight $\gamma' = 110$ pcf (given by CalTrans)

For nonlinear analysis, the Friction Angle $\phi = 33^\circ$ (given by CalTrans) and the peak shear stress occurs at a shear strain $\gamma_{\max} = 10\%$ (at the 11.6 psi confinement). The parameter γ_{\max} along with the shear modulus define the nonlinear soil stress-strain curve. Other values of γ_{\max} should be explored in the future.

Axial Load

An axial load of 243 kips is applied at the pile head (free head connection).

Finite Element Simulation

In view of symmetry, a half-mesh (2,900 8-node brick elements, 19 beam-column elements and 180 rigid beam-column elements in total) is studied as shown in Figure G.1. Length of the mesh in the longitudinal direction is 520 ft, with 260 ft transversally (in this half-mesh configuration, resulting in a 520 ft x 520 soil domain in plan view). Layer thickness is 60 ft (the bottom of the soil domain is 25 ft below the pile tip, so as to mimic the analytical half-space solution).

The floating pile is modeled by beam-column elements (Mazzoni et al. 2006), and rigid beam-column elements are used to model the pile size (diameter).

The following boundary conditions are enforced:

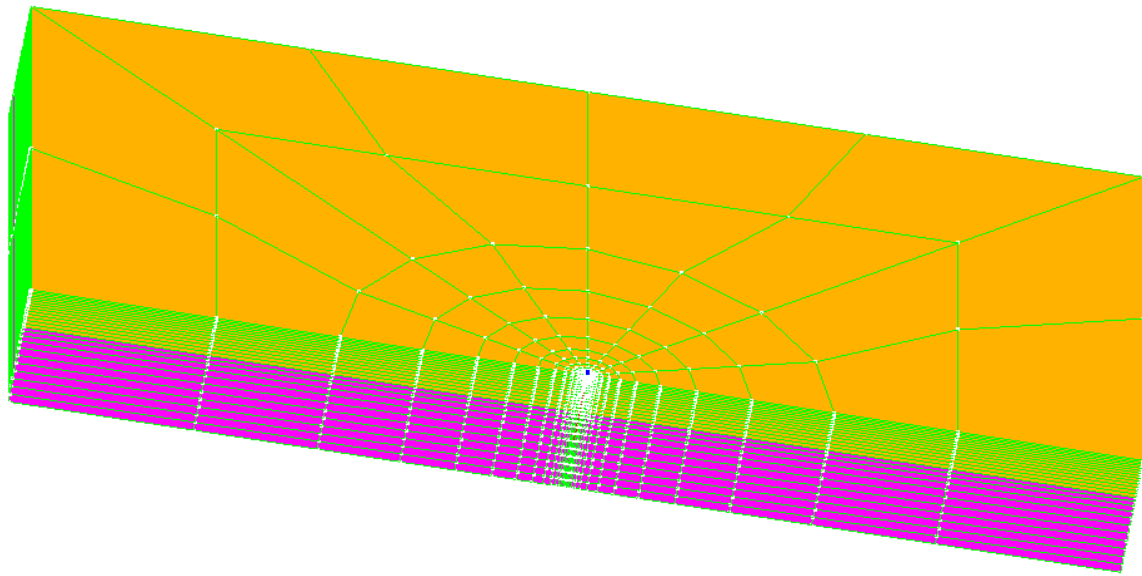
- I) The bottom of the domain is fixed in the longitudinal (x), transverse (y), and vertical (z) directions.
- II) Left, right and back planes of the mesh are fixed in x and y directions (the lateral directions) and free in z direction.
- III) Plane of symmetry is fixed in y direction and free in z and x direction (to model the full-mesh 3D solution).

The axial load is applied at the pile head (ground level) in z (vertical) direction.

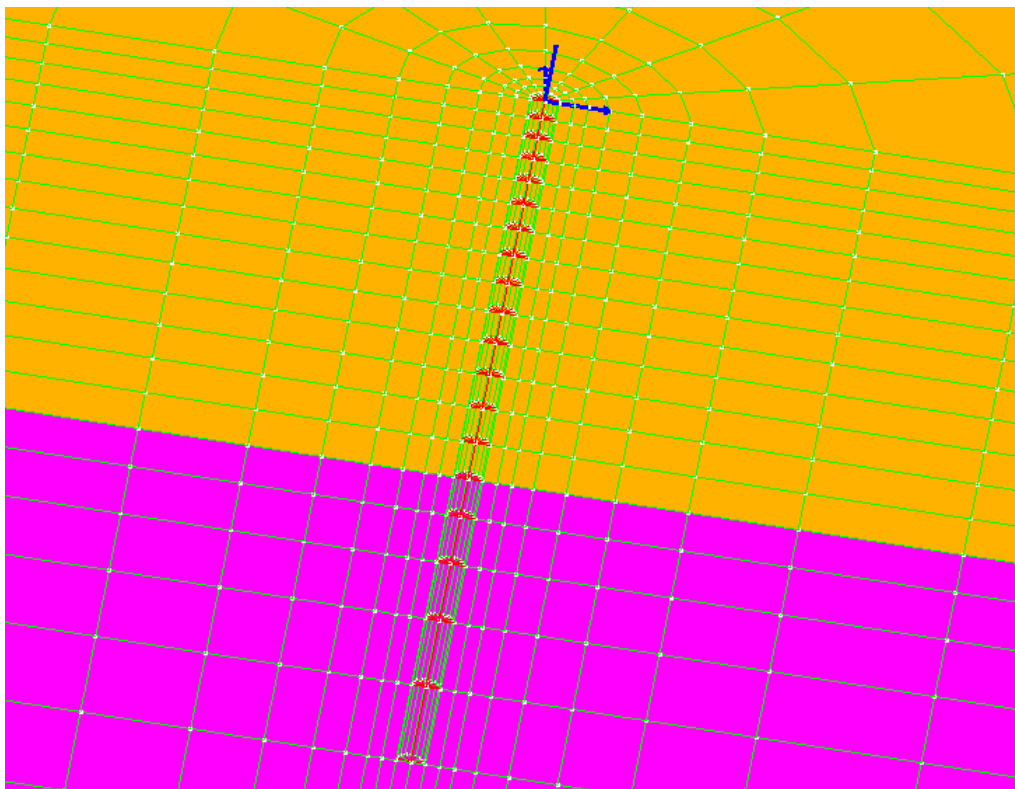
The above simulations were performed using OpenSeesPL (Lu et al. 2006).

Simulation Results

The pile vertical displacement and axial force profiles at the axial load of 243 kips are shown in Figure G.2. The final deformed mesh is shown in Figure G.3. Figure G.4 displays the stress ratio contour fill.



(a) Isometric view



(b) Pile head close-up

Figure G.1: Finite element mesh employed in this study.

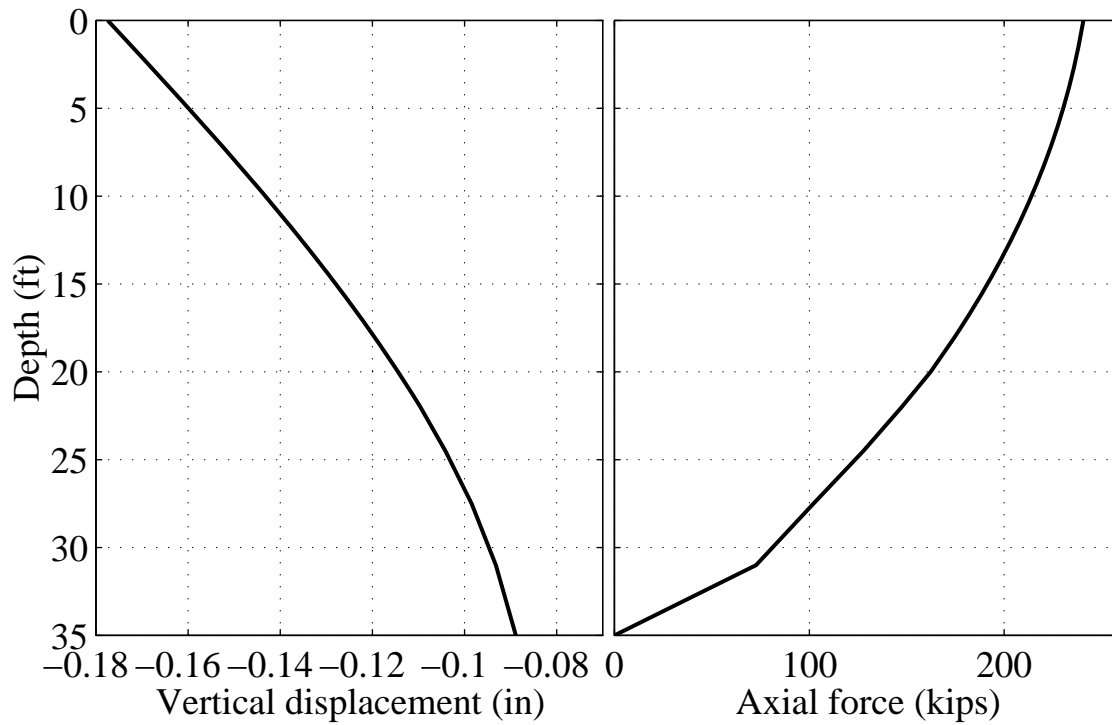


Figure G.2: Pile profile response at the axial load of 243 kips.

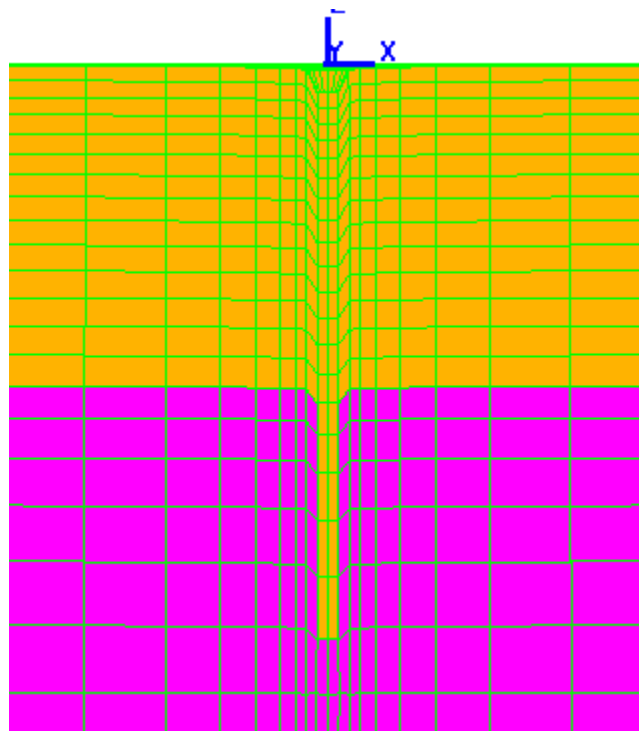
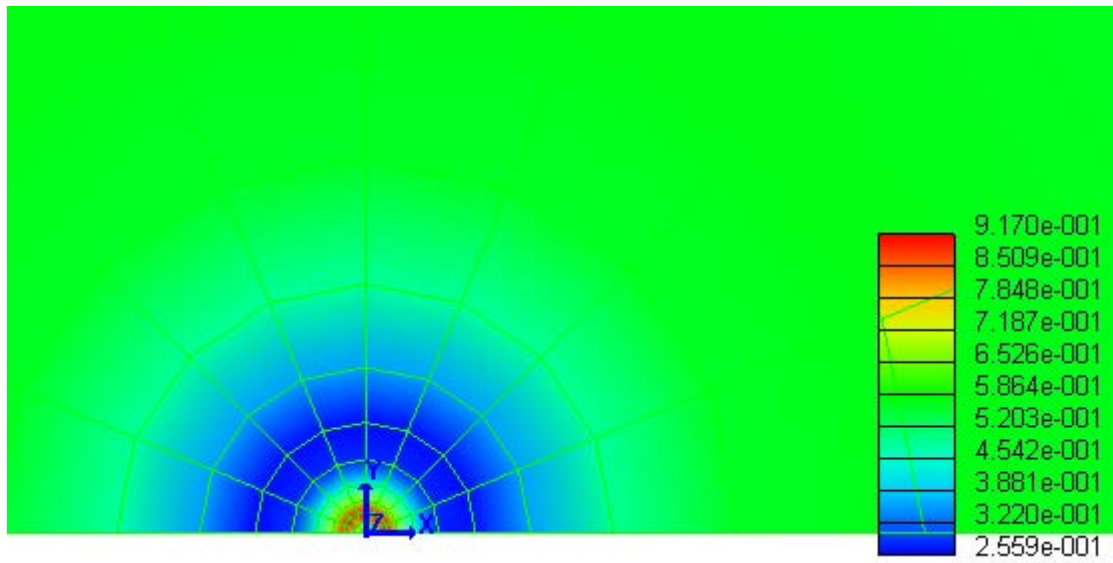
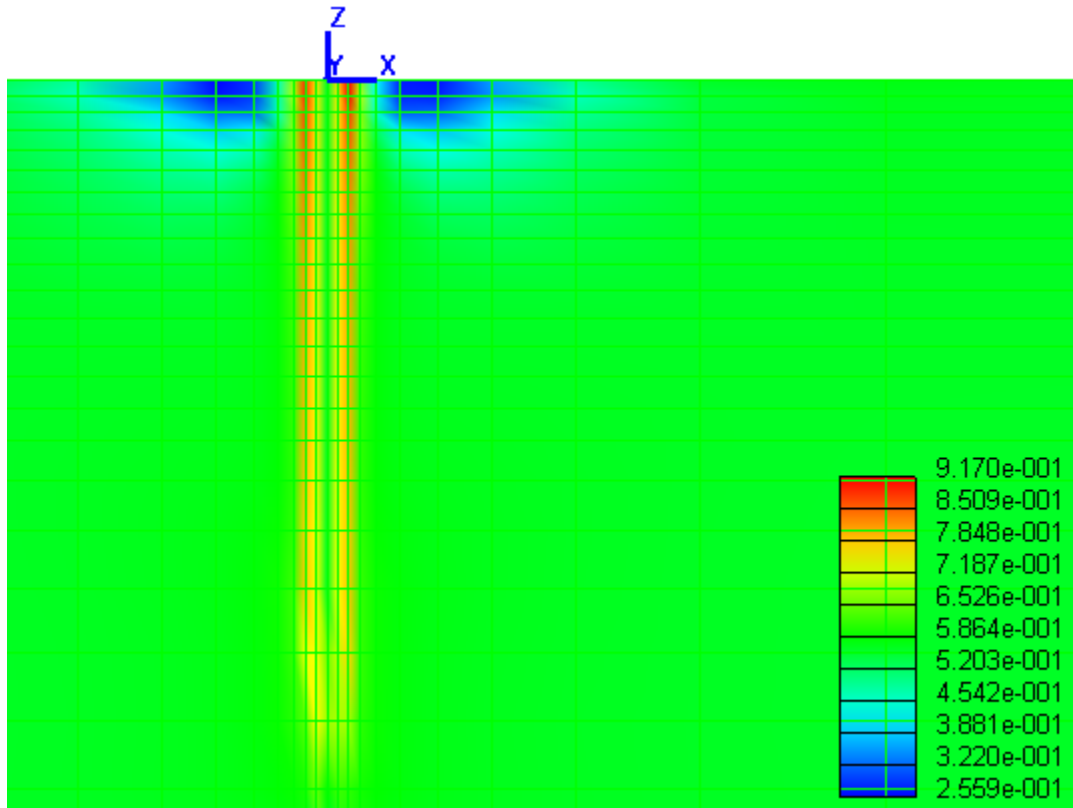


Figure G.3: Close-up of final deformed mesh (factor of 120).



a) plan view



b) Side view

Figure G.4: Stress ratio contour fill for the nonlinear analysis (red color shows yielded soil elements).

Appendix H Moment-Curvature Analysis of Circular Nonlinear RC Beam (Fiber Section)

Introduction

In this study, we compare with an OpenSees moment-curvature pushover analysis input file (see appendix). A single circular reinforced concrete column is rigidly attached to the soil mesh for that purpose. The soil domain is assumed rigid so as to simulate a cantilever beam scenario.

The OpenSees input file is Example 9 listed in the OpenSees Example Manual (<http://opensees.berkeley.edu/OpenSees/manuals/ExamplesManual/HTML/>). This OpenSees example introduces the moment-curvature procedures for sections in 3D space. The moment-curvature analysis of the section in this OpenSees example is by creating a zero-length rotational-spring element. This section is subjected to a user-defined constant axial load and to a linearly-increasing moment to a user-defined maximum curvature (Mazzoni et al. 2006).

Laterally Loaded Pile

The circular pile is 5 ft in diameter (D). The pile length above the ground surface is 10 ft. Therefore the equivalent pile length is 10 ft.

Fiber section is used to model the nonlinear behavior of the pile. The fiber section properties are listed in Tables F.1-4. The schematic of the fiber section definition is also shown in Figure F.1 (also see Figure F.2 for the input interface for fiber section in OpenSeesPL):

Table H.1: Material parameters of the concrete material.

	Core	Cover
Concrete Compressive Strength (ksi)	-5.2	-4
Concrete Strain at Maximum Strength	-0.002885	-0.003
Concrete Crushing Strength (ksi)	-1.04	-0.8
Concrete Strain at Crushing Strength	-0.0144	-0.01

Table H.2: Material parameters of the steel material.

	Steel
Yield Strength (ksi)	66.8
Initial Elastic Tangent (ksi)	29000
Strain-hardening Ratio	0.01

Table H.3: Patch information for the pile circular cross section.

	Core	Cover
Number of Subdivisions (fibers) in the Circumferential Direction	8	8
Number of Subdivisions (fibers) in the Radial Direction	8	4
Internal Radius (in)	0	25
External Radius (in)	25	30

Table H.4: Layer information for the pile circular cross section.

Number of Reinforcing Bars along Layer	16
Area of Individual Reinforcing Bar (in ²)	2.25
Radius of Reinforcing Layer (in)	25

Pile head (lateral) displacement of 0.69 in is applied in 25 equal steps. An axial load of 1800 kips is applied at the pile head (free head connection) during loading.

Simulation Results

The finite element mesh employed is shown in Figure F.3. As mentioned before, the soil domain is rigid therefore the meshing of the soil domain is insignificant. 10 `nonlinearBeamColumn` elements are used for the pile.

The comparison of the moment-curvature curves is shown in Figure F.4. Both curves match quite well.

Response profiles of the single pile are shown in Figure F.5. A shear load of 662 kips is reached at the pile head longitudinal displacement of 0.69 in (Figure F.5 & F.6). The maximum moment reached 6609 kip-ft, occurring at the ground surface (Figure F.6).

The moment-curvature curve of the single pile at the ground surface location is shown in Figure F.7.

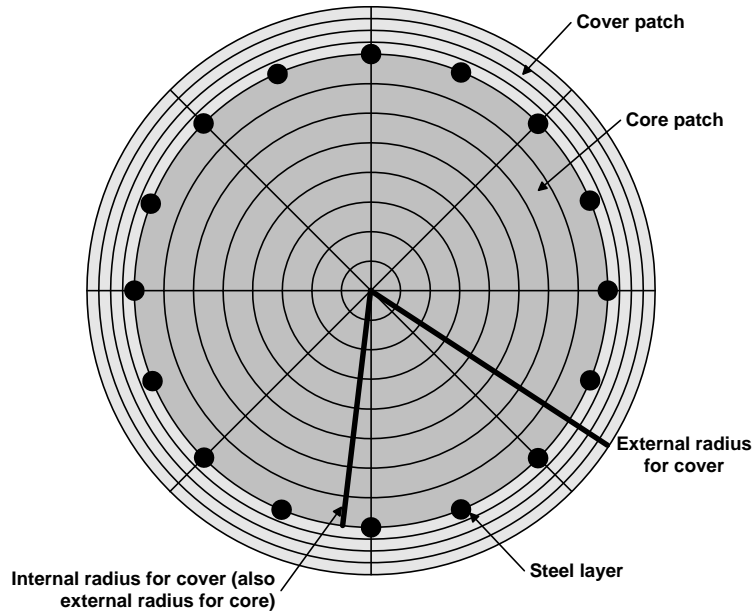


Figure H.1: Schematic of the fiber section definition for the circular pile cross section.

Material		Core	Cover	
Concrete01:	Concrete Compressive Strength	-5.2	-4	[ksi]
	Concrete Strain at Maximum Strength	-0.002885	-0.003	
	Concrete Crushing Strength	-1.04	-0.8	[ksi]
	Concrete Strain at Crushing Strength	-0.0144	-0.01	
Steel01:	Yield Strength	66.8		[ksi]
	Initial Elastic Tangent	29000		[ksi]
	Strain-hardening Ratio	0.01		

Circular Shape		Core	Cover	
Patch:	Number of Subdivisions (fibers) in the Circumferential Direction	8	8	
	Number of Subdivisions (fibers) in the Radial Direction	8	4	
	Internal Radius	0	25	[in]
	External Radius	25	30	[in]
Layer:	Number of Reinforcing Bars along Layer	16		
	Area of Individual Reinforcing Bar	2.25		[in ²]
	Radius of Reinforcing Layer	25		[in]

Figure H.2: Material properties for the Fiber section.

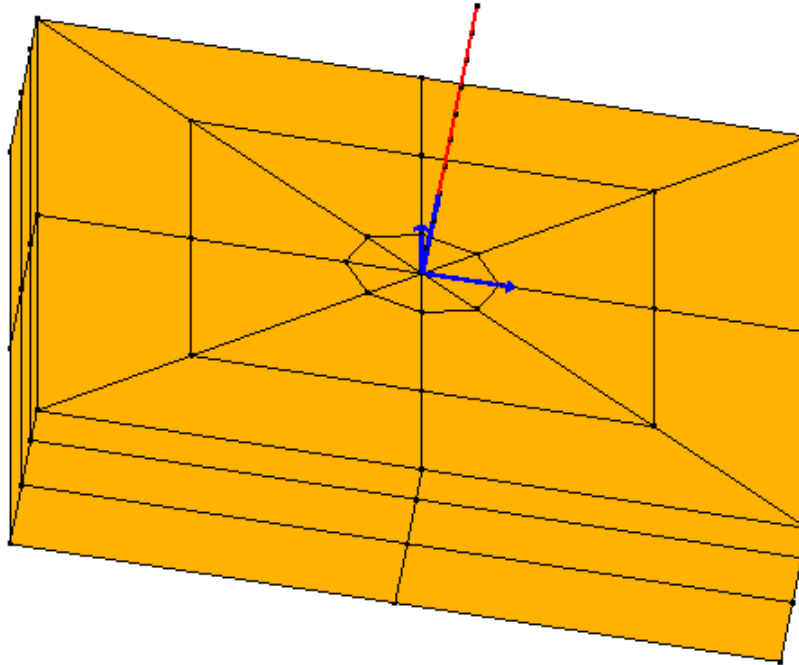


Figure H.3: Finite element mesh employed in this study.

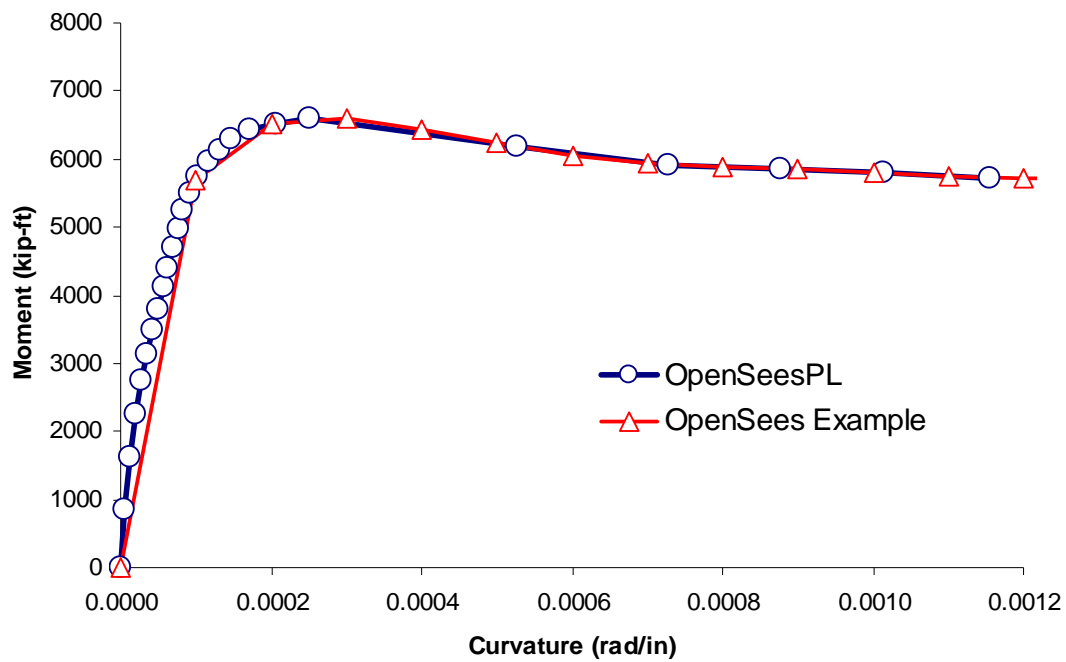
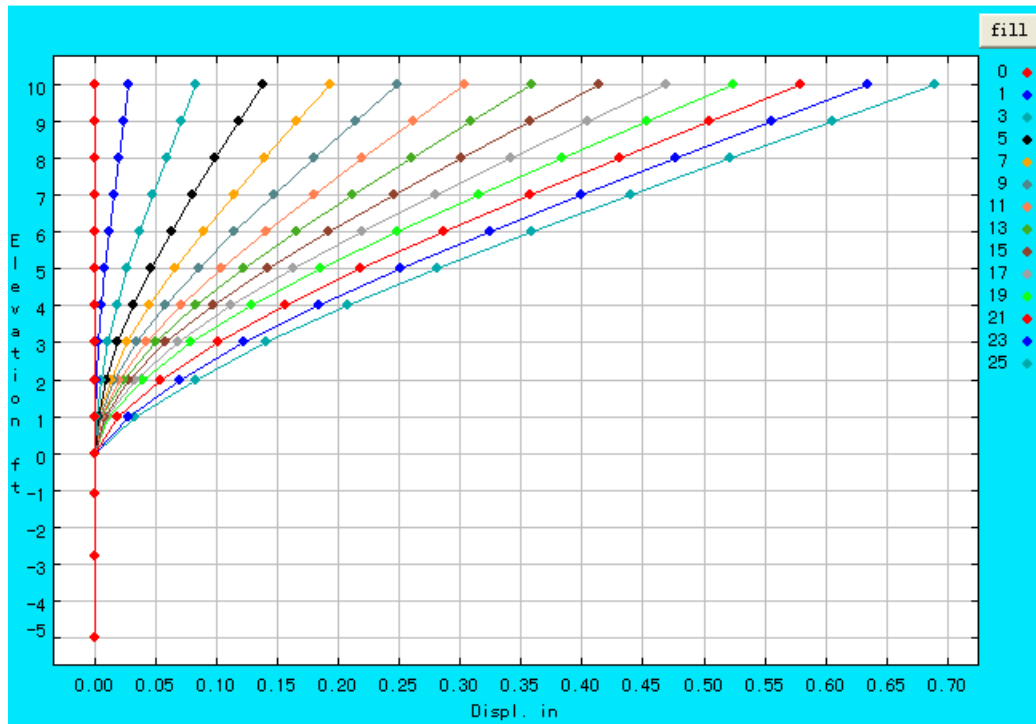
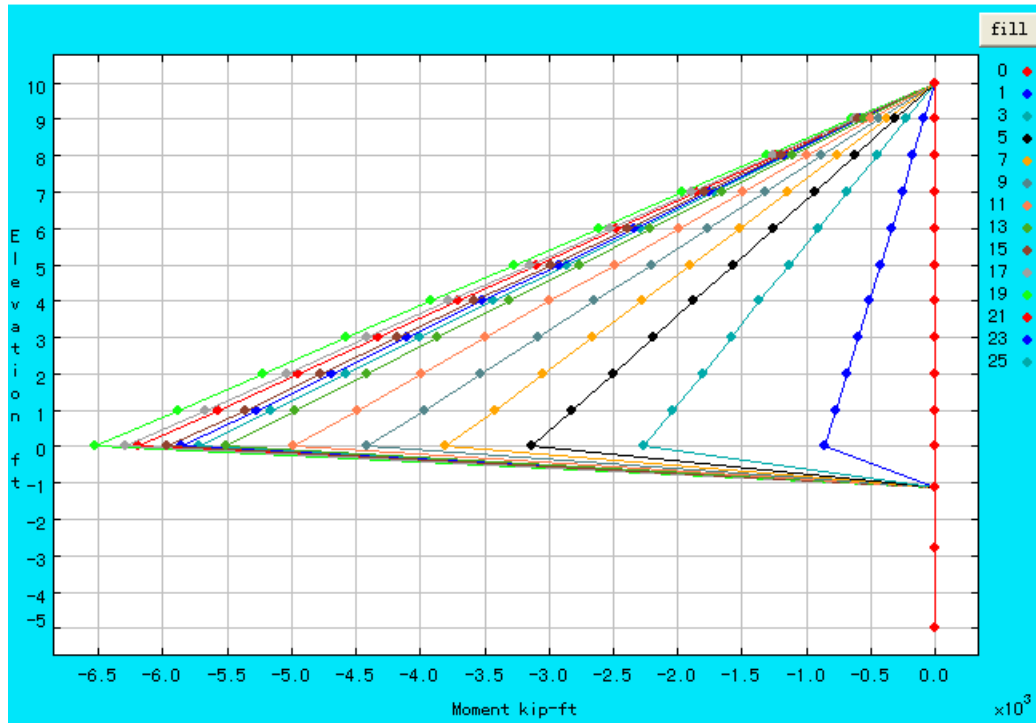


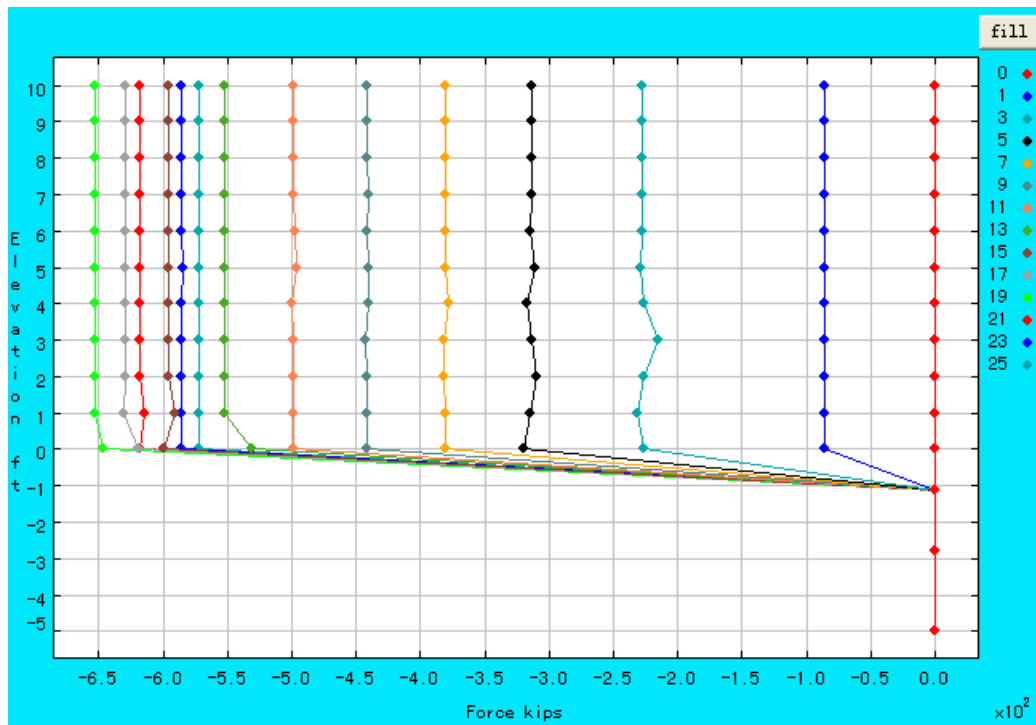
Figure H.4: Comparison of the moment-curvature curves calculated by using OpenSeesPL and OpenSees Example.



a) Longitudinal displacement



b) Moment in the longitudinal plane



c) Longitudinal shear force

Figure H.5: Displacement response profiles histories of the pile.

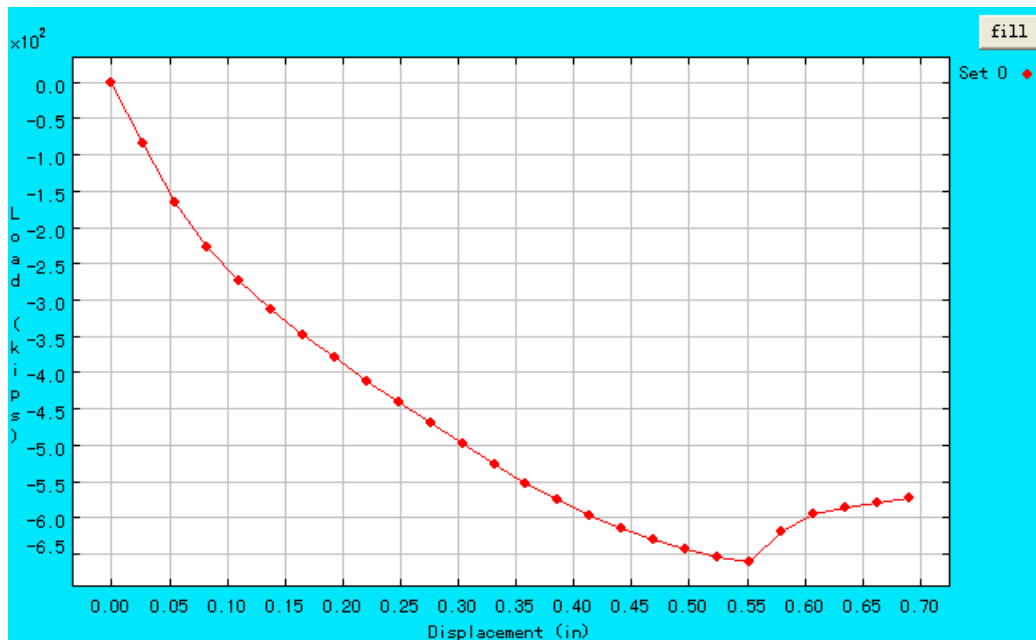


Figure H.6: Lateral (longitudinal) shear versus displacement at the pile head.

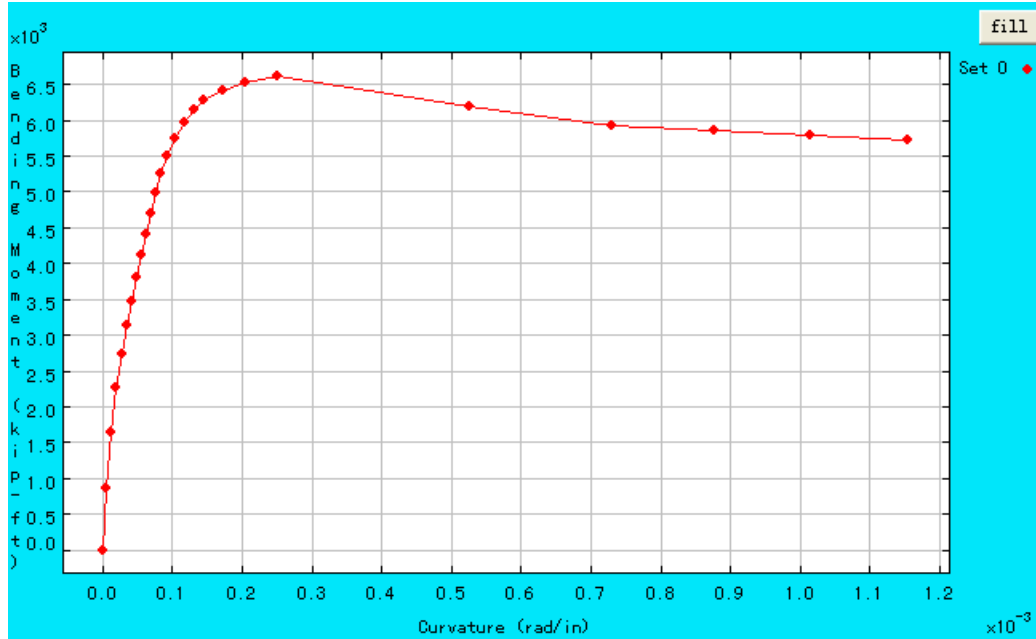


Figure H.7: Moment-curvature relation at the maximum moment location (ground surface) in OpenSeesPL.

Appendix: OpenSees Moment-Curvature Pushover Analysis Input File
(Available at
<http://opensees.berkeley.edu/OpenSees/manuals/ExamplesManual/HTML/>**)**

Source code of file ex9f.tcl:

```
# -----
# build a section
#       Silvia Mazzoni & Frank McKenna, 2006
#

# SET UP -----
wipe;                # clear memory of all past model definitions
model BasicBuilder -ndm 3 -ndf 6;    # Define the model builder, ndm=#dimension, ndf=#dofs
set dataDir Data;    # set up name of data directory -- simple
file mkdir $dataDir; # create data directory
source LibUnits.tcl; # define units

# MATERIAL parameters -----
set IDconcCore 1;    # material ID tag -- confined core concrete
```

```

set IDconcCover 2;          # material ID tag -- unconfined cover concrete
set IDreinf 3;              # material ID tag -- reinforcement
# nominal concrete compressive strength
set fc [expr -4.0*$ksi];    # CONCRETE Compressive Strength, ksi (+Tension, -
                             Compression)
set Ec [expr 57*$ksi*sqrt(-$fc/$psi)]; # Concrete Elastic Modulus
# confined concrete
set Kfc 1.3;                # ratio of confined to unconfined concrete strength
set fc1C [expr $Kfc*$fc];   # CONFINED concrete (mander model), maximum stress
set eps1C [expr 2.*$fc1C/$Ec]; # strain at maximum stress
set fc2C [expr 0.2*$fc1C];   # ultimate stress
set eps2C [expr 5*$eps1C];   # strain at ultimate stress
# unconfined concrete
set fc1U $fc;               # UNCONFINED concrete (todeschini parabolic model), maximum
                             stress
set eps1U -0.003;           # strain at maximum strength of unconfined concrete
set fc2U [expr 0.2*$fc1U];   # ultimate stress
set eps2U -0.01;            # strain at ultimate stress
set lambda 0.1;             # ratio between unloading slope at $eps2 and initial slope $Ec
# tensile-strength properties
set ftC [expr -0.14*$fc1C];  # tensile strength +tension
set ftU [expr -0.14*$fc1U];  # tensile strength +tension
set Ets [expr $ftU/0.002];   # tension softening stiffness
# -----
set Fy [expr 66.8*$ksi];     # STEEL yield stress
set Es [expr 29000.*$ksi];   # modulus of steel
set Bs 0.01;                 # strain-hardening ratio
set R0 18;                   # control the transition from elastic to plastic branches
set cR1 0.925;               # control the transition from elastic to plastic branches
set cR2 0.15;                # control the transition from elastic to plastic branches
uniaxialMaterial Concrete01 $IDconcCore $fc1C $eps1C $fc2C $eps2C ; # build core concrete
(confined)
uniaxialMaterial Concrete01 $IDconcCover $fc1U $eps1U $fc2U $eps2U ; # build cover concrete
(unconfined)
uniaxialMaterial Steel01 $IDreinf $Fy $Es $Bs ; # build reinforcement material
puts "Ec = $Ec"
puts "uniaxialMaterial Concrete01 $IDconcCore $fc1C $eps1C $fc2C $eps2C ; # build core concrete
(confined)"
puts "uniaxialMaterial Concrete01 $IDconcCover $fc1U $eps1U $fc2U $eps2U ; # build cover concrete
(unconfined)"
puts "uniaxialMaterial Steel01 $IDreinf $Fy $Es $Bs ; # build reinforcement material"
#uniaxialMaterial Concrete02 $IDconcCore $fc1C $eps1C $fc2C $eps2C $lambda $ftC $Ets; # build
core concrete (confined)
#uniaxialMaterial Concrete02 $IDconcCover $fc1U $eps1U $fc2U $eps2U $lambda $ftU $Ets; # build
cover concrete (unconfined)
#uniaxialMaterial Steel02 $IDreinf $Fy $Es $Bs $R0 $cR1 $cR2; # build reinforcement
material

# section GEOMETRY -----
set DSec [expr 5.*$ft];     # Column Diameter
set coverSec [expr 5.*$in]; # Column cover to reinforcing steel NA.
set numBarsSec 16;          # number of uniformly-distributed longitudinal-reinforcement bars
set barAreaSec [expr 2.25*$in2]; # area of longitudinal-reinforcement bars
set SecTag 1;                # set tag for symmetric section

# Generate a circular reinforced concrete section

```

```

# with one layer of steel evenly distributed around the perimeter and a confined core.
# confined core.
#         by: Michael H. Scott, 2003
#
#
# Notes
# The center of the reinforcing bars are placed at the inner radius
# The core concrete ends at the inner radius (same as reinforcing bars)
# The reinforcing bars are all the same size
# The center of the section is at (0,0) in the local axis system
# Zero degrees is along section y-axis
#
set ri 0.0;          # inner radius of the section, only for hollow sections
set ro [expr $DSec/2]; # overall (outer) radius of the section
set nfCoreR 8;      # number of radial divisions in the core (number of "rings")
set nfCoreT 8;      # number of theta divisions in the core (number of "wedges")
set nfCoverR 4;     # number of radial divisions in the cover
set nfCoverT 8;     # number of theta divisions in the cover

# Define the fiber section
section fiberSec $SecTag {
    set rc [expr $ro-$coverSec];          # Core radius
    patch circ $IDconcCore $nfCoreT $nfCoreR 0 0 $ri $rc 0 360;    # Define the core patch
    patch circ $IDconcCover $nfCoverT $nfCoverR 0 0 $rc $ro 0 360; # Define the cover patch
    set theta [expr 360.0/$numBarsSec];    # Determine angle increment between bars
    layer circ $IDreinf $numBarsSec $barAreaSec 0 0 $rc $theta 360; # Define the reinforcing layer
}

# assign torsional Stiffness for 3D Model
set SecTagTorsion 99;    # ID tag for torsional section behavior
set SecTag3D 3;         # ID tag for combined behavior for 3D model
uniaxialMaterial Elastic $SecTagTorsion $Ubig; # define elastic torsional stiffness
section Aggregator $SecTag3D $SecTagTorsion T -section $SecTag; # combine section properties

source ex9.tcl

```

Source code of file ex9. tcl:

```

# -----
# Moment-Curvature analysis of section
#         Silvia Mazzoni & Frank McKenna, 2006
#
# define procedure
source MomentCurvature3D.tcl

# set AXIAL LOAD -----
set P [expr -1800*$kip]; # + Tension, - Compression

# set maximum Curvature:
set Ku [expr 0.01/$in];
set numIncr 100; # Number of analysis increments to maximum curvature (default=100)
# Call the section analysis procedure
MomentCurvature3D $SecTag3D $P $Ku $numIncr

```

Source code of file MomentCurvature3D.tcl:

```
proc MomentCurvature3D { secTag axialLoad maxK {numIncr 100} } {  
    #####  
    # A procedure for performing section analysis (only does  
    # moment-curvature, but can be easily modified to do any mode  
    # of section response.)  
    #  
    # MHS  
    # October 2000  
    # modified to improve convergence by Silvia Mazzoni, 2006  
    #  
    # Arguments  
    #     secTag -- tag identifying section to be analyzed  
    #     axialLoad -- axial load applied to section (negative is compression)  
    #     maxK -- maximum curvature reached during analysis  
    #     numIncr -- number of increments used to reach maxK (default 100)  
    #  
    # Sets up a recorder which writes moment-curvature results to file  
    # section$secTag.out ... the moment is in column 1, and curvature in column 2  
  
    # Define two nodes at (0,0)  
    node 1001 0.0 0.0 0.0  
    node 1002 0.0 0.0 0.0  
  
    # Fix all degrees of freedom except axial and bending  
    fix 1001 1 1 1 1 1  
    fix 1002 0 1 1 1 1 0  
  
    # Define element  
    #         tag ndI ndJ secTag  
    element zeroLengthSection 2001 1001 1002 $secTag  
  
    # Create recorder  
    recorder Node -file data/Mphi.out -time -node 1002 -dof 6 disp;      # output moment (col 1) &  
    curvature (col 2)  
  
    # Define constant axial load  
    pattern Plain 3001 "Constant" {  
        load 1002 $axialLoad 0.0 0.0 0.0 0.0 0.0  
    }  
  
    # Define analysis parameters  
    integrator LoadControl 0 1 0 0  
    system SparseGeneral -piv;      # Overkill, but may need the pivoting!  
    test EnergyIncr 1.0e-9 10  
    numberer Plain  
    constraints Plain  
    algorithm Newton  
    analysis Static  
  
    # Do one analysis for constant axial load  
    analyze 1  
  
    # Define reference moment
```

```

pattern Plain 3002 "Linear" {
    load 1002 0.0 0.0 0.0 0.0 0.0 0.0 1.0
}

# Compute curvature increment
set dK [expr $maxK/$numIncr]

# Use displacement control at node 1002 for section analysis, dof 6
integrator DisplacementControl 1002 6 $dK 1 $dK $dK

# Do the section analysis
set ok [analyze $numIncr]

# -----if convergence failure-----
set IDctrlNode 1002
set IDctrlDOF 6
set Dmax $maxK
set Dincr $dK
set TolStatic 1.e-9;
set testTypeStatic EnergyIncr
set maxNumIterStatic 6
set algorithmTypeStatic Newton
if {$ok != 0} {
    # if analysis fails, we try some other stuff, performance is slower inside this loop
    set Dstep 0.0;
    set ok 0
    while {$Dstep <= 1.0 && $ok == 0} {
        set controlDisp [nodeDisp $IDctrlNode $IDctrlDOF ]
        set Dstep [expr $controlDisp/$Dmax]
        set ok [analyze 1];          # this will return zero if no
convergence problems were encountered
        if {$ok != 0} {};          # reduce step size if still fails to
converge

        set Nk 4;                  # reduce step size
        set DincrReduced [expr $Dincr/$Nk];
        integrator DisplacementControl $IDctrlNode $IDctrlDOF
$DincrReduced

        for {set ik 1} {$ik <= $Nk} {incr ik 1} {
            set ok [analyze 1];          # this will return
zero if no convergence problems were encountered
            if {$ok != 0} {
                # if analysis fails, we try some other stuff
                # performance is slower inside this loop      global
maxNumIterStatic;          # max no. of iterations performed before "failure to converge" is ret'd
                puts "Trying Newton with Initial Tangent .."
                test NormDispIncr $TolStatic 2000 0
                algorithm Newton -initial
                set ok [analyze 1]
                test $testTypeStatic $TolStatic

$maxNumIterStatic 0

                algorithm $algorithmTypeStatic
            }
            if {$ok != 0} {
                puts "Trying Broyden .."
                algorithm Broyden 8
                set ok [analyze 1 ]
            }
        }
    }
}

```

```

        algorithm $algorithmTypeStatic
    }
    if {$ok != 0} {
        puts "Trying NewtonWithLineSearch .."
        algorithm NewtonLineSearch 0.8
        set ok [analyze 1]
        algorithm $algorithmTypeStatic
    }
    if {$ok != 0} {; # stop if still fails
to converge
        puts [format $fmt1 "PROBLEM" $IDctrlNode
$IDctrlDOF [nodeDisp $IDctrlNode $IDctrlDOF] $LunitTXT]
        return -1
    }; # end if
}; # end for
integrator DisplacementControl $IDctrlNode $IDctrlDOF $Dincr;
# bring back to original increment
}; # end if
}; # end while loop
}; # end if ok != 0
# -----
global LunitTXT; # load time-unit text
if { [info exists LunitTXT] != 1 } {set LunitTXT "Length"}; # set blank if it has not
been defined previously.

    set fmt1 "%s Pushover analysis: CtrlNode %.3i, dof %.1i, Curv=%.4f /%s"; # format for
screen/file output of DONE/PROBLEM analysis
    if {$ok != 0} {
        puts [format $fmt1 "PROBLEM" $IDctrlNode $IDctrlDOF [nodeDisp $IDctrlNode
$IDctrlDOF] $LunitTXT]
    } else {
        puts [format $fmt1 "DONE" $IDctrlNode $IDctrlDOF [nodeDisp $IDctrlNode
$IDctrlDOF] $LunitTXT]
    }
}
}

```


References

- M. Alizadeh and M. T. Davisson (1970). "Lateral Load Tests on Piles – Arkansas River Project", JSMFD, ASCE, Vol. 96, SM5, September, pp. 31-40
- J. E. Bowles (1988). *Foundation Analysis and Design, 4th Edition*, McGraw-Hill Book Co., New York, NY 10020.
- Farzad Abedzadeh and Y. S. Pak (2004). "Continuum Mechanics of Lateral Soil–Pile Interaction", *Journal of Engineering Mechanics*, Vol. 130, No. 11, November, pp. 1309-1318
- Iwan, W. D. (1967). "On a class of models for the yielding behavior of continuous and composite systems." *J. Appl. Mech.*, ASME 34, 612-617.
- Kondner, R. L. (1963). "Hyperbolic stress-strain response: Cohesive soils." *Journal of the Soil Mechanics and Foundations Division*, 89(SM1), 115-143.
- Mazzoni, S., McKenna, F., and Fenves, G. L. (2006). *Open system for earthquake engineering simulation user manual*, Pacific Earthquake Engineering Research Center, University of California, Berkeley
(<http://opensees.berkeley.edu/OpenSees/manuals/usermanual/>).
- Mroz, Z. (1967). "On the description of anisotropic work hardening." *Journal of Mechanics and Physics of Solids*, 15, 163-175.
- Parra, E. (1996). "Numerical modeling of liquefaction and lateral ground deformation including cyclic mobility and dilation response in soil systems," PhD Thesis, Department of Civil Engineering, Rensselaer Polytechnic Institute, Troy, NY.
- Prevost, J. H. (1985). "A simple plasticity theory for frictional cohesionless soils." *Soil Dynamics and Earthquake Engineering*, 4(1), 9-17.
- Yang, Z. (2000). "Numerical modeling of earthquake site response including dilation and liquefaction," PhD Thesis, Department of Civil Engineering and Engineering Mechanics, Columbia University, New York, NY.
- Yang, Z., and Elgamal, A. (2002). "Influence of permeability on liquefaction-induced shear deformation." *Journal of Engineering Mechanics*, 128(7), 720-729.
- Yang, Z., Elgamal, A., and Parra, E. (2003). "A computational model for cyclic mobility and associated shear deformation." *Journal of Geotechnical and Geoenvironmental Engineering*, 129(12), 1119-1127.

OpenSeesPL-Related References

"Numerical Analysis of Seismically Induced Deformations In Saturated Granular Soil Strata," (1994), Ahmed M. Ragheb, PhD Thesis, Dept. of Civil Engineering, Rensselaer Polytechnic Institute, Troy, NY.

"Identification and Modeling of Earthquake Ground Response," (1995), A. -W. Elgamal, M. Zeghal, and E. Parra, First International Conference on Earthquake Geotechnical Engineering, IS-TOKYO'95, Vol. 3, 1369-1406, Ishihara, K., Ed., Balkema, Tokyo, Japan, Nov. 14-16. (Invited Theme Lecture).

"Prediction of Seismically-Induced Lateral Deformation During Soil Liquefaction," (1995), T. Abdoun and A. -W. Elgamal, Eleventh African Regional Conference on Soil Mechanics and Foundation Engineering, International Society for Soil Mechanics and Foundation Engineering, Cairo, Egypt, Dec. 11-15.

"Liquefaction of Reclaimed Island in Kobe, Japan," (1996), A. -W. Elgamal, M. Zeghal, and E. Parra, Journal of Geotechnical Engineering, ASCE, Vol. 122, No. 1, 39-49, January.

"Analyses and Modeling of Site Liquefaction Using Centrifuge Tests," (1996), E. Parra, K. Adalier, A. -W. Elgamal, M. Zeghal, and A. Ragheb, Eleventh World Conference on Earthquake Engineering, Acapulco, Mexico, June 23-28.

"Numerical Modeling of Liquefaction and Lateral Ground Deformation Including Cyclic Mobility and Dilation Response in Soil Systems," (1996), Ender Parra, PhD Thesis, Dept. of Civil Engineering, Rensselaer Polytechnic Institute, Troy, NY.

"Identification and Modeling of Earthquake Ground Response II: Site Liquefaction," (1996), M. Zeghal, A. -W. Elgamal, and E. Parra, Soil Dynamics and Earthquake Engineering, Vol. 15, 523-547, Elsevier Science Ltd.

"Soil Dilation and Shear Deformations During Liquefaction," (1998a), A.-W. Elgamal, R. Dobry, E. Parra, and Z. Yang, , Proc. 4th Intl. Conf. on Case Histories in Geotechnical Engineering, S. Prakash, Ed., St. Louis, MO, March 8-15, pp1238-1259.

"Liquefaction Constitutive Model," (1998b), A.-W. Elgamal, E. Parra, Z. Yang, R. Dobry and M. Zeghal, Proc. Intl. Workshop on The Physics and Mechanics of Soil Liquefaction, Lade, P., Ed., Sept. 10-11, Baltimore, MD, Balkema.

"Modeling of Liquefaction-Induced Shear Deformations," (1999), A. Elgamal, Z. Yang, E. Parra and R. Dobry, Second International Conference on Earthquake Geotechnical Engineering, Lisbon, Portugal, 21-25 June, Balkema.

"Numerical Modeling of Earthquake Site Response Including Dilation and Liquefaction," (2000), Zhaohui Yang, PhD Thesis, Dept. of Civil Engineering and Engineering

Mechanics, Columbia University, NY, New York.

"Dynamic Soil Properties, Seismic Downhole Arrays and Applications in Practice," (2001), A.-W. Elgamal, T. Lai, Z. Yang and L. He, 4th International Conference on Recent Advances in Geotechnical Earthquake Engineering and Soil Dynamics, S. Prakash, Ed., San Diego, California, USA, March 26-31.

"Computational Modeling of Cyclic Mobility and Post-Liquefaction Site Response," (2002), A. Elgamal, Z. Yang and E. Parra, Soil Dynamics and Earthquake Engineering, 22(4), 259-271.

"Influence of Permeability on Liquefaction-Induced Shear Deformation," (2002), Z. Yang and A. Elgamal, J. Engineering Mechanics, ASCE, 128(7), 720-729.

"Numerical Analysis of Embankment Foundation Liquefaction Countermeasures," (2002), A. Elgamal, E. Parra, Z. Yang, and K. Adalier, J. Earthquake Engineering, 6(4), 447-471.

"Modeling of Cyclic Mobility in Saturated Cohesionless Soils," (2003), A. Elgamal, Z. Yang, E. Parra and A. Ragheb, Int. J. Plasticity, 19, (6), 883-905.

"Application of unconstrained optimization and sensitivity analysis to calibration of a soil constitutive model ," (2003), Z. Yang and A. Elgamal, Int. J for Numerical and Analytical Methods in Geomechanics, 27 (15), 1255-1316.

"Computational Model for Cyclic Mobility and Associated Shear Deformation," (2003), Z. Yang, A. Elgamal and E. Parra, J. Geotechnical and Geoenvironmental Engineering, ASCE, 129(12), 1119-1127.

"A Web-based Platform for Live Internet Computation of Seismic Ground Response," (2004), Z. Yang, J. Lu, and A. Elgamal, Advances in Engineering Software, 35, 249-259.

"Earth Dams on Liquefiable Foundation: Numerical Prediction of Centrifuge Experiments," (2004), Z. Yang, A. Elgamal, K. Adalier, and M. Sharp, J. Engineering Mechanics, ASCE, 130(10), 1168-1176.

"Dynamic Response of Saturated Dense Sand in Laminated Centrifuge Container," (2005), A. Elgamal, Z. Yang, T. Lai, B.L. Kutter, and D. Wilson, J. Geotechnical and Geoenvironmental Engineering, ASCE, 131(5), 598-609.

"Modeling Soil Liquefaction Hazards for Performance-Based Earthquake Engineering," (2001), "S. Kramer, and A. Elgamal, Pacific Earthquake Engineering Research (PEER) Center Report No. 2001/13, Berkeley, CA.